Journal of Research of the National Bureau of Standards

Volume 92 Number 1 January-February 1987

The Journal of Research of the National Bureau of Standards features advances in measurement methodology and analyses consistent with the NBS responsibility as the nation's measurement science laboratory. It includes reports on instrumentation for making accurate and precise measurements in fields of physical science and engineering, as well as the mathematical models of phenomena which enable the predictive determination of information in regions where measurements may be absent. Papers on critical data, calibration techniques, quality assurance programs, and well-characterized reference materials reflect NBS programs in these areas. Special issues of the Journal are devoted to invited papers in a particular field of measurement science. Occasional survey articles and conference reports appear on topics related to the Bureau's technical and scientific programs.

ISSN 0160-1741 **Library of Congress Catalog Card No.: 63-37059**

In This Issue:

Letter

Articles

Conference Reports

Contents and Errata

News Briefs and Reports

Ordering

The U.S. Government Printing Office will accept payment for the

Journal of Research of the National Bureau of Standards

by check, money order, VISA, or MasterCard. The Journal is issued six times a year and has a cost schedule as follows:

	Subscription	Single Copy
Domestic	$17.00	$3.00
Foreign	21.25	3.75

Payment should be made to the Superintendent of Documents, U.S. Government Printing Office, Washington, DC 20402.

The Secretary of Commerce has determined that the publication of the periodical is necessary in the transaction of the public business required by law of the Department. Use of funds for printing this periodical has been approved by the Director of the Office of Management and Budget through October 1, 1987.

United States Government Printing Office, Washington: 1987

Dear Reader:

Dr. Hans Oser has left the National Bureau of Standards (NBS) to take on new challenges in Philadelphia, PA. We shall miss him. I have been appointed Chief Editor and Julianne W. Chappell has been appointed Managing Editor of the *Journal of Research.* To Ms. Chappell will fall the task of developing and assembling the non-archival material for the *Journal* and of presenting the work and achievements of NBS in measurement science in a clear and interesting manner. We intend to continue the work started by Dr. Oser to expand the part of the *Journal* devoted to general interest news in areas of measurement as well as publishing archival articles on measurement research. We hope to make this journal required reading for scientists, engineers, and technicians working in precision measurement.

Karl G. Kessler

Journal of Research of the National Bureau of Standards

The Continuity of the Meter: The Redefinition of the Meter and the Speed Of Visible Light

Volume 92 Number 1 January–February 1987

D. A. Jennings, R. E. Drullinger, K. M. Evenson, C. R. Pollock, and J. S. Wells

National Bureau of Standards
Boulder, CO 80303

The product of the frequency and wavelength of the i^{th} hyperfine component of the 11-5, R(127) transition of $^{127}I_2$ yields a value for the speed of visible red light. This value of c, the most accurate ever measured for visible light, agrees with the value defined in the redefinition of the meter within the 3σ error limits of the krypton length standard.

Key words: frequency; laser; meter; speed of light.

Accepted: September 15, 1986

The speed of light has intrigued scientists for several centuries and during the short quarter century of the laser it has not been different. The measurement of the speed of light, c, by a group of scientists at the National Bureau of Standards in 1972 [1][1] reported a value for c from the product of the wavelength and frequency of a 3.39 μm He-Ne laser which was limited in accuracy by the uncertainty in the krypton length standard. This definitive measurement for c followed by other confirmative measurements prompted the international scientific community, through the Comité Consultatif pour la Definition du Metre (CCDM), to a new definition for the meter. The new definition for the meter, adopted by the Conférence Générale des Poids et Mesures (CGPM) in October 1983 reads, "The meter is the length of the path travelled by light in vaccum during a time interval of 1/299 792 458 of a second." [2] This definition for the meter fixes the speed of light to be *exactly* 299 792 458 m/s. With this definition the meter could be realized from the wavelength of any coherent optical source whose frequency is known, for example, a laser which is stabilized to a narrow atomic or molecular absorption for which the frequency is known. The wavelength λ would be determined from the relation $\lambda = c/\nu$, where c is the fixed value of the speed of light, and ν is the measured frequency of the transition. Since the measurement in 1972 there have been four speed of light measurements [3–6]; two at a wavelength of 3.39 μm and two at a wavelength of 9.31 μm.These measurements have been summarized [7], and the average value for the speed of light is 299 792 458.1 m/s with a fractional uncertainty of $\pm 4 \times 10^{-9}$ (3σ), which is the recognized uncertainty in the realization of the meter from the krypton definition.

About the Authors: D. A. Jennings, R. E. Drullinger, K. M. Evenson, and J. S. Wells are physicists with the NBS Time and Frequency Division. C. R. Pollock, an electrical engineer, is a former member of the division who is now with the School of Electrical Engineering, Cornell University, Ithaca, NY 14853.

[1]Figures in brackets indicate literature references.

We are reporting a value of c using visible rather than infrared radiation. This has been made possible by the absolute frequency measurement of the visible He-Ne laser stabilized on the i^{th} hyperfine component of the 11-5, R(127) transition of the molecule $^{127}I_2$ [8]. The reported value for the frequency of this transition is 473 612 214.830 MHz with a fractional uncertainty of 1.6×10^{-10}. The wavelength for this transition is obtained from four published values which are 632 991 399.0±0.8 fm [9], 632 991 399.8±0.9 fm [10], 632 991 400.0±1.2 fm [11], and 632 993 398.0±3 fm [12]. These four wavelengths are from direct wavelength measurements referred to the wavelength of krypton. The weighted average of these measurements is 632 991 399.4±0.6 fm. The value for the speed of light is, of course, the product of the frequency and wavelength and is $c=299\ 792\ 458.6\pm0.3$ m/s, with a one sigma uncertainty.

This value of c, the most accurate ever measured for visible light, is in good agreement with the defined value of c proposed by the CCDM within the recognized uncertainties in the use of the krypton length standard (±1.2 m/s, 3σ) [11], and was the final confirmation in the choice of the new definition for the standard of length.

The fractional uncertainty of the meter realized through the new definition and use of a laser stabilized on either this frequency measured iodine transition [8], or another in the yellow region [13] is 10 times smaller than the uncertainty as realized through the krypton definition and would represent a tenfold improvement in accuracy for length metrology. Future frequency measurements in the visible will undoubtedly be even more accurate, ultimately being limited by the time standard itself. In fact, length metrology need not be limited by the frequency measurement of the laser used to realize the meter. Thus, with the new definition, a new era of length metrology is at hand, one in which the uncertainty will not be due to the length standard but with the measurement techniques.

It is always interesting to speculate on the dispersion of the speed of light. The most accurate values to date are at the CH_4 transition at 88.4 THz and the one reported here. Using formula

$$\frac{\Delta c}{\Delta \nu}=\frac{c_{88}-c_{473}}{\nu_{88}-\nu_{473}}$$

and using the best values (CGPM for 88 THz and this paper for 473 THz) gives the result

$$\Delta c/\Delta \nu < 1.5\times10^{-15}\ \text{m/s}^2.$$

References

[1] Evenson, K. M.; J. S. Wells, F. R. Petersen, B. L. Danielson, D. W. Day, R. L. Barger, and J. L. Hall, Phys. Rev. Lett. **29** 1346 (1972).

[2] Giacomo, P., IEEE Trans. on Instr. and Mea., **IM-34** 116 (1985).

[3] Layer, H. P.; R. D. Deslattes and W. G. Schweitzer, Appl. Opt. **15** 734 (1976).

[4] Monchalin, J. P.; M. J. Kelly, J. E. Thomas, N. A. Kurmit, A. Szoke, and A. Javan, Opt. Lett. **1** 4 (1977).

[5] Woods, P. T.; K. C. Shotton and W. R. C. Rowley, Appl. Opt. **17** 1048 (1978).

[6] Baird, K. M.; D. S. Smith and W. E. Berger, Opt. Commun. **31** 367 (1979).

[7] Proceedings: NATO School on Quantum Metrology and Fundamental Physical Constants, Erice, Sicily, Nov. 16–28, 1981.

[8] Jennings, D. A.; C. R. Pollock, F. R. Petersen, R. E. Drullinger, K. M. Evenson, J. S. Wells, J. L. Hall, and H. P. Layer, Opt. Lett. **8** 136 (1983).

[9] Rowley, W. R. C., and A. J. Wallard, J. Phys. **E6** 647 (1973).

[10] Schweitzer, W. G. Jr.; E. G. Kessler, R. D. Deslattes, H. P. Layer, and J. R. Whetstone, Appl. Opt. **12** 2829 (1973).

[11] Rapport: Comité Consultatif pour la Definition du Metre, 5th Session, page M54 (1973) Bureau International des Poids et Mesures, Sevres, France.

[12] Hanes, G. R.; K. M. Baird and J. DeRemigis, Appl. Opt. **12** 1600 (1973).

[13] Pollock, C. R.; D. A. Jennings, F. R. Petersen, J. S. Wells, R. E. Drullinger, E. C. Beaty, and K. M. Evenson, Opt. Lett. **8** 133 (1983).

Appendices

Appendix I. Practical Realization of the Definition of the Meter

The following recommendations for the practical realization of the definition of the meter were adopted by the International Committee for Weights and Measures (Comité International de Poids et Mesures, CIPM) in 1983.

The CIPM *recommends* that the meter be realized by one of the following methods:

a) by means of the length l of the path travelled in vacuum by a plane electromagnetic wave in a time t; this length is obtained from the measured time t, using the relation $l=c \cdot t$ and the value of the speed of light in vacuum $c=299\ 792\ 458$ m/s;

b) by means of the wavelength in vacuum λ of a plane electromagnetic wave of frequency f; this wavelength is obtained from the measured frequency f, using the relation $\lambda=c/f$· and the value of the speed of light in vacuum $c=299\ 792\ 458$ m/s;

c) by means of one of the radiations from the list below, whose stated wavelength in vacuum or whose stated frequency can be used with the uncertainty shown, provided that the given specifications and accepted good practice are followed;

and that in all cases any necessary corrections be applied to take account of actual conditions such as diffraction, gravitation, or imperfection in the vacuum.

List of recommended radiations, 1983

In this list, the values of the frequency f and of the wavelength λ should be related exactly by the relation $\lambda f=c$, with $c=299\ 792\ 458$ m/s but the values of λ are rounded.

1. *Radiations of Lasers Stabilized by Saturated Absorption*[a]

1.1. Absorbing molecule CH_4, transition ν_3, P(7), component $F_2^{(2)}$.

The values $f=88\ 376\ 181\ 608$ kHz
$\lambda=3\ 392\ 231\ 397.0$ fm

with an estimated overall relative uncertainty of $\pm 1.3\times 10^{-10}$ [which results from an estimated relative standard deviation of 0.44×10^{-10}] apply to the radiation of a He-Ne laser stabilized with a cell of methane, within or external to the laser, subject to the conditions:

methane pressure $\leqslant 3$ Pa
mean one-way axial intracavity surface power density[b] $\leqslant 10^4$ W · m^{-2}
radius of wavefront curvature $\geqslant 1$ m
inequality of power between counter-propagating waves $\leqslant 5\%$.

Notes

[a]Each of these radiations can be replaced, without degrading the accuracy, by a radiation corresponding to another component of the same transition or by another radiation, when the frequency difference is known with sufficient accuracy. Details of methods of stabilization are described in numerous scientific and technical publications. References to appropriate articles, illustrating accepted good practice for a particular radiation, may be obtained by application to a member laboratory of the CCDM, or the BIPM.

[b]The one-way-intracavity beam power is obtained by dividing the output power by the transmittance of the output mirror.

1.2. Absorbing molecule $^{127}I_2$, transition 17-1, P(62), component o.

The values $f = 520\ 206\ 808.51$ MHz
$\lambda = 576\ 294\ 760.27$ fm

with an estimated[c] overall relative uncertainty of $\pm 6 \times 10^{-10}$ [which results from an estimated relative standard deviation of 2×10^{-10}] apply to the radiation of a dye laser (or frequency-doubled He-Ne laser) stabilized with a cell of iodine, within or external to the laser, having a cold-finger temperature of 6 °C±2 °C.

1.3. Absorbing molecule $^{127}I_2$, transition 11-5, R(127), component i.

The values $f = 473\ 612\ 214.8$ MHz
$\lambda = 632\ 991\ 398.1$ fm

with an estimated overall relative uncertainty of $\pm 1 \times 10^{-9}$ [which results from an estimated relative standard deviation of 3.4×10^{-10}] apply to the radiation of a stabilized He-Ne laser containing an iodine cell, subject to the conditions:

cell-wall temperature between 16 °C and 50 °C with a cold-finger temperature of 15 °C±1 °C
one-way intracavity beam power[b] 15 mW±10 mW
frequency modulation amplitude, peak to peak, 6 MHz±1 MHz.

1.4. Absorbing molecule $^{127}I_2$, transition 9-2, R(47), component o.

The values $f = 489\ 880\ 355.1$ MHz
$\lambda = 611\ 970\ 769.8$ fm

with an estimated overall relative uncertainty of $\pm 1.1 \times 10^{-9}$ [which results from an estimated relative standard deviation of 3.7×10^{-10}] apply to the radiation of a He-Ne laser stabilized with a cell of iodine, within or external to the laser, having a cold-finger temperature of −5 °C±2 °C.

1.5. Absorbing molecule $^{127}I_2$, transition 43-0, P(13), component a_3 (sometimes called component s).

The values $f = 582\ 490\ 603.6$ MHz
$\lambda = 514\ 673\ 466.2$ fm

with an estimated overall relative uncertainty of $\pm 1.3 \times 10^{-9}$ [which results from an estimated relative standard deviation of 4.3×10^{-10}] apply to the radiation of an Ar^+ laser stabilized with a cell of iodine, within or external to the laser, having a cold-finger temperature of −5 °C±2 °C.

[c]This uncertainty, and the frequency and wavelength values, are based on the weighted mean of only two determinations. The more precise of the two, however, was a measurement dependent only on frequency mixing and multiplication techniques relative to the radiation in 1.1. above.

Appendix II. Decisions of the Conférence Générale des Poids et Mesures (CGPM) Regarding the Definition of the Meter

1st CGPM, 1889:

"Sanction of the international prototype of the meter.

"The General Conference, considering

"..that ... the fundamental measurements of the international and national prototypes of the meter [has] been made with all the accuracy and reliability that the present state of science permits; that the international and national prototypes of the meter are made of an alloy of platinum with 10 percent iridium, to within 0.0001; the equality in length of the international Meter ... with the length of the Meter kept in the Archives of France;

"that the differences between the national Meters and the international Meter lie within 0.01 millimeter and that these differences are based on a hydrogen thermometer scale which can always be reproduced..;

"that the international Meter ... and the national Meters ... fulfill the requirements of the Meter Convention,

"**Sanctions** The Prototype of the meter chosen by the Comité International des Poids et Mesures (CIPM). This Prototype, at the temperature of melting ice, shall henceforth represent the metric unit of length."

7th CGPM, 1927:

"Definition of the meter by the international Prototype.

The unit of length is the meter, defined by the distance, at 0°, between the axes of the two central lines marked on the bar of platinum-iridium kept at the BIPM, and declared Prototype of the meter by the 1st CGPM, this bar being subject to standard atmospheric pressure and supported on two cylinders of at least one centimeter diameter, symmetrically placed in the same horizontal plane at a distance of 571 mm from each other."

11th CGPM, 1960:

"Considering that the international Prototype does not define the meter with an accuracy adequate for the present needs of metrology, [the CGPM] decides that it is moreover desirable to adopt a natural and indestructible standard.

"The meter is the length equal to 1 650 763.73 wavelengths in vacuum of the radiation corresponding to the transition between the levels 2 p_{10} and 5 d_5 of the krypton 86 atom."

15th CGPM, 1975:

considering the excellent agreement among the results of wavelength measurements on the radiations of lasers locked on a molecular absorption line in the visible or infrared region, with an uncertainty estimated at $\pm 4 \times 10^{-9}$ which corresponds to the uncertainty of the realization of the meter,

considering also the concordant measurements of the frequencies of several of these radiations,

recommends the use of the resulting value for the speed of propagation of electromagnetic waves in vacuum $c = 299\ 792\ 458$ meters per second.

17th CGPM, 1983:

"Considering: that the present definition does not allow a sufficiently precise realization of the meter for all requirements,

that progress made in the stabilization of lasers allows radiations to be obtained that are more reproducible and easier to use than the standard radiation emitted by a krypton 86 lamp,

that progress made in the measurement of the frequency and wavelength of these radiations has resulted in concordant determinations of the speed of light whose accuracy is limited principally by the realization of the present definition of the meter,

that wavelengths determined from frequency measurements and a given value for the speed of light have a reproducibility superior to that which can be obtained by comparison with the wavelength of the standard radiation of krypton 86,

that there is an advantage, notably for astronomy and geodesy, in maintaining unchanged the value of the speed of light recommended in 1975 by the 15th CGPM in its Resolution 2 ($c = 299\,792\,458$ m/s),

that a new definition of the meter has been envisaged in various forms all of which have the effect of giving the speed of light an exact value, equal to the recommended value, and that this introduces no appreciable discontinuity into the unit of length, taking into account the uncertainty of $\pm 4 \times 10^{-9}$ of the best realizations of the present definition of the meter,

that these various forms, making reference either to the path travelled by light in a specified time interval or to the wavelength of a radiation of measured or specified frequency, have been the object of consultations and deep discussions, have been recognized as being equivalent and that a consensus has emerged in favor of the first form,

that the CCDM is now in a position to give instructions for the practical realization of such a definition, instructions which could include the use of the orange radiation of krypton 86 used as standard up to now, and which may in due course be extended or revised,

"The 17th CGPM invites the CIPM to draw up instructions for the practical realization of the new definition of the meter to choose radiations which can be recommended as standards of wavelength for the interferometric measurement of length and to draw up instructions for their use."

[See "Practical Realization of the Definition of the Meter," *above*.]

Appendices 1 and 2 are taken from NBS Special Publication 330, The International System of Units (SI) and are the official translations from the minutes of the General Conferences on Weights and Measures.

Journal of Research of the National Bureau of Standards

The NBS Scale Of Radiance Temperature

Volume 92 Number 1 January–February 1987

William R. Waters,
James H. Walker,
and Albert T. Hattenburg

National Bureau of Standards
Gaithersburg, MD 20899

This paper describes the measurement methods and instrumentation used in the realization and transfer of the International Practical Temperature Scale (IPTS-68) above the temperature of freezing gold. The determination of the ratios of spectral radiance of tungsten-strip lamps to a gold-point blackbody at a wavelength of 654.6 nm is detailed. The response linearity, spectral responsivity, scattering error, and polarization properties of the instrumentation are described. The analysis of sources of error and estimates of uncertainty are presented. The assigned uncertainties (three standard deviations) in radiance temperature range from ±2 K at 2573 K to ±0.5 K at 1073 K.

Key words: calibrations; gold-point blackbody; radiance temperature; response linearity; standards; tungsten-strip lamps.

Accepted: October 17, 1986

1. Introduction

Temperatures above the freezing point of gold (1337.58 K) are defined on the International Practical Temperature Scale (IPTS-68) [1][1] in terms of the ratio of spectral radiances of two blackbody sources, one of which is maintained at the gold point. Thus, the accurate measurement of the spectral radiance ratio of two sources is required for the realization and dissemination of the radiance temperature scale. Currently, such measurements are performed at NBS using a spectroradiometer operated by a computer-controlled data acquisition system, which permits rapid comparison of the spectral radiances from a variety of sources. With this system, lamp standards of radiance temperature are calibrated in the range 1337.58 K to 2573 K. For convenience, the calibrations are extended to 1073 K, where the scale is defined in terms of thermocouples. Calibration services are also available for optical pyrometers. The purpose of this paper is to provide a detailed description of the instrumentation and procedures used to realize and disseminate the radiance temperature scale. Detailed information on the calibration services appears in a separate report [2].

About the Authors: William R. Waters and James H. Walker are with the Center for Radiation Research in the NBS National Measurement Laboratory. Albert T. Hattenburg was with the center and is now retired.

[1]Figures in brackets indicate literature references.

2. Basic Theory

Spectral radiance is the radiant power contained in a defined area, solid angle, and wavelength interval,

$$L_\lambda = d^3\Phi/dA \cdot \cos\Theta \cdot d\Omega \cdot d\lambda \quad (1)$$

where L_λ is the spectral radiance, Φ is the radiant

flux, A is the area, Θ is the angle between the surface normal and the direction of propagation, Ω is the solid angle about that direction, and λ is the wavelength. The relation between spectral radiance, wavelength and temperature is given by Planck's Law,

$$L_\lambda = c_1/\pi \cdot \lambda^5 \cdot [\exp(c_2/\lambda \cdot T) - 1] \quad (2)$$

where c_1 and c_2 are the first and second radiation constants, λ is the wavelength in vacuo, and T is the temperature. The defining equation for the IPTS above 1337.58 K is therefore

$$r = L_\lambda(T)/L_\lambda(T_{Au}) = [\exp(c_2/\lambda \cdot T_{Au}) - 1]/[\exp(c_2/\lambda \cdot T) - 1] \quad (3)$$

where $L_\lambda(T)$ and $L_\lambda(T_{Au})$ are the spectral radiances of the two blackbodies at temperatures T and T_{Au}, T_{Au} is the temperature of freezing gold defined as 1337.58 K, r is their ratio, and c_2 is defined as 1.4388 cm-K. In principle, a measurement of the ratio at a discrete wavelength with a linear response instrument yields the value of T.

In practice, the radiance temperature scale is realized with an instrument of finite bandpass, and an integral form of eq (2) must be used.

$$r = \int L_\lambda(T) \cdot R_\lambda \cdot d\lambda / \int L_\lambda(T_{Au}) \cdot R_\lambda \cdot d\lambda \quad (4)$$

where R_λ is the spectral responsivity of the instrument and includes the spectral transmittance of the wavelength-limiting element (e.g., interference filter or monochromator), the spectral transmittance of all other optical elements, and the spectral responsivity of the detector. A determination of R_λ allows a calculation of T from eqs (2 and 4). Determination of the ratio for a range of values provides a temperature scale over the corresponding temperature range.

The radiance temperature scale is typically maintained and disseminated on tungsten-strip lamps, which possess a repeatable current vs. radiance-temperature relationship not available in present variable-temperature blackbodies. Realization of the scale with these lamps and a gold-point blackbody is also practical, and is the typical procedure followed by standards laboratories [3]. This scale is valid only for the wavelength of realization, since the spectral distributions of the lamps are not known functions. Traditionally the wavelength of realization has been near 650 nm, a convenient region for visual optical pyrometers. At NBS, a spectroradiometer system is presently being used and a wavelength of 654.6 nm (wavelength of a thorium spectral line) has been chosen. This method requires that the instrument relative spectral responsivity function extend only over an acceptably small spectral range, or is known accurately enough to determine the wavelength at which the integrands of eq (4) have the same ratio as the integrals.

3. Measurement Apparatus

The radiance temperature calibrations described in this report are performed on the NBS Facility for Automated Spectroradiometric Calibrations (FASCAL). This system employs a prism-grating double monochromator, mirror optics, a highly stable external tungsten reference source, and a photomultiplier tube operated in a linear response mode. A block diagram of the system is shown in figure 1. Prior calibrations were carried out on the NBS

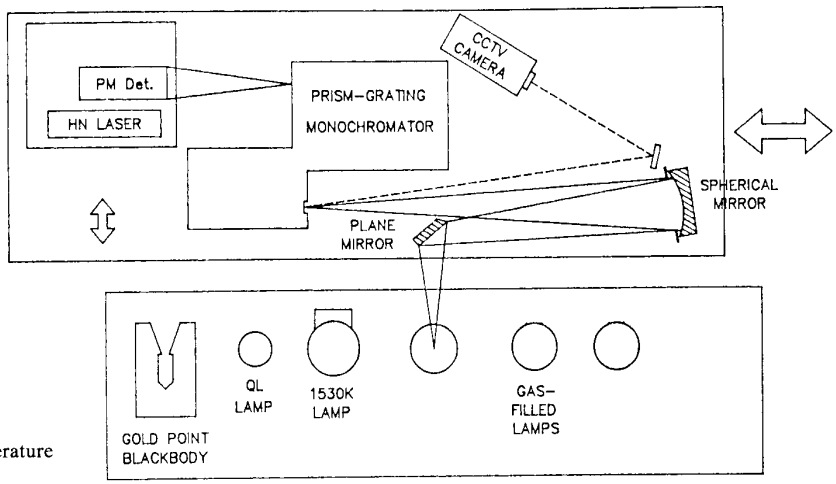

Figure 1–FASCAL radiance temperature measurement.

Photoelectric Pyrometer [4]. A new version of this instrument is under development, which will employ interference filters (1 nm bandpass) and refractive optics. The measurement process will be nearly identical to that of the FASCAL system, utilizing an external reference source and a linear-response photomultiplier tube. A schematic diagram of the new instrument is shown in figure 2.

3.1 Gold-Point Blackbody

The Gold-Point Blackbody (GPBB) is a graphite cylinder with a small viewing hole (diameter 1 mm) at one end, and a conical cavity at the other. The cylinder is surrounded by 0.99999 pure gold, and the crucible containing the gold is surrounded by heating coils and an insulated case. The construction and characterization of the GPBB have been detailed in prior reports [4]. The estimated emissivity is 0.9999. The duration of a melt or freeze plateau is approximately 5 minutes, and the time delay between these observation periods is about 5 minutes.

3.2 Lamp Sources

Tungsten-strip filament lamps are used both in the realization of the radiance temperature scale and as secondary standards for scale dissemination. Each filament has a small notch in one edge, about midway along its length, to aid in determination of the filament portion to be calibrated (target area). A small mark is placed on the rear of the lamp envelope to permit reproducible angular positioning.

3.2.1 Vacuum Lamps: Vacuum tungsten-strip lamps of the Quinn-Lee type [5,6] are used in the scale realization. One lamp is operated at a single current to produce a spectral radiance equal to that of the gold-point blackbody at 654.6 nm. A second lamp is operated at a single current to produce a spectral radiance of about eight times that of the gold-point blackbody at 654.6 nm (about 1530 K radiance temperature). Both lamps are stable to better than 0.02% over 200 burning hours when operated under these single-level conditions.

3.2.2 Gas-Filled Lamps: Gas-filled tungsten-strip lamps are calibrated as secondary standards for dissemination of the radiance temperature scale. Prior to calibration, the lamps are annealed at a radiance temperature of 2350 °C for 2 hours on direct current. Each lamp is examined for the variations in spectral radiance with angle of emission, while set at a radiance temperature of 1700 °C. The lamp orientation is chosen to minimize variations in spectral radiance with rotation, and an alignment arrow is then etched on the rear of the envelope. The amount and orientation of polarization effects are also determined. Lamps selected for calibration display a degree of polarization of 0.005 or less.

3.3 Spectroradiometer

3.3.1 Fore-optics: Sources are imaged with unit magnification at the entrance slit of the monochromator by the two front-surface aluminized mirrors shown in figure 1. The mirror surfaces are stripped and recoated at intervals to reduce signal loss due to oxidation. The plane mirror directs the beam to the spherical mirror (radius of curvature 1220 mm)

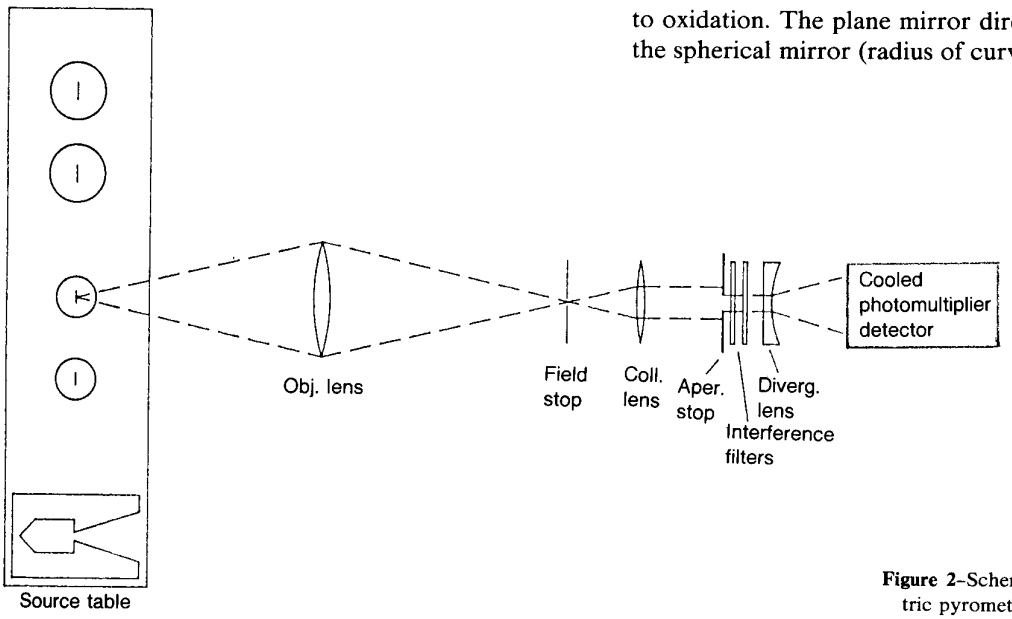

Figure 2–Schematic of photoelectric pyrometer.

along a line about 1.5 degrees from the spherical mirror axis. The spherical mirror focuses the beam onto a mirror-surfaced mask, placed immediately in front of the entrance slit. The mask is engraved with horizontal and vertical scales with 0.1 mm divisions, and is viewed at high magnification by either a telescope or a video camera to allow for precise positioning of the sources. The mask determines the height of the system field stop (source target area). The entrance slit determines the width. The stop dimensions are 0.8 mm high by 0.6 mm wide for the scale realization and transfer. The system aperture stop is located within the monochromator.

3.3.2 Monochromator: A prism-grating double monochromator is employed to minimize spectral scattering and avoid multiple orders. The dispersion is about 4 nm/mm at the 654.6 nm wavelength setting. The entrance aperture (solid angle) is rectangular in shape, with a vertical angle of 0.125 radians and a horizontal angle of 0.0625 radians. The wavelength setting is calibrated against a spectral line standard (thorium) and is repeatable to within 0.05 nm. The entrance, intermediate, and exit slits are adjustable from 0.01 to 3.0 mm as a unit, resulting in a nearly triangular-shaped spectral responsivity function.

3.3.3 Detector: For the radiance temperature determinations an end-on 11-stage photomultiplier with quartz window and S-20 spectral response is placed behind the exit slit. The detector is cooled to 258 K with a thermoelectric cooler. The anode current is amplified and converted to a 0–10 volt signal by a programmable amplifier.

3.4 Control and Data Acquisition System

The FASCAL system employed for the radiance temperature calibrations permits control of the entire measurement process from a remote operator console after initial source alignment. Component positions, instrument settings, sequence of operations, and data collection are effected by either stored computer programs, operator commands, or a combination of the two.

The system is directed by a microcomputer and a high-speed disk system for program and data storage. A modular interface controller [7] provides the link between instruments and computer. All measurement signals are multiplexed into the digital voltmeter through the interface scanner, and the instruments are remotely programmed and controlled through interface modules. All instrument settings and signal outputs are printed and stored on disk for later analysis. The spectroradiometer (fore-optics, monochromator, and detector) and a closed-circuit TV camera are mounted on a carriage. The carriage can be positioned by remote command along a linear track, to align the spectroradiometer with one of the sources mounted at fixed stations along the track. The average move time between stations is a few seconds, and positions are repeatable to about 0.1 mm. The TV camera presents a highly magnified image of the monochromator entrance slit mask to video displays at the spectroradiometer and at the operator console for initial source alignment and subsequent monitoring.

4. Measurement of Instrument and Source Parameters

4.1 Spectral Responsivity Function

The relative spectral responsivity function of the spectroradiometer is determined by the indirect method [8]. In this method, the relative responsivity function is treated as the product of two terms, the responsivity factor and the slit-scattering function, where the responsivity factor depends only upon the wavelength of the observed flux and the slit-scattering function depends only upon the difference between the wavelength setting of the monochromator and the wavelength of the flux. This factorization of the spectral responsivity function is valid if the instrument dispersion, aberrations, scattering, and diffraction are constant over the wavelength region of interest. This assumption is valid in the central portion of the relative responsivity function, but values for the distant wings are subject to error due primarily to changes in scattering and dispersion.

The responsivity factor is obtained by spectrally scanning a continuous source standard of spectral radiance with narrow (0.1 mm) slits. To determine the slit-scattering function, an integrating sphere irradiated by a krypton or argon laser is spectrally scanned by the spectroradiometer, with the slit widths set at the 0.6 mm width used in the scale realization and transfer. The plot of the output signal versus wavelength is the mirror image of the plot of the slit-scattering function versus wavelength [8]. For a 647 nm krypton laser, the function is nearly triangular in shape with a width at half-height of 2.2 nm. Relative to the peak value, the measured values decrease to about 10^{-3} at 3 nm, 10^{-4} at 15 nm, and 10^{-7} at 70 nm from the central wavelength. At 150 nm from the central wavelength, the value decreases to 10^{-8} in the short-wavelength wing and to 10^{-9} in the long-wavelength wing. Scans with 488 and 514 nm (ar-

gon), and 676 nm (krypton) yield similar results. These values were confirmed over the central and near wings portion of the function by measurements with the direct method, using a dye laser tuned through a series of wavelengths with the spectroradiometer set at a fixed wavelength [9]. Since the function changes very slowly with wavelength in the visible region, the measurement at 647 nm yields the slit-scattering function at 654.6 nm.

4.2 Linearity of Response

The degree of linearity of the spectroradiometer response is determined with an automated beam conjoiner [10]. A beam from a constant source is split into two branches, whose fluxes are independently attenuated or blocked before recombination and further attenuation. The flux contribution from both branches is equal to the sum of the fluxes from each branch when measured separately (additivity). The device provides 96 levels of flux over a range of about 1 to 500. The levels are presented in random order to avoid systematic errors, and are interspersed with 29 zero flux levels. A microcomputer controls the attenuating filters and records the filter positions and radiometer signals. The data is least-squares fitted to a polynomial response function, to determine a correction factor by which the radiometer output signal must be multiplied to obtain a quantity proportional to radiant flux.

The measured instrument response is linear to within $\pm 0.2\%$ for a range of photomultiplier anode currents from 1 to 500 nanoamperes. For currents much less than 1 nanoampere, the signal is limited by noise. For currents greater than 1 microampere, the linearity correction increases rapidly, rising to 3% at 7 microamperes. The anode current is restricted to less than 500 nanoamperes during measurements by selection of appropriate photomultiplier tube voltage. Correction factors for the amplifier ranges are determined from measurement of a known electrical current and combined with the linearity correction factor.

4.3 Polarization

The polarization properties of the spectroradiometer and the gas-filled lamps are measured with the aid of dichroic (linear) polarizers positioned in motorized rotating mounts. The sheet polarizer properties and those of the spectroradiometer are determined in an initial set of experiments, using an illuminated integrating sphere as a source of unpolarized radiation. The characterized polarizer and spectroradiometer are then used to measure the polarization properties of the lamp sources.

The determination of spectroradiometer and sheet polarizer properties consists of spectral radiance measurements of the sphere source alone, with a pair of similar polarizers interposed in the beam and set at a number of angular positions (rotations about the optic axis), and with each polarizer individually placed in the beam at the same angular positions. In order to account for departure from ideal behavior, a Mueller transmittance matrix [11] containing six parameters is assumed for the sheet polarizers. Circular polarization is assumed to be negligible. The spectroradiometer polarization direction is determined in a preliminary experiment and chosen as the polarization reference direction, leaving only the degree of polarization to be determined for the instrument. Our measurements provide about 200 equations involving 10 unknowns, whose values are then obtained by a non-linear least-squares solution.

The sphere source is replaced by the lamp source whose properties are to be measured using a characterized sheet polarizer and spectroradiometer. Measurements are made with the lamp alone and with the polarizer set at the same angular positions as before. This results in 25 equations involving the two source unknowns, whose values are obtained by a least-squares solution. The polarization of the lamp source is specified by the direction of maximum linear polarization τ, and the degree of polarization

$$P=(L_{max}-L_{min})/(L_{max}+L_{min}) \tag{5}$$

where L_{max} and L_{min} are the maximum and minimum readings of a polarization-indifferent radiometer when an ideal linear polarizer is rotated in the source beam. The factor (see Appendix) required to reduce the signal ratio of eq (4) to a value which would be obtained with a polarization-indifferent radiometer is

$$(1+Bp_l)^{-1}$$

where $p_l=p\cdot\cos 2\tau$ and B is the spectroradiometer polarizance (degree of linear polarization introduced by the spectroradiometer). For the spectroradiometer employed here, the measured polarizance is 0.26 at 654.6 nm. The degree of polarization of a typical lamp selected for calibration is about 0.003. The uncertainty in the radiometer polarizance B is estimated as ± 0.0005, and the lamp polarization uncertainties are estimated as ± 0.002 (uncertainties are stated at the three standard deviations level).

4.4 Size of Source

The "size of source" effect (signal contribution due to flux which originates outside the target area and is scattered into the measured beam by the fore-optics) is determined by observing the signal from a 0.6 by 0.8 mm segment of a uniform diffuse source, and noting the change in signal when the surrounding area of the source is changed by placing various masks on the diffuse source. The masks expose source areas which closely approximate the radiant areas of the lamp and blackbody sources used in the scale realization and transfer. As a check, the effect is also evaluated by observing changes in the near-zero signal from a "black hole" (an absorbing cavity slightly larger than the 0.6 by 0.8 mm field stop) as the various surrounding area masks are positioned. The observed differences are used to apply a correction to the signals observed in source comparisons. The measured effect varies from 0.04% to 0.1% at 654.6 nm depending upon the elapsed time since the last mirror recoating.

5. Process of Realization and Transfer

The process of realization and transfer consists of three steps, all carried out at a wavelength of 654.6 nm. In step one, the gold-point spectral radiance is transferred to a Quinn-Lee vacuum lamp. In step two, a second vacuum lamp at about 1530 K radiance temperature (about eight times the gold-point spectral radiance) is compared to the first vacuum lamp. In step three, the second lamp is compared to the test lamp. After resetting the test lamp current, step three is repeated for each desired radiance temperature. If the vacuum lamps remain constant between observations, the product of the signal ratios from the three comparisons is the signal ratio of the test lamp to the GPBB. With appropriate corrections for size of source and polarization, the spectral radiance and thus the radiance temperature of the test lamp can be evaluated from eqs (4 and 2). The polarization and the spectral radiance distributions over Ω, A, and λ of the vacuum lamps are of no concern here, since the lamps serve only to reproduce the spectroradiometer signal between comparisons. The only requirement is that the vacuum lamp parameters remain constant between comparisons with the gold-point blackbody (GPBB) and with the test lamp. This is satisfied by the constant-current operation of the stable (0.02% per 200 hours) vacuum lamps. Comparison with the GPBB is performed about every 50 to 100 hours of lamp operation, and the vacuum lamps are compared with each other weekly during experiments. The use of the first vacuum lamp avoids the inconvenience of manipulating the GPBB through its melting and freezing point cycles and provides a continuous measure of gold-point radiance. It also increases the number of experiments allowed between maintenance or replacement of the gold-point furnace. The use of the second vacuum lamp keeps all signal ratios within the linear response region of the spectroradiometer (i.e., within the 1 to 500 nanoampere range of anode current).

6. Data Analysis and Uncertainties

6.1 Temperature Values

The signal ratio of the test lamp to the GPBB is obtained from the product of the signal ratios measured in the first vacuum lamp comparison with the GPBB, the second (1530 K) vacuum lamp comparison to the first, and the test lamp comparisons to the second lamp. The ratio is then multiplied by correction factors to account for the size-of-source disparity, polarization error, and departure from linear response where appropriate. An estimated test lamp radiance temperature is then calculated from the ratio of Planck functions for two blackbodies which have the same signal ratio (one blackbody at the gold point), using 654.6 nm as the wavelength. This temperature can then be used to determine by iteration the exact temperature which will satisfy eq (4). For the spectral responsivity function of this spectroradiometer, this exact temperature differs from the estimated temperature obtained from the Planck ratio by an amount which is small (less than 0.2 K) and is a simple function of the temperature. Therefore, to avoid the repetitive iteration process, the temperature calculated from the Planck ratio is corrected to the desired eq (4) value by this known difference.

6.2 Uncertainties

The uncertainties in the radiance temperature values assigned to the calibrated lamps are obtained from the observed imprecision of the measurements and the estimated systematic error in both the measured and the provided quantities (e.g., temperature of melting gold). Uncertainties obtained from observed imprecision and from published values for the physical constants are based upon three standard deviations. Uncertainties of systematic errors are estimated at the equivalent of three standard deviations.

In order to examine the contributions of the various errors to the uncertainty in radiance temperature, an approximate equation for the complete measurement process can be developed by using the Wien approximation to eq (2),

$$L_\lambda \cong (c_1/\pi)\cdot\lambda^{-5}\cdot\exp(-c_2/\lambda\cdot T) \tag{6}$$

to express the spectral radiance of a blackbody. With this approximation, eq (3) becomes

$$\begin{aligned} r &= \exp(c_2/\lambda\cdot T_{Au})/\exp(c_2/\lambda\cdot T) \\ &= \exp[(c_2/\lambda)\cdot(1/T_{Au} - 1/T)]. \end{aligned} \tag{7}$$

Solving for T, and expressing r in terms of the measured ratios and their correction factors, we can express the complete measurement process as

$$T = \{(1/T_{Au}) - (\lambda/c_2)\cdot\ln[s\cdot d\cdot f\cdot M_0\cdot M_1\cdot M_2/(1+B\cdot p_1)]\}^{-1} \tag{8}$$

where the definitions of the quantities and their estimated 3σ uncertainties are:

M_0, signal ratio GPBB vs. first vacuum lamp (0.12%)

M_1, signal ratio first vacuum lamp vs. 1530 K lamp (0.12%)

M_2, signal ratio 1530 K lamp to test lamp (0.2–0.5%)

s, size-of source correction for GPBB vs. test lamp (0.1%)

d, correction for test lamp drift during calibration (0.1%)

f, linearity-range factor correction (0.04–0.1%)

T_{Au}, IPTS-68 temperature of freezing gold (0.4 K)

c_2, second radiation constant (0.00014 cm·K)

B, spectroradiometer polarizance (0.05%)

p_1, lamp polarization component (0.2%)

λ, wavelength setting at 654.6 nm (0.15 nm)

Radiance temperature uncertainties due to the factors of eq (8) are obtained from the partial derivative with respect to those factors and the estimated uncertainty in the factor (propagation of error). For example, the calculated uncertainty in radiance temperature at the 2300 °C (2573.15 K) point due to the 0.4 K uncertainty in T_{Au} is

$$\Delta T = (2573.15/1337.58)^2\cdot(0.4) = 1.48 \text{ K}.$$

Differences between errors calculated by eq (8) and those calculated by the exact Planck equation are negligible. Note that for the wavelength λ this process yields the error due to inserting the wrong wavelength in the calculation, not the error due to incorrect wavelength setting.

In addition to the factors which appear explicitly in this relation, uncertainties in the ratios M_0, M_1, and M_2 arise from errors in the wavelength setting λ, in the current measurements of the vacuum (0.2 ma) and gas-filled (2 ma) lamps, in the alignment of lamps and in the measured spectral responsivity function. The uncertainties in the ratios due to wavelength setting and current are assessed by measurement of the change in signal ratio when varying these quantities. The effect upon the signal ratios due to the uncertainty in the measured spectral responsivity function is determined by solving eq (4) for a range of $R(\lambda_0, \lambda)$ values, using the known spectral radiance distribution of the GPBB and an approximate test lamp distribution derived from spectral scans of such lamps. The radiance temperature uncertainties due to these factors are then deduced from the ratio uncertainties as before. The uncertainties in signal ratio, wavelength setting, lamp currents and lamp alignment are considered random errors; the remaining errors are systematics. Table 1 summarizes the uncertainties obtained by this process.

References

[1] The International Practical Temperature Scale of 1968, Metrologia **5** 2, 35–44: April 1969.

[2] Waters, W. R.; J. H. Walker and A. T. Hattenburg, Radiance Temperature Calibrations at NBS, Natl. Bur. Stand. (U.S.) Spec. Publ. 250-7; to be published.

[3] Supplementary Information for the IPTS-68 and the EPT-76, 1983, Comité Consultatif de Thermometrie, Bureau Internationale Des Poids et Mesures Monographie; Pavillon de Breteuil, F-92310, Sevres, France.

[4] Lee, R. D., The NBS photoelectric pyrometer and its use in realizing the International Practical Temperature Scale above 1063 °C, Metrologia **2** 4, 150–162: October 1966.

[5] Quinn, T. J., and R. D. Lee, Vacuum tungsten strip lamps with improved stability as radiance temperature standards, in Temperature, Its Measurement and Control in Science and Industry (Instrument Society of America, Pittsburgh: 1972), Vol. 4, Part 1, p. 395.

[6] Lee, R. D.; H. J. Kostkowski, T. J. Quinn, P. R. Chandler, T. N. Jones, J. Tapping and H. Kunz, Intercomparison of the IPTS-68 above 1064 °C by four national laboratories, in Temperature, Its Measurement and Control in Science and Industry (Instrument Society of America, Pittsburgh: 1972), Vol. 4, Part 1, p. 377.

[7] Popenoe, C. H., and M. S. Campbell, MIDAS Modular Interactive Data Acquisition System—Description and Specification, Natl. Bur. Stand. (U.S.) Tech. Note 790, 49 pages, 1973 August.

[8] Kostkowski, H. J., The relative spectral responsivity and slit-scattering function of a spectroradiometer, Chapter 7 of Self-Study Manual on Optical Radiation Measurements: Part I—Concepts, Natl. Bur. Stand. (U.S.) Tech.

Note 910-4, 134 pages, June 1979, pp. 2–34.
[9] Saunders, R. D., and J. B. Shumaker, Apparatus function of a prism-grating double monochromator. (Submitted to Applied Optics.)
[10] Saunders, R. D., and J. B. Shumaker, Automated radiometric linearity tester, Appl. Opt. **23** 20, 3504–3506: 1984 October 15.
[11] Shumaker, J. B., The distribution of optical radiation with respect to polarization, Chapter 6 of Self-Study Manual on Optical Radiation Measurements: Part I—Concepts, Natl. Bur. Stand. (U.S.) Tech. Note 910-3, 53 pages, June 1977.

Table 1. Summary of estimated uncertainties in degrees C.

Source of Uncertainty	Temperature (°C)				
	800	1100	1400	1800	2300
Signal Ratio M_0 (r)	0.06	0.10	0.15	0.23	0.36
Signal Ratio M_1 (r)	0.06	0.10	0.15	0.23	0.36
Signal Ratio M_2 (r)	0.27	0.27	0.28	0.37	0.67
Size of Source (s)	0.05	0.09	0.13	0.20	0.30
Lamp Drift (s)	0.05	0.09	0.13	0.20	0.30
Linearity (s)	0.05	0.03	0.05	0.13	0.30
Temperature Freezing Gold (s)	0.26	0.42	0.62	0.96	1.48
Second Radiation Constant (s)	0.02	0.0	0.04	0.11	0.22
Polarization (s)	0.04	0.06	0.09	0.14	0.21
Wavelength Setting (r)	0.08	0.05	0.08	0.20	0.44
Vacuum Lamp Current (r)	0.05	0.08	0.13	0.18	0.29
Test Lamp Current (r)	0.29	0.18	0.12	0.09	0.07
Spectral Responsivity (s)	0.03	0.01	0.0	0.02	0.03
Lamp Alignment (r)	0.13	0.21	0.32	0.49	0.76
Total estimated 3σ uncertainty on Thermodynamic Scale (square root of sum of squares)	0.5	0.6	0.8	1.3	2.0

Note: Random errors denoted by (r), systematic by (s).

APPENDIX

Measurement of Instrument and Source Polarization

The measurement of source polarization and the determination of its effect on the measurement of spectral radiance is carried out with a sheet polarizer mounted in a motorized rotating mount. This mount fits a slot milled into a bracket attached to the front of the spectroradiometer. By this means the polarizer can be reproducibly positioned in the same location between the source and the spectroradiometer whenever required.

Before the polarizer can be used for source polarization measurements its polarization and that of the spectroradiometer must be measured. This is accomplished with the help of an integrating sphere and a second polarizer similar to the first. The integrating sphere is mounted in the radiometer source plane so that its exit port serves as a source of unpolarized radiance. Its entrance port, located at about 90° from the exit port, is irradiated with a suitable light source, such as a quartz-halogen lamp. Then a series of spectral radiance measurements of this source is recorded: a) with no polarizer, b) with the first polarizer in its slot, c) with the second polarizer added in a second milled slot in the mounting bracket between the first polarizer and the source, and, d) with the first polarizer removed leaving only the second polar-

izer. At each wavelength of interest measurements are taken as a function of polarizer orientation as the polarizers are rotated about the optic axis. The first polarizer is typically sampled every 15° and the second every 30°. The second polarizer is tilted in its mount by about 10° to avoid polarizer-polarizer interreflections. All of these measurements are automated and require typically about an hour at each wavelength.

In the analysis of this data we write the first row Mueller matrix elements of the spectroradiometer responsivity as

$$R = R_0 \left| 1 \; B \; 0 \; 0 \right| \tag{1a}$$

where R_0 is the ordinary responsivity neglecting polarization and we take the reference direction for polarization to be in whatever direction the radiometer polarizance lies, thus forcing the 45° component to vanish. The reference direction was determined to be horizontal by simply observing the effect of a hand-held polarizer of known polarization axis upon a lamp measurement. The polarization axis of the polarizer, in turn, was confirmed by viewing sunlight reflected at glancing incidence through the polarizer. Circular polarization is assumed to be negligible for the type of instrument and sources employed here. The quantity B represents the degree of linear polarization of the spectroradiometer. The Mueller matrix of a polarizer is taken to be of the form

$$P = \begin{vmatrix} s & d\mathrm{C} & d\mathrm{S} & 0 \\ d\mathrm{C} & e\mathrm{C}^2+f & g\mathrm{SC} & 0 \\ d\mathrm{S} & \mathrm{X} & \mathrm{X} & \mathrm{X} \\ 0 & \mathrm{X} & \mathrm{X} & \mathrm{X} \end{vmatrix} \tag{2a}$$

where $\mathrm{C}=\cos 2(\phi-\phi_0)$, $\mathrm{S}=\sin 2(\phi-\phi_0)$ and the parameters s, d, e, f, g, and ϕ_0 are obtained by least-squares fitting of the measurements. The angle ϕ is the orientation angle of the polarizer read from a scale on the polarizer mount. The matrix elements marked X are not involved in these measurements. This form of the Mueller matrix was found, by trial and error, to fit our data well. The simpler model of an ideal dichroic polarizer in which $e=s$ and $g=s-f$ (where, in terms of the principle transmittances k_1 and k_2, we have $s=[k_1+k_2]/2$ and $d=[k_1-k_2]/2$) is adequate for our visible and infrared polarizers but fails to fit the ultraviolet polarizer data. Finally, the Stokes vector of the unpolarized source is given by

$$L = L_0 \begin{vmatrix} 1 \\ 0 \\ 0 \\ 0 \end{vmatrix} \tag{3a}$$

The various measurements then lead to equations of the following forms.

No polarizer: $V = R \cdot L = R_0 L_0$ (4a)

Polarizer #1: $V(\phi) = R \cdot P \cdot L$

$$= R_0 L_0 (s + Bd\mathrm{C}) \tag{5a}$$

Both polarizers: $V(\phi, \phi') = R \cdot P \cdot P' \cdot L$

$$= R_0 L_0 (ss' + Bs'd\mathrm{C} + dd'\mathrm{CC}' + Bd'f\mathrm{C}' + dd'\mathrm{SS}' + Bd'g\mathrm{SCS}' + Bd'e\mathrm{C}^2\mathrm{C}') \tag{6a}$$

Polarizer #2: $V(\phi') = R \cdot P' \cdot L$

$$= R_0 L_0 (s' + Bd'\mathrm{C}') \tag{7a}$$

where $\mathrm{C}'=\cos 2(\phi'-\phi_0')$, $\mathrm{S}'=\sin 2(\phi'-\phi_0')$, and V represents the recorded radiometer signal output as a function, in general, of polarizer orientation angles. Altogether our measurements produce about 200 equations. The values of the ten unknowns s, s', d, d', e, f, g, B, ϕ_0, and ϕ_0' are then obtained by a non-linear least squares solution. As far as polarization is concerned the parameters s, d, e, f, g, and ϕ_0 completely characterize the first polarizer, at least within the accuracy of the model represented by the Mueller matrix of eq (10), and the parameter B characterizes the spectroradiometer. Since the factor R_0L_0 is common to all equations these measurements yield no information about it.

Using the characterized polarizer and radiometer we are now able to measure the polarization of an unknown source by recording spectroradiometer measurements obtained from the source: a) without a polarizer, and b) with the first polarizer again mounted on the bracket as when it was characterized. As before, the measurements are made at 15° intervals of the polarizer. We take the Stokes vector of the unknown source to be

$$L = L_0 \begin{vmatrix} 1 \\ p_1 \\ p_2 \\ 0 \end{vmatrix} \tag{8a}$$

where, as always, we have neglected circular polarization. p_1 and p_2 are given by $p_1=p\cdot\cos 2\tau$ and $p_2=p\cdot\sin 2\tau$, where τ is the direction of polarization measured from the reference direction of the radiometer and p is the degree of polarization,

$$p = (L\max - L\min)/(L\max + L\min). \tag{9a}$$

In eq (17) $L\max$ and $L\min$ are the maximum and minimum readings of a polarization-indifferent radiometer when an ideal linear polarizer is rotated in the source beam. Then our measurements lead to a no-polarizer equation:

$$V=R_0L_0(1+Bp_1) \tag{10a}$$

and to 24 equations:

$$V(\tau)=R_0L_0[(s+Bd\,\mathrm{C})+(d\,\mathrm{C}+Be\,\mathrm{C}^2+Bf)p_1 + (d\,\mathrm{S}+Bg\,\mathrm{SC})p_2]. \tag{11a}$$

Aside from the factor R_0L_0 which is common to all equations and cancels out, the only unknowns in these 25 equations are p_1 and p_2 which we can then obtain by a least-squares solution. These two parameters completely characterize the state of (linear) polarization of the source. Normally, only the second described experiment of 25 measurements need be performed to measure the polarization of a source since the polarizers and radiometer are relatively stable and, once characterized, will only infrequently need to be measured.

Equation (10a) gives the relationship between the spectral radiance of a source, L_0, and the radiometer output signal, V, assuming linearity of response and only linear polarization. If we apply this equation both to the measurement of an unknown source and to the measurement of a spectral radiance standard used to calibrate the radiometer we obtain:

$$L_0=L_0^s[\mathrm{V}/\mathrm{V}^s][(1+Bp_1^s)/(1+Bp_1)] \tag{12a}$$

where L_0^s is the known spectral radiance of the standard, V/V^s is the measured signal ratio, B is the radiometer polarizance, and p_1^s and p_1 are the relative Stokes components measured as described above for the standard and for the unknown source. (For a blackbody standard, presumably, $p_1^s=0$.) This shows that the presence of polarization introduces the extra factor

$$(1+Bp_1^s)/(1+Bp_1)$$

into the simple measurement relationship which is valid in the absence of source polarization or if the radiometer is indifferent to polarization.

The polarization measurement uncertainty by this process can be judged by the statistics of the least-squares fitting and by the measurement reproducibility when different polarizers are used. Both indications suggest typical uncertainties (one standard deviation) in the visible where the polarizers are very good and the noise level very low of ± 0.0003 in the radiometer polarizance B and uncertainties of ± 0.001 in the source relative Stokes components p_1 and p_2.

Journal of Research of the National Bureau of Standards

Detection and Sizing of Surface Flaws With a SQUID-Based Eddy Current Probe

Volume 92 Number 1 January–February 1987

J. C. Moulder and T. E. Capobianco

National Bureau of Standards
Boulder, CO 80303

In a new approach to eddy current detection and sizing of surface-breaking flaws, we have coupled a conventional reflection probe to a superconducting quantum interference device (SQUID) to produce an eddy current probe with increased sensitivity and signal to noise ratio. The reflection probe consists of an air-core excitation coil surrounding two counterwound ferite-core pickup coils connected in series. A room-temperature probe is inductively coupled to a SQUID, which operates in a liquid helium bath. The new probe was used to obtain flaw signals from a number of electrical-discharge machined slots in aluminum alloy 6061. Results indicated that by scanning the probe along the length of the flaw, the length could be determined from the extent of the flaw signal. The peak amplitude of the flaw signal was found to be proportional to the cross-sectional area of the flaw. Empirical calibration curves relating these quantities were used to invert successfully the experimental data obtained for the EDM slots.

Key words: aluminum alloy; eddy current testing; flaw sizing; nondestructive evaluation; reflection probe; superconducting quantum interference device; surface flaw.

Accepted: September 24, 1986

Introduction

The development of superconducting quantum interference devices (SQUIDs) two decades ago [1][1] introduced to the metrologist a new sensor of extraordinary sensitivity. The SQUID comprises a small superconducting inductance in series with a weak Josephson junction [2]. The rf impedance of the junction is a periodic function of the flux linking the series inductor, with a period of precisely one quantum of flux, $\phi_0 = h/2e = 2.07 \times 10^{-15}$ webers. If a feedback circuit is used to maintain a constant amount of flux linking the inductor in response to changes in the externally applied field, an error signal that is linear in flux results with wide dynamic range and a sensitivity of a fraction of a flux quantum [3]. The operating principles of such rf-biased devices are described in detail elsewhere [3–5]. The commercial availability of SQUIDs has led to their application to a wide variety of measurement problems: from magnetic-monopole detectors to magnetocardiography and magnetoencephalography. They have been used in magnetometers and gradiometers, for susceptibility measurements and noise thermometry, to name but a few applications.

One of the first applications of SQUIDS to measurement problems in nondestructive evalua-

About the Authors: J. C. Moulder is with the Fracture and Deformation Division in NBS' Institute for Materials Science and Engineering, and T. E. Capobianco is with the Electromagnetic Technology Division in the Bureau's National Engineering Laboratory. The work they describe was supported by the NBS Office of Nondestructive Evaluation.

[1] Bracketed figures indicate literature references.

tion was the use of a SQUID magnetometer to measure and map the magnetic fields of eddy current probes [6,7]. The success of this application led to the development of a SQUID-based eddy current probe for flaw detection [8]. This instrument consisted of a reflection probe, operated at room temperature, coupled inductively to the SQUID, which is operated in a liquid helium bath (4 K).

Our first studies with this probe characterized its responses to flaws by scanning the probe along or across several rectangular, electrical-discharged machined (EDM) slots in 6061 Al. We found that the magnitude of the flaw signal scaled linearly with cross-sectional area of the flaws (length times depth for these rectangular flaws). A linear response to flaw area has also been reported for electric-current perturbation (ECP) probes [9].

A linear response to flaw area suggests a particularly simple and direct method for determining the length and depth of surface-breaking cracks, the two parameters of most interest in a fracture-mechanics assessment of fitness for service. Measurements made by scanning the probe along the length of EDM slots [8] indicated that the length of the slot could be inferred from the "flaw profile" so produced, a procedure proposed for absolute probes by B. A. Auld et al. [10]. If the length and area of a flaw can be determined from the width and height of the flaw profile, and if the flaw shape is known, then it is quite simple to determine the flaw's depth.

The objective of the present study was to evaluate the ability of the SQUID-based eddy current probe to detect and size surface-breaking flaws using the inversion method outlined above. A series of 16 EDM slots of different length, depth, and shape was machined in 6061 Al and scanned with the SQUID-based eddy current probe. Calibration curves relating the breadth and amplitude of the flaw signal to flaw length and cross-sectional area were derived from the experimental data. We then used these calibration curves to predict the size of the slots from the experimental data and compared the predictions with the known slot dimensions.

Experiment

The eddy current probe used in these studies consists of a large (8.1-mm i.d.) air-core coil surrounding two smaller ferrite-core coils. The axes of all the coils are normal to the workpiece. The outer coil is driven with an oscillator to provide excitation; the flaw signal is taken from the two inner pickup coils connected in series opposing. Tuning slugs are located above each of the pickup coils to permit nulling of the signal in the absence of a flaw. The probe has been described in greater detail elsewhere [7,8].

Connection of the eddy current probe to the SQUID is shown in figure 1. The room-temperature probe is connected to a single loop of copper wire in the liquid-helium Dewar through a shielded twisted pair. The eddy current signal is coupled to the SQUID inductively through the mutual inductance of the one-turn coil and a nine-turn Nb coil that is directly connected to the SQUID input terminals. The one-turn coil and the nine-turn coil are wound on separate coil forms; one coil is mounted on a translator so that the spacing (and strength of coupling) can be varied from outside the cryostat.

The SQUID and the detection electronics associated with it are commercial instruments. The output of the SQUID detector circuit was fed into a

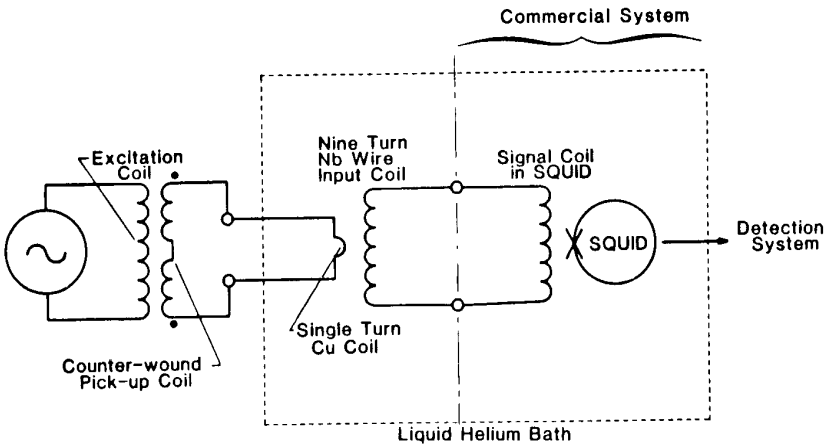

Figure 1–Schematic diagram of SQUID-based eddy current probe.

lock-in amplifier locked to the phase of the excitation voltage. In this way we could determine both the magnitude and phase of the flaw signals. The lock-in amplifier was interfaced to a laboratory computer through the IEEE-488 bus.

The eddy current probe was scanned over the flaws with a two-axis, computer-controlled positioner. Two types of scans were made: longitudinal and transverse. For longitudinal scans, one pickup coil is scanned along the length of the flaw with the other coil remaining to one side of the flaw. For transverse scans, the probe scans across the center of the flaw with the line connecting the two pickup coils at 90° to the flaw axis.

The EDM slots we used for this study are described in table 1. Four of the slots were semi-elliptical in cross section; the remainder were rectangular. They ranged in depth from 0.35 to 2.46 mm and in length from 3.69 to 7.08 mm. The widths of all the slots were about 0.2 mm. All the specimens were machined in 6061 Al alloy.

Table 1. Flaw specimens used in experiments.

Specimen	Flaw Type	Length (mm)	Width (mm)	Depth (mm)
NBS-2A	R	6.54	0.24	0.49
NBS-2B	R	7.07	0.25	1.51
NBS-2C	R	7.08	0.32	1.90
NBS-2D	R	7.08	0.36	2.46
NBS-3A	S	3.70	0.19	0.70
NBS-3B	S	3.82	0.20	0.95
NBS-3C	S	4.15	0.22	1.25
NBS-3D	S	4.20	0.22	1.44
NBS-4A	R	3.69	0.17	0.35
NBS-4B	R	3.85	0.18	0.64
NBS-4C	R	4.16	0.19	0.75
NBS-4D	R	4.20	0.21	0.92
NBS-5A	R	3.75	0.24	0.88
NBS-5B	R	3.90	0.20	1.17
NBS-5C	R	4.24	0.18	1.32
NBS-5D	R	4.27	0.19	1.88

Flaw Types: S=semi-elliptical EDM notch, R=rectangular EDM notch.

Measurements were performed under computer control in a step-and-measure mode. The probe was stepped along or across the flaws in 0.25-mm increments, remaining stationary at each point along the scan for a sequence of measurements of the flaw signal to be acquired by the computer from the lock-in amplifier. The operating frequency for the measurements reported here was 10 kHz. Previous measurements showed this to be the frequency of greatest sensitivity for the system [8]. Only results of longitudinal scans were used for signal inversion.

Results and Discussion

Flaw profiles obtained by making longitudinal scans of the EDM slots in specimen NBS-5 are shown in figures 2a and 2b. Figure 2a shows the magnitude of the flaw signal and figure 2b shows the phase. There is a residual imbalance of about 50 mV in the magnitude of the SQUID output owing to our inability to perfectly balance the pickup of the two ferrite-core coils with the tuning slugs.

The double-peaked structure of the flaw profiles is characteristic of longitudinal scans; the two peaks occur when the pickup coil is near the ends of the flaw. In a way, the differential pickup coils are a magnetic field gradiometer; the emf developed across these coils is proportional to the gradient of the magnetic field normal to the surface. The double peaks indicate a concentration of eddy currents circulating around the flaw. The asymmetry of the two peaks appears to be related to probe construction, since the relative height of the two peaks reverses when the probe is rotated by 180°.

The structure of the phase flaw profiles shown in figure 2b is closely related to the structure of the magnitude profiles. Extrema in the phase curves occur at inflection points of the magnitude curves.

The characteristic flaw profiles shown in figure 2 may be used in a type of imaging to determine the length of the flaws. If we draw lines tangent to the flanks of the flaw profiles and determine the distance between intersections of these lines with the signal base line, we find this distance to be proportional to the actual flaw length as shown in figure 3 for all the specimens studied. The solid line in figure 3 is the result of a linear least-squares fit to the data.

The linear relationship between the peak amplitude of the flaw profile and cross-sectional area of the flaw is shown in figure 4 for the 16 flaws we studied. For this plot the amplitude of the larger peak was used. The solid line in figure 4 is a least-squares fit to the data. The results for the semi-elliptical flaws (NBS-3) can be seen to conform to the same response as the rectangular flaws.

If we now take the least-squares fits from figures 3 and 4 as calibration curves and use them to predict flaw lengths and depths from the experimental data, the results we obtain are shown in figure 5 and table 2. Table 2 lists the predicted and actual lengths and depths for the 16 EDM slots

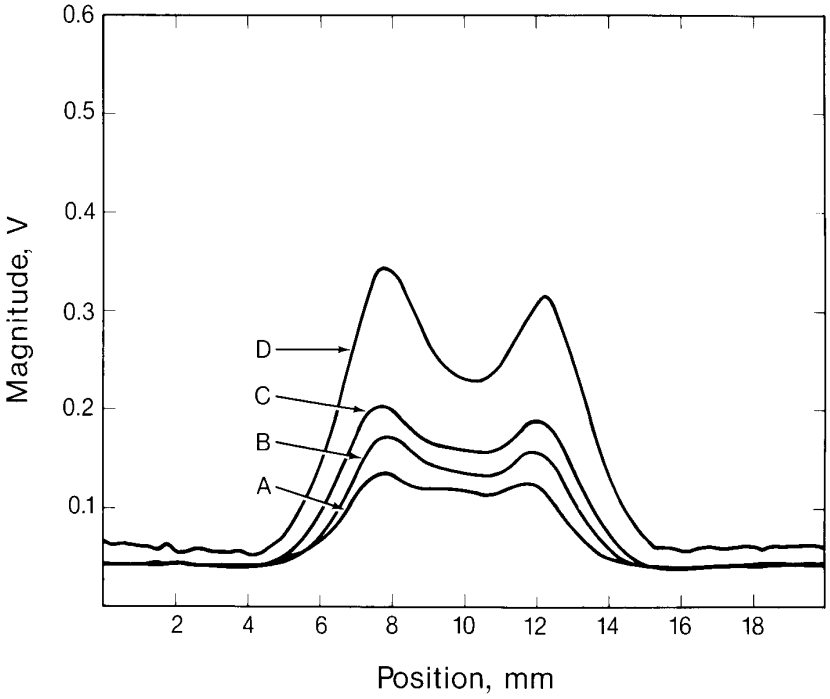

Figure 2a–Magnitude of flaw signals from SQUID-based eddy current probe for longitudinal scans of four rectangular EDM slots in specimen NBS-5 (see table 1).

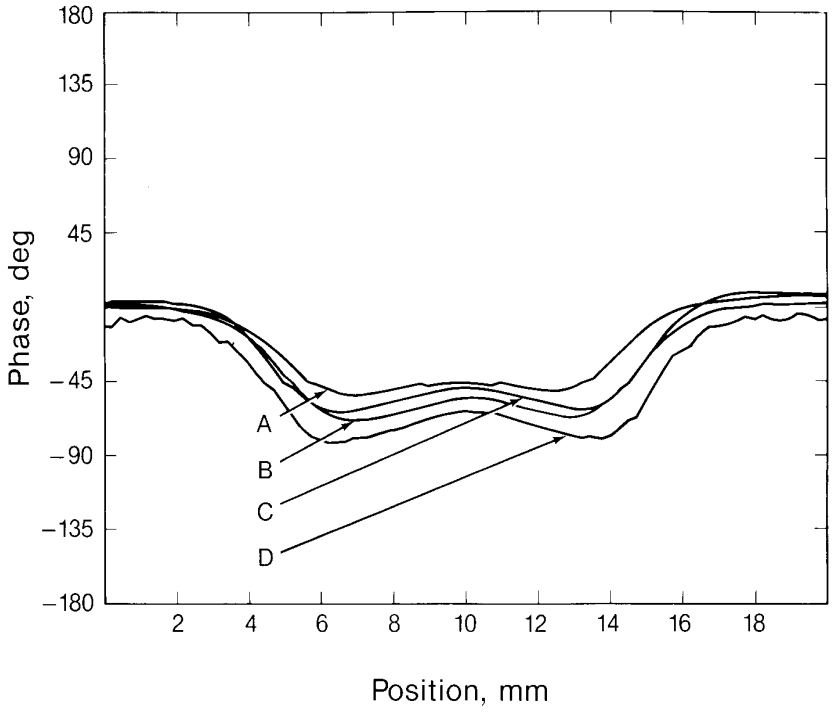

Figure 2b–Phase of flaw signals for the same flaws shown in figure 2a.

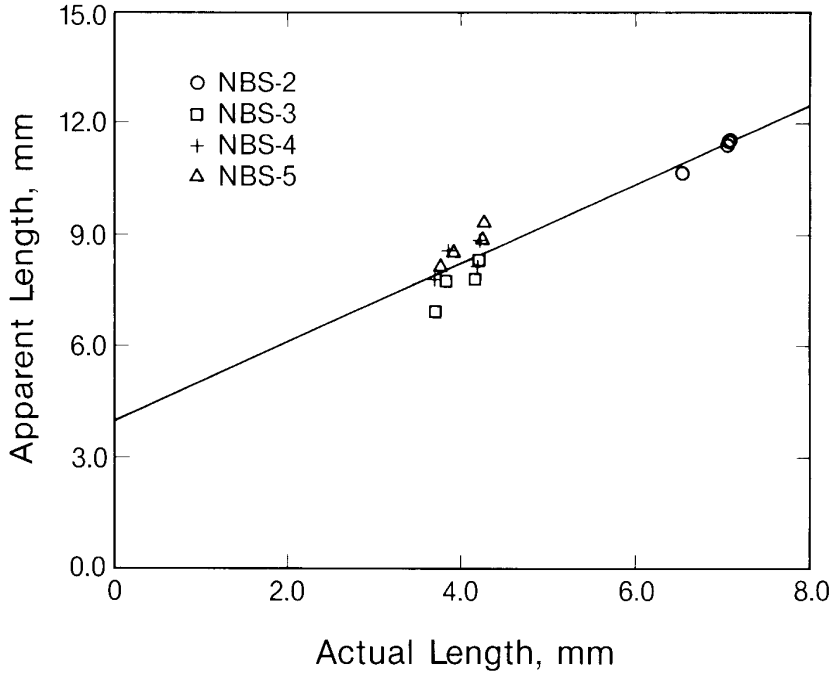

Figure 3–Correlation between flaw length and the width of the flaw signal obtained from a longitudinal flaw scan. Line is a least-squares fit to the data.

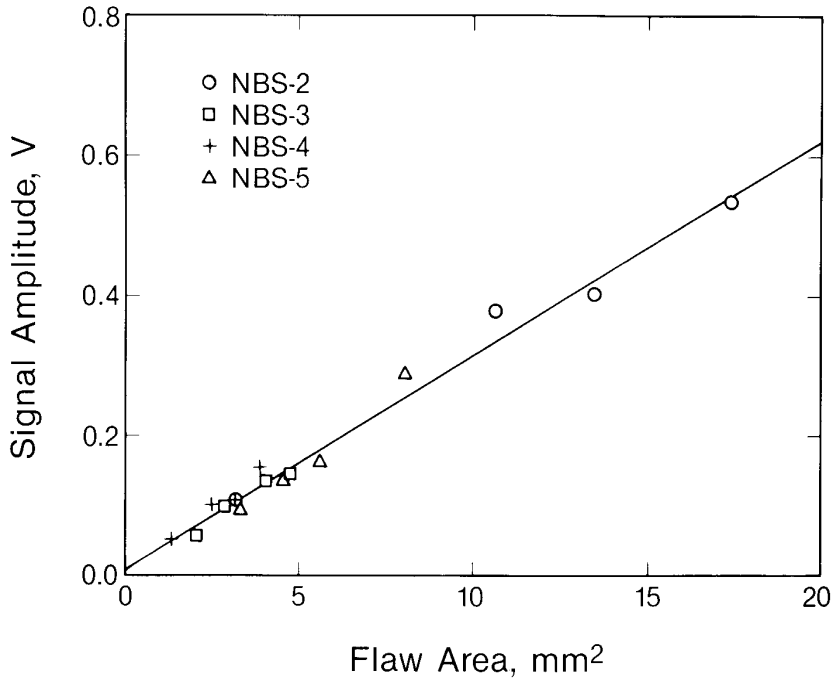

Figure 4–Relation between maximum flaw signal and cross sectional area of flaw. Line is a least-squares fit to the data.

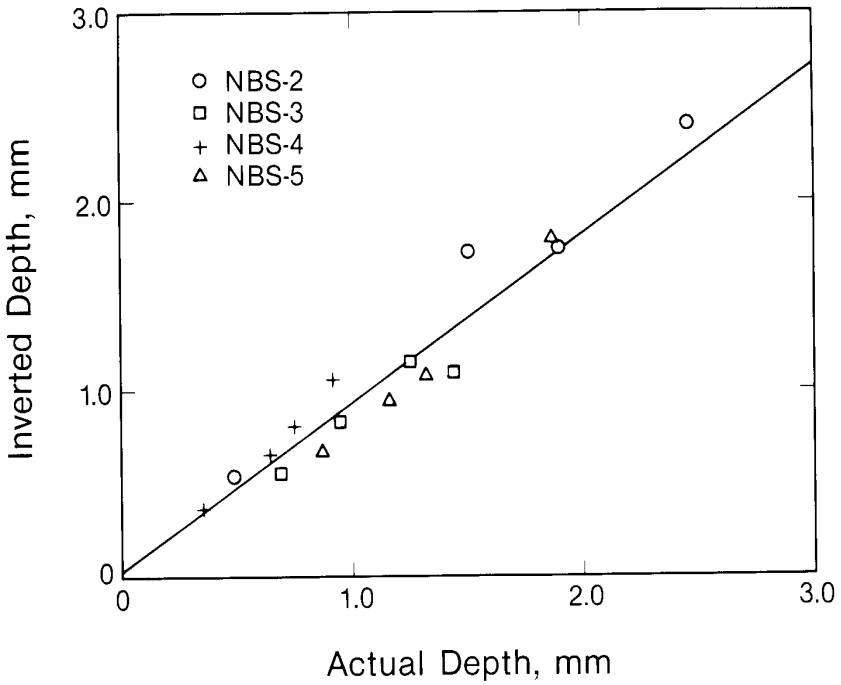

Figure 5–Flaw depth determined by inversion of eddy current flaw signals in relation to actual flaw depth. Line is a least-squares fit to the data.

Table 2. Results of inverting flaw measurements.

Specimen	Length (mm) Inverted	Length (mm) Actual	Depth (mm) Inverted	Depth (mm) Actual
NBS-2A	6.28	6.54	0.52	0.49
NBS-2B	7.01	7.07	1.72	1.51
NBS-2C	7.10	7.08	1.75	1.90
NBS-2D	7.13	7.08	2.40	2.46
NBS-3A	2.75	3.70	0.55	0.70
NBS-3B	3.55	3.82	0.82	0.95
NBS-3C	3.57	4.15	1.15	1.25
NBS-3D	4.05	4.20	1.05	1.44
NBS-4A	3.57	3.69	0.37	0.35
NBS-4B	4.30	3.85	0.66	0.64
NBS-4C	3.91	4.16	0.80	0.75
NBS-4D	4.54	4.20	1.05	0.92
NBS-5A	3.91	3.75	0.68	0.88
NBS-5B	4.25	3.90	0.95	1.17
NBS-5C	4.59	4.24	1.08	1.32
NBS-5D	5.02	4.27	1.80	1.88

we studied. Figure 5 plots inverted depth against the actual depth. The solid line in figure 5 is a least-squares fit to the data. The fact that the slope of this line is slightly less than 45° indicates a tendency for the method to slightly underestimate the depth of flaws. On the whole, however, there is excellent agreement between predicted and actual flaw dimensions. In most cases the variance was less than 20 percent.

Conclusions

A SQUID-based eddy current probe was used to obtain flaw signals from a number of EDM slots in Al 6061. The results indicated that the breadth of the flaw signal determined from the longitudinal scan of a flaw was proportional to the flaw length. The peak amplitude of the flaw signal was found to be proportional to cross-sectional area of the flaws. Empirical calibration curves relating these quantities were used to invert successfully the experimental data. The success of the simple inversion method used here indicates that this type of probe could be used to accurately size surface-breaking cracks with only a single calibration. Although the SQUID increased the magnitude of the response of the probe to a flaw by 80 dB, the main features of the flaw signal are related to the nature of the eddy current probe and not any special characteristics of the SQUID.

The authors are grateful to Dr. Leonard Mordfin of the NBS Office of Nondestructive Evaluation for his encouragement and interest in this work. We also gratefully acknowledge the contributions of S. Kleinbach and R. Benson in performing experiments and developing the software for data acquisition.

References

[1] Zimmerman, J. E., and A. H. Silver, Phys. Rev. **141** 367 (1966).

[2] Josephson, B. D., Advan. Phys. **14** 419 (1965).

[3] Giffard, R. P.; R. A. Webb and J. C. Wheatley, J. Low Temp. Phys. **6** 533 (1972).

[4] Zimmerman, J. E.; P. Thiene and J. T. Harding, J. Appl. Phys. **41** 1572 (1970).

[5] Sullivan, D. B., Superconducting quantum interference devices: an operational guide for rf-biased systems, NBS TN 629, November 1972, National Bureau of Standards, Boulder, CO.

[6] Fickett, F. R., and T. E. Capobianco, Review of Progress in Quantitative Nondestructive Evaluation 4, D. O. Thompson and D. E. Chimenti, eds. Plenum Press: New York p. 401 (1985).

[7] Capobianco, T. E.; F. R. Fickett and J. C. Moulder, in Review of Progress in Quantitative Nondestructive Evaluation 5, D. O. Thompson and D. E. Chimenti, eds. Plenum Press: New York p. 705 (1986).

[8] Capobianco, T. E.; J. C. Moulder and F. R. Fickett, in Proceedings of the 15th Symposium on Nondestructive Evaluation, D. W. Moore and G. A. Matzkanin, eds. Nondestructive Testing Information Analysis Center: San Antonio p. 15 (1986).

[9] Beisner, R. E.; C. M. Teller, G. L. Burkhardt, R. T. Smith, and J. R. Barton, in Eddy Current Characterization of Materials and Structures, ASTM STP 722, G. Birnbaum and G. Free, eds. American Society for Testing and Materials: Philadelphia p. 428 (1981).

[10] Auld, B. A.; G. McFetridge, M. Riaziat, and S. Jefferies, Review of Progress in Quantitative Nondestructive Evaluation 4, D. O. Thompson and D. E. Chimenti, eds. Plenum Press: New York p. 623 (1985).

Journal of Research of the National Bureau of Standards

Ideal Gas Thermodynamic Functions For Water

Volume 92 Number 1 January–February 1987

Harold W. Woolley

National Bureau of Standards
Gaithersburg, MD 20899

The calculation of ideal gas thermodynamic properties for steam to 10,000 K is examined. Centrifugal effects are included using spectroscopic data for the lowest vibrational levels, with extension to higher bending levels based on estimates from a bending model. Modifications are examined for rotational and vibrational cut-off effects. Uncertainties in obtaining a suitably regularized representation of energy versus bond stretching vibration in approaching the dissociation energy region appear relevant to the reliability of the extrapolation.

Key words: anharmonicities; centrifugal effects; ellipsoidal shell; Hamiltonian; semi-axes; vibrational states.

Accepted: October 27, 1986

Introduction

A calculation made in 1979 of the ideal gas thermodynamic properties for water [1][1] is the background for this study on improving the extrapolation to higher temperatures. The procedure under consideration is to calculate the internal partition function and its first two temperature derivatives, using direct summation over vibrational levels.

Direct summation was also used for the 1979 work. It was used not only for vibrational levels, but for rotational ones as well for temperatures up to 230 K. In the earlier work of Friedman and Haar [2], sums over vibrational levels were computed according to a procedure similar to that of Mayer and Mayer [3] for diatomic molecules. Such a formulation is in principle a low temperature form, analogous to a power series in increasing powers of temperature, and as such encounters questions of convergence in extension to very high temperature.

While it is not too difficult in such an approach to include effects of lowest order anharmonicities in their first power contribution, the inclusion of higher power contributions of even the lowest order of anharmonicities including cross product effects and rotational dependence is more complex. The extension to cover still higher order terms such as might satisfactorily describe the approach to the energy of dissociation would involve too many terms of cross product power type for easy confidence in the adequacy of their enumeration. There is in fact no formal end to the number of possible orders of the expansion, and each succeeding order would be enormously more complex than the one before it.

In the presentation that follows, the problem of the myriads of correction terms is circumvented by using direct summation over the three vibrational

About the Author: Harold W. Woolley, a physicist, retired from NBS some years ago but continues his affiliation with the Bureau as a guest worker in its Thermophysics Division, Center for Chemical Engineering.

[1]Figures in brackets indicate literature references.

quantum numbers for this triatomic molecule. The problems which remain are the physical ones of obtaining reliable energies for the vibrational levels and reliable rotational parameters, including the way in which the rotational energy behaves in the extension to high rotational quantum numbers.

1) As a first step, this last item is discussed with a study of an empirical bending model, including its implications as to bending energy.

2) The next topic to be covered is the implied centrifugal thermodynamic effect based on empirical constants fitting the spectroscopically-determined rotational levels as represented by a Watson Hamiltonian [4]. This applies to eight low lying vibrational levels, extending up to 5331 cm^{-1}.

3) Following this, the problem of extending the representation of rotational details to high energy and high temperature is considered, including the termination of rotational levels due to lack of bond stability.

4) Finally, considerations are introduced pertaining to a suitable extrapolation for energies of vibrational levels in approaching the dissociation region, a problem that is not regarded as solved.

The calculation range of new estimates for ideal gas thermodynamic functions for water is from 200 K to 10,000 K. It uses

$$Q=\sum_v Q_v \exp(-G_v hc/kT), \tag{1}$$

with v indicating all sets of values for v_1, v_2 and v_3 giving stable vibrational states. G_v is the vibrational energy in cm^{-1} units. Q_v is the rotational partition function for the given vibrational state. This is taken as

$$Q_v=Q_v^{\,0} f_v + dQ_v \tag{2}$$

with the usual semi-classical relation

$$Q_v^{\,0}=\pi^{1/2}(kT/hc)^{3/2}(A_vB_vC_v)^{-1/2}\sigma^{-1} \tag{3}$$

where the symmetry number σ is equal to 2 for the H_2O molecule. A_v, B_v and C_v are the principal rotational constants and dQ_v is a "low temperature" quantum correction such as that of Stripp and Kirkwood [5] as used in reference [1]. The centrifugal distortion and stretching effects are here represented by the factor f_v, related to the "Wilson [6] centrifugal effect constant ρ_v" by $f_v=\exp(h_v)$, where $h_v=\rho_v T$. The treatment of centrifugal effects for eight of the lowest vibrational levels is based on spectroscopic data interpreted with a Watson type rotational Hamiltonian. The extension to high bending quantum number is made on the basis of model estimates.

An examination is also made as to plausible magnitudes for effects of rotational cut-off in the dissociation region. Ad hoc adjustments in the approach to the dissociation energy region have been made to preserve approximate symmetry versus v_1 and v_3 quantum numbers.

For temperatures upward of 200 K, the data and empirical representations of Camy-Peyret et al. [7] could be used for seven vibrational levels above the ground state for which detailed parameters for rotational Hamiltonians are available. These include values for the principal rotational constants A_v, B_v and C_v, and for G_v, the energy for the vibrational level at zero rotation. Their reported values for G_v were used also for four other vibrational levels. Their G_v data for the (1,1,1) state were not used, as its partner in resonance, (0,3,1), had not apparently been similarly covered. A placement estimate for a (0,4,0) level based on a resonance shift from Benedict [8] was used to complete G_v values for the resonating triad including the (2,0,0) and (1,2,0) levels. For the ground vibrational state, however, the slightly differing results of the more recent analysis by Kyro [9] were accepted in the later calculations. The overall course of vibrational energies versus vibrational quantum number was taken to follow an empirical data fit by Benedict [8], but with some adjustment in the higher energy regions to be consistent with other data, such as dissociation and heats of reaction.

The Bending Model

On the basis of spectroscopic data it can be inferred that vibrational bending produces large effects on f_v and special effects on the total energy. The lack of extensive data and the impossibility of making reliable long range extrapolations of directly fitted polynomial representations of data have led to the present numerical exploration based on a simple bending model. For this, somewhat crude evaluations of WKBJ integrals have been used, based on an approximate bending potential.

The potential U is taken as the product of an empirical basic function U_0 and an empirical correction function U_c, as

$$U=U_0 \cdot U_c. \tag{4}$$

The basic function U_0 here involves two Lorentz type terms,

$$U_0=k_1/(q_1+x)+k_2/(q_2+x)-k_1/q_1-k_2/q_2 \tag{5}$$

with the correction function U_c taken as

$$U_c=(1+B_1x+B_2x^2+B_3x^3-B_4gx^4)$$

$$\div[1-B_4(g+1)x^4], \quad (6)$$

where $x=(\phi^2-\phi_e^2)/\phi_e^2$ with ϕ as the angle of bending of H-O-H out of a straight line as shown in figure 1. The even power of ϕ in the definition of x gives symmetry about the angle for full barrier height, at $\phi=0$. The subscript e refers to the equilibrium configuration.

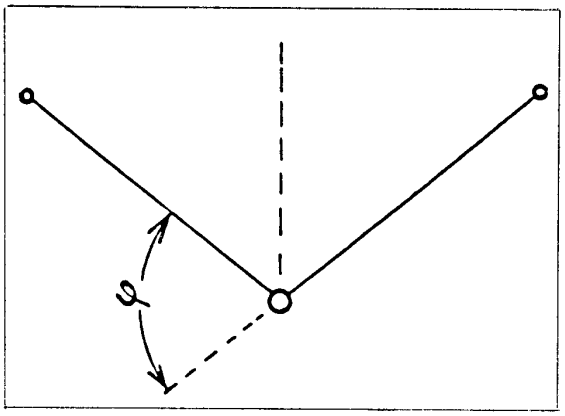

Figure 1–A schematic model of the water molecule.

The calculations were made with bonds of fixed length "d," taking the atoms as point masses. The quantum phase integral

$$v_2+1/2=m_H^{1/2}\,d\,h^{-1}\int_{\phi_{\min}}^{\phi_{\max}}[1-(1+\cos\phi)$$

$$\div(m_O/m_H+2)]^{1/2}\,[G-U(i)]^{1/2}\,d\phi \quad (7)$$

may be put in the form

$$v_2+1/2=(2^{1/2}/4\pi)(1+\cos\phi_e)^{-1/2}\int_{\phi_{\min}}^{\phi_{\max}}$$

$$\times[1-(1+\cos\phi)/(m_O/m_H+2)]^{1/2}$$

$$\times\{[G-U(i)]/B_e\}^{1/2}\,d\phi \quad (8)$$

for which conventional wave number energy units are convenient. The quantities m_O and m_H represent masses of the respective atoms.

In the absence of rotation, $U(i)$ is identical with U of eq (4). For rotation purely about the principal axes there are three cases:

$$(i=a): U(a)=U+J_a^2\,A_e(1-\cos\phi_e)/(1-\cos\phi)$$

$$(i=b): U(b)=U+J_b^2\,B_e(1+\cos\phi_e)/(1+\cos\phi)$$

$$(i=c): U(c)=U+J_c^2\,C_e[1+m_H(m_O+m_H)^{-1}$$

$$\cos\phi_e]/[1+m_H(m_O+m_H)^{-1}\cos\phi]. \quad (9)$$

Evaluations were made using cm^{-1} energy units, with

$$U_0=40266.9[1/(1-0.21507x)-1]$$

$$+13464.5[1/(1+0.6432x)-1] \quad (10)$$

and

$$U_c=(1-0.2467x-0.1526x^2+0.5678x^3$$

$$+1.3708x^4)/(1+1.7442x^4). \quad (11)$$

A value of 75.73 degrees was used for ϕ_e in adjusting between A_e and B_e indications of a preliminary data fit of Benedict [8].

Energy values on effective potential curves including rotation were approximated by

$$U(a)=U+20.24J_a^2/(1.0001-\cos\phi) \quad (12)$$

$$U(b)=U+17.97J_b^2/(1.0001+\cos\phi) \quad (13)$$

and

$$U(c)=U+9.5J_c^2/(1+0.0593\cos\phi) \quad (14)$$

where 0.0001 has been added in two of the denominators to avoid accidental division by zero.

Values of $v_2+1/2$ were computed at 17 to 40 suitably spaced values for energy "E" or "G" up into the 100,000 cm^{-1} region for these three cases of rotation about the principal axes, for several values of each J_i^2 ranging from zero to 400 in the "a" and "c" cases and somewhat further in the "b" instance. Four point Lagrangian interpolation was then used to obtain energies corresponding to integer v_2 values at each of the chosen J_i^2 values. Effective values for the principal rotational constants were estimated according to

$$A_v=(E_{Ja}-E_0)/J_a^2 \quad (15)$$

$$B_v=(E_{Jb}-E_0)/J_b^2 \quad (16)$$

$$C_v=(E_{Jc}-E_0)/J_c^2. \quad (17)$$

Figures 2, 3, and 4 show results from these calculations. Extrapolation to zero rotation appears reliable for B_v and C_v and for A_v for v_2 small.

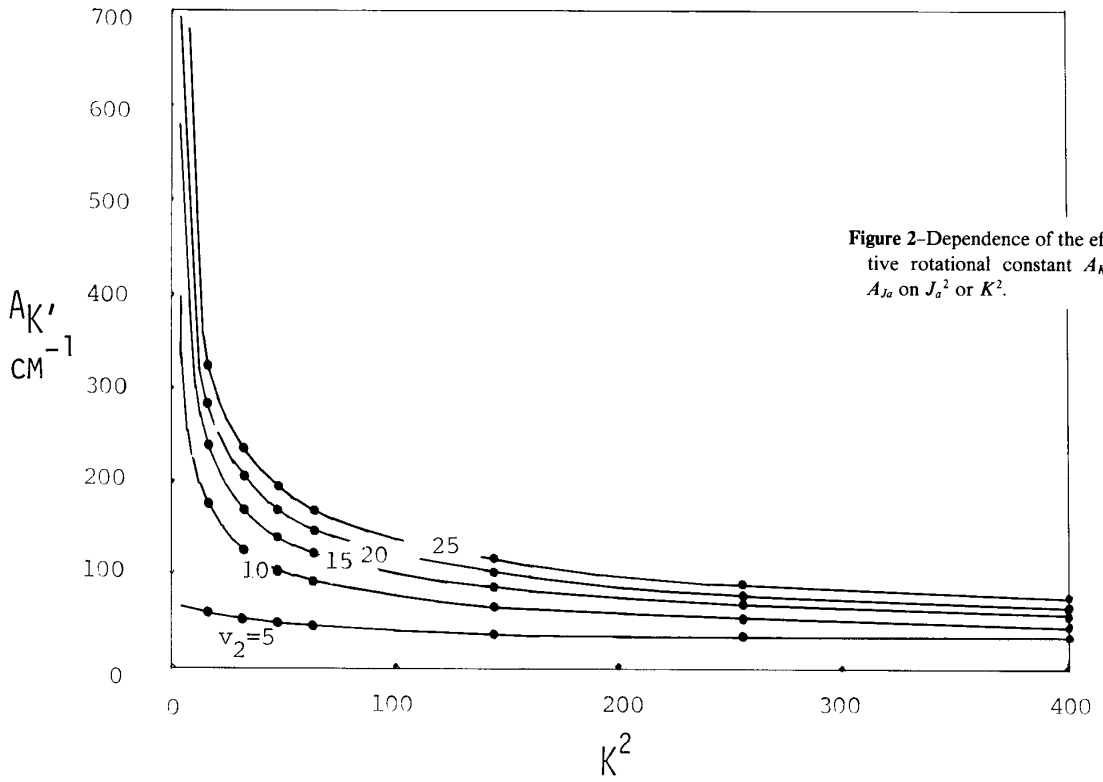

Figure 2–Dependence of the effective rotational constant A_K or A_{Ja} on J_a^2 or K^2.

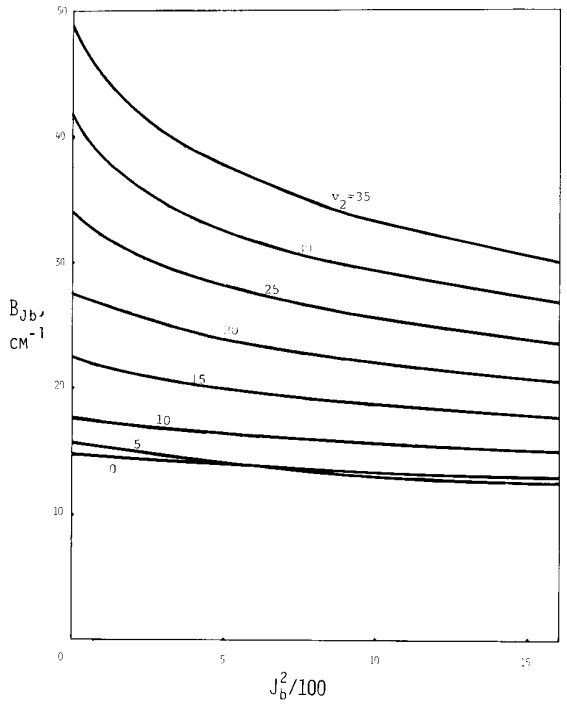

Figure 3–Dependence of the effective rotational constant B_{Jb} on J_b^2.

Estimates for the centrifugal effect contribution associated with rotation about separate principal axes were obtained in the following way. In the case of the "B" rotation, for example, and empirical representation for B versus J_b^2 was used for each of various v_2 values. Numerical quadratures were performed for a partition function contribution as

$$(Q)_B=\int_0^\infty \exp(-\beta B J_b^2)\, dJ_b \tag{18}$$

for various temperatures where $\beta=hc/kT$. This determined an effective B according to

$$B_{\text{eff}}=\pi/(4\beta (Q)_B^2). \tag{19}$$

The corresponding contribution to the Wilson centrifugal effect constant then followed as

$$(\rho_{\text{eff}})_B=(2T)^{-1}\ln(B_0/B_{\text{eff}}). \tag{20}$$

A similar procedure was used for the "A" rotation. No appreciable contribution came from the "C" case.

The combined contributions to the Wilson centrifugal effect constant based on the rigid bender model are shown in figure 5 for values of v_2 ranging

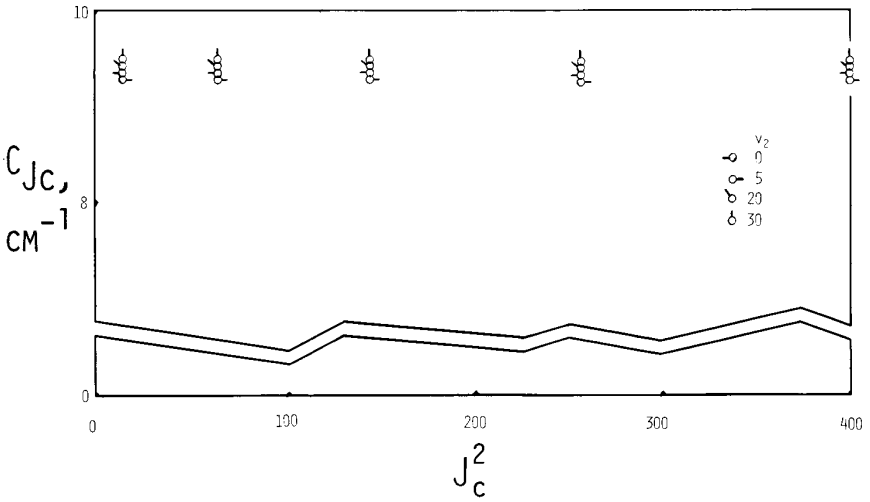

Figure 4–Effective values for the rotational constant C_{Jc}.

by unit steps from 4 to 9 and also for 10, 15, 20, 25, and 35. (The sizes of symbols in the figure are not intended to indicate relative importance of the plotted values.) Corresponding curves are shown for the empirical representation

$$10^5\rho=(b_0+b_1t+b_2t^2)/(1+d_1t+d_2t^2), \qquad (21)$$

where $t=T/1000$. For these, the numerical parameters that follow are based on combined estimates as from eq (21), fitted approximately by inspection and graphical processes. With v representing v_2, the constants b_i and d_i were taken as

$$b_0=2.2616(1+0.242v+0.037v^2+0.00083v^3)$$
$$\div(1-0.0175v+0.0033v^2)+8/[1+0.8(v-7.3)^2]$$

$$b_1=1/\{.122+[-1.6+1$$
$$\div(0.31+0.02v+0.0019v^2-0.000028v^3)]^2\}$$

$$b_2=1/[1.3+0.106(12-v)^2+(1E-06)(12-v)^6$$
$$+(2E-08)(12-v)^8]-1/[5+14.3(8.3-v)^2]$$

$$d_1=12.6/[35.+(v-5)^2]$$

$$d_2=3./[25.+(v-11)^2]$$

as an approximate representation of the calculated values.

Values for A_v, B_v, and C_v as interpreted via data of figures 2, 3, and 4 are shown in figures 6, 7, and 8 by solid circles. The solid curves are from a fit of spectroscopic data by Benedict [8] running up to $v_2=4$, with v_1 and v_3 also extending up to 4.

The x's in figure 6 show individual estimates at the quantum number $K=1$, indicating that for A_v extrapolation above $v_2=7$ encounters some imperfection in the traditional representation.

The dashed curves in figures 6, 7, and 8 are given respectively by

$$A=27.8847\Big(1+\{0.0895v+0.0228v^2+(0.0022v^2$$
$$+0.00012v^3-0.000185v^4+0.35E-04v^5$$
$$-0.7E-06v^6)/[(1-0.17v+0.008v^2)$$
$$\times(1-0.15v+0.007v^2)^2+1E-06v^5]\}\Big) \qquad (22)$$

$$B=14.5118\{(1.0012771+0.05266v+0.00779v^2)$$
$$\div(1+0.04v+0.008v^2)+(2.51E-08v^3+6.4E$$
$$-06v^4+6.3E-06v^5)/(1+0.04v+0.008v^2)$$
$$+0.009(v-7)/[(0.00032)^2+(v-7)^2]\} \qquad (23)$$

$$C=[9.2806+0.0073v(v-1)]/(1+H+H^2+H^3) \qquad (24)$$

with $H=0.1473v/9.2806$, where v represents v_2.

The expressions for A_v and B_v are roughly representative of the directly indicated model results as shown by the solid circles. For C_v, the equation here is basically a rearrangement of Benedict's equation, although the model results suggest that a different curve might be better.

The open circles show values that have been adjusted from the solid circles according to an allowance for bond stretching based on OH bond data. The effects may be summarized in part as due

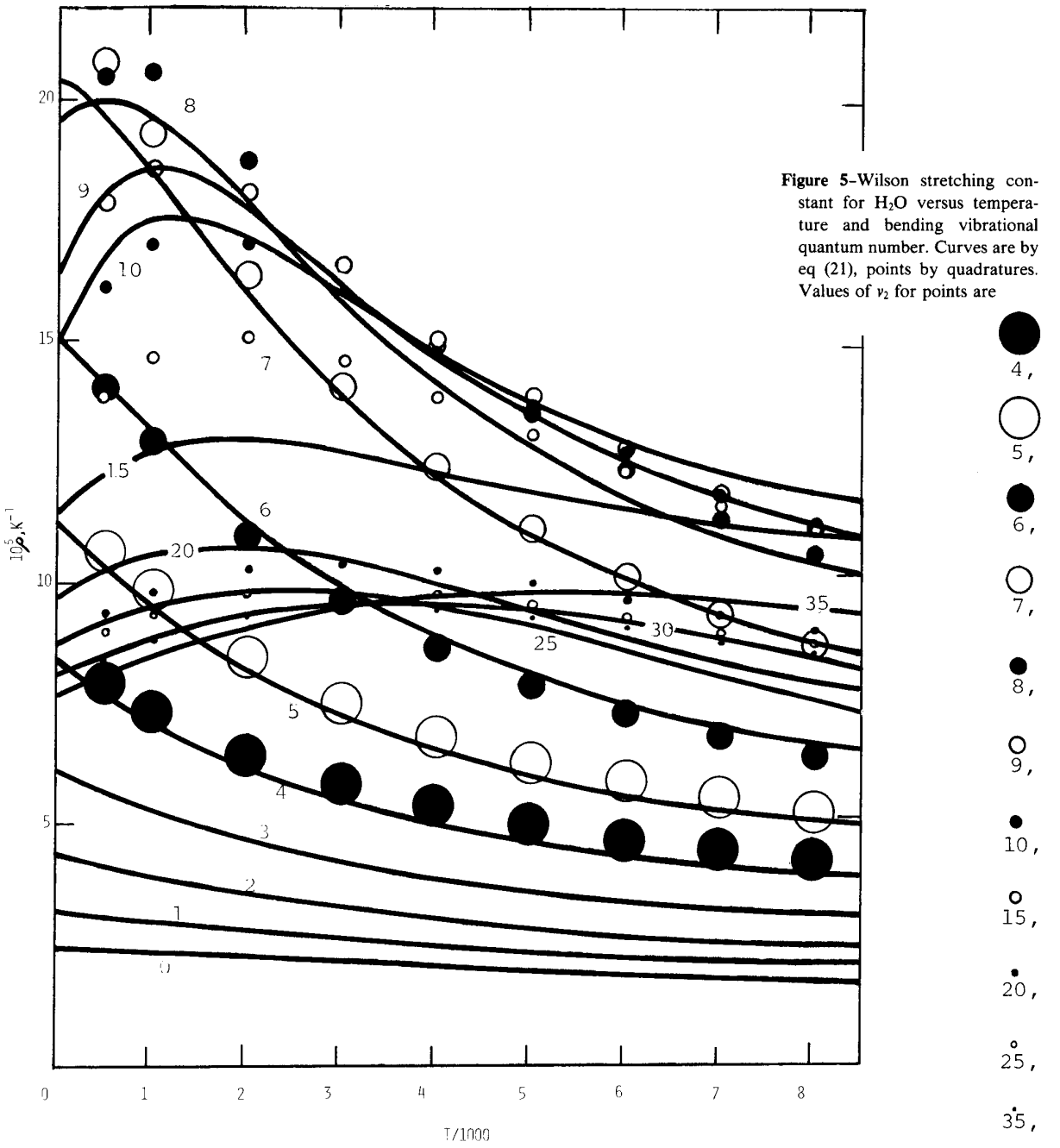

Figure 5–Wilson stretching constant for H_2O versus temperature and bending vibrational quantum number. Curves are by eq (21), points by quadratures. Values of v_2 for points are

to the "effective" v_2 value, v_2 (eff), being less than the true v_2 in accord with

$$v_2(\text{eff}) = v_2/[1+(1.60E-03)v_2+(6.12E-05)v_2^2 - (5.81E-07)v_2^3+(9.7E-09)v_2^3]. \quad (25)$$

This causes the adjusted value for the "true" v corresponding to each model estimate to occur for a larger value than the v (eff). The change in bond length also reduces the magnitudes of principal rotational constants from the model according to the square of the same ratio.

An indication via the bending model as to the dependence of vibrational energy on the v_2 quantum number is also given directly by the $v_2+1/2$ values versus E_0 values from the WKBJ integrals with $J_i^2=0$. The results are shown graphically in figure 9 by the large open circles, obtained directly using the bending model without any bond stretching allowance. Ad hoc adjustments for bond

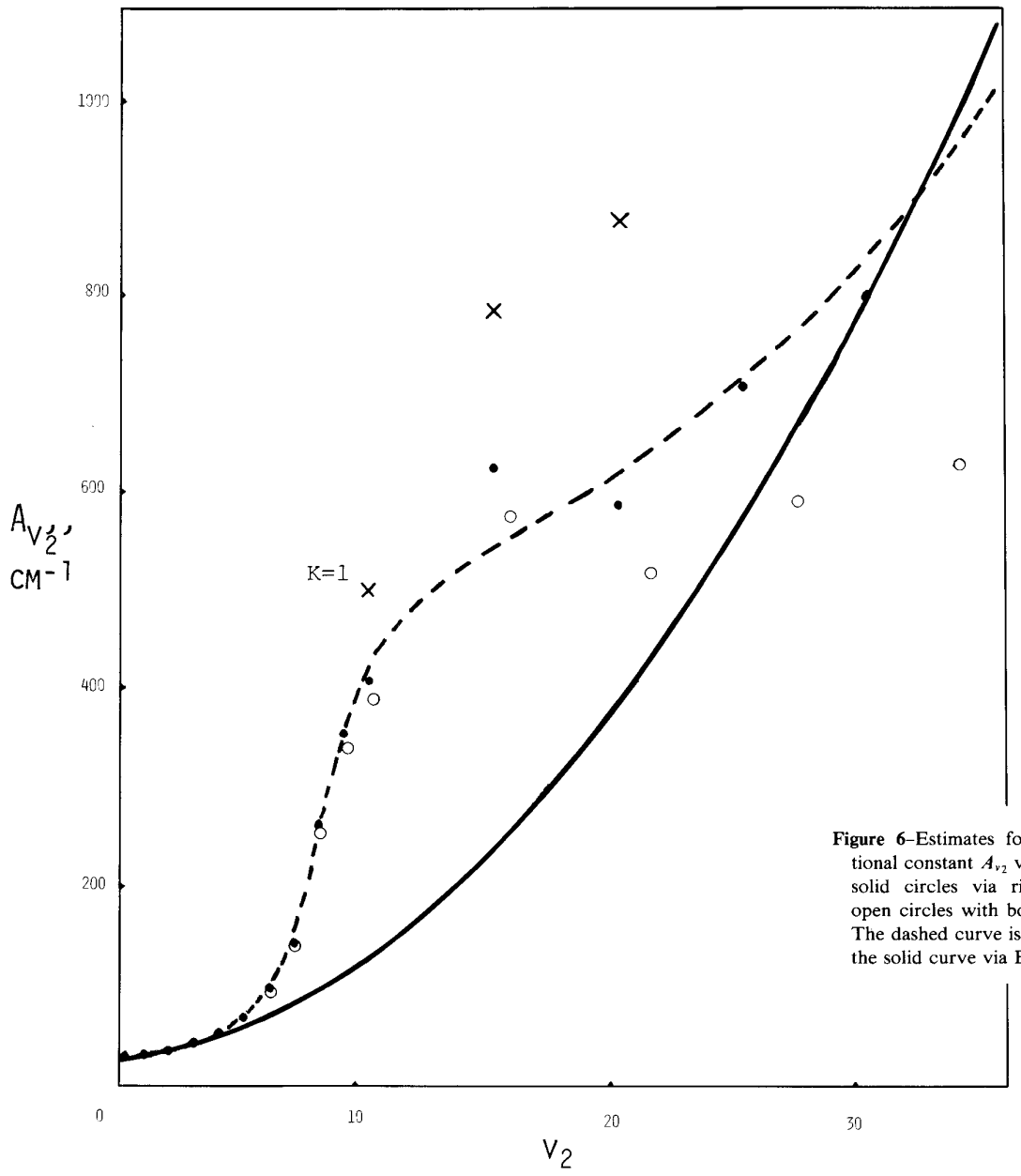

Figure 6–Estimates for the rotational constant A_{v_2} versus v_2 — solid circles via rigid bonds, open circles with bond stretch. The dashed curve is by eq (22), the solid curve via Benedict.

stretching were then taken from $v_2+1/2$ differences between the small open circles for free rotation without bond stretch and the small solid circles for free rotation with bond stretch obtained with bond data transferred from the OH bond of the OH diatomic molecule.

As to the curves of figure 9, the one labelled "a" is for three terms in v_2 when $v_1=v_3=0$, from a fit by Benedict with Σv_i's up to 4. Curve "c," as

$$G=1608.034v_2-11.748v_2^2-1.643v_2^3+0.0937v_2^4, \quad (26)$$

is obtained versus v_2 alone from basically the same data with a fourth term included in the fitting. Curve "b," used in the ideal gas calculations of 1979 [1], was obtained from "a" by adding the two terms

$$0.05v_2(v_2-1)(v_2-2)(v_2-3)$$

$$-0.00051v_2(v_2-1)(v_2-2)(v_2-3)(v_2-4).$$

Curve "d" is represented by a rational function with coefficients chosen to fit the large open circles

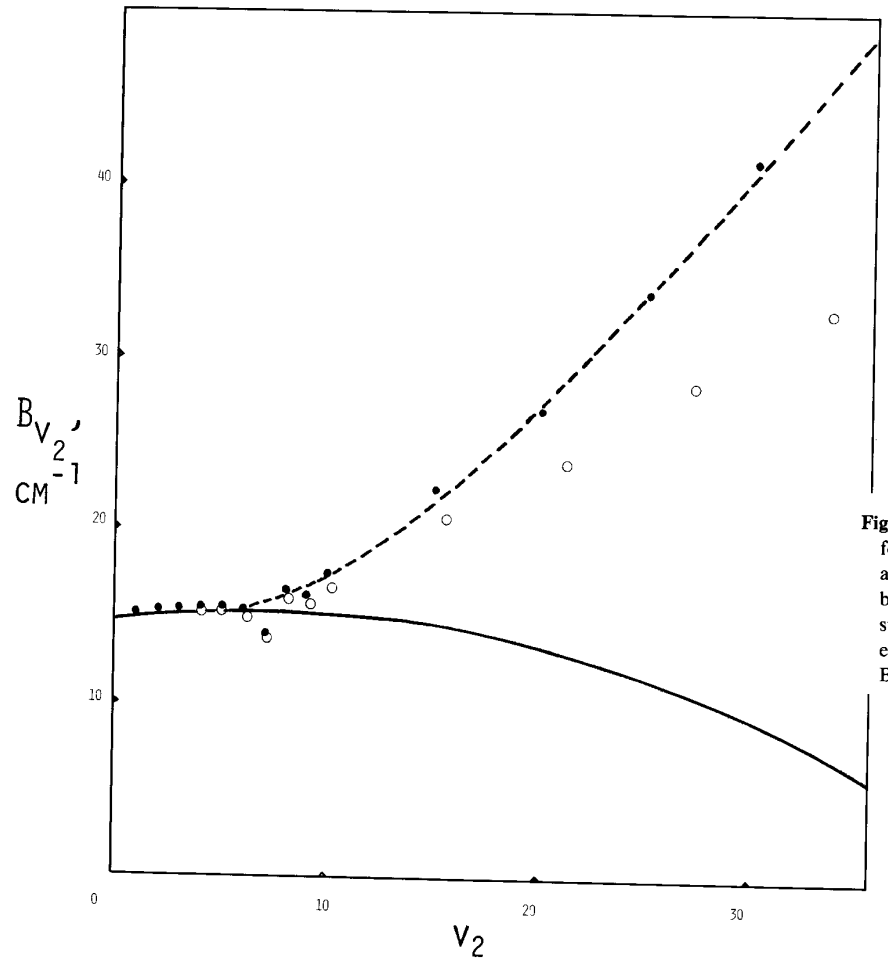

Figure 7–Rotational constant B_{v_2} for rotation about intermediate axis – solid circles via rigid bonds, open circles with bond stretch. The dashed curve is by eq (23), the solid curve via Benedict.

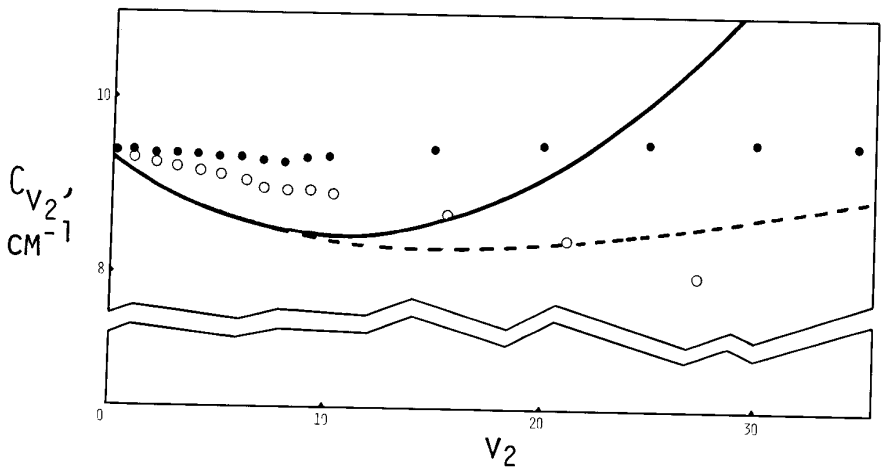

Figure 8–Estimates for the rotational constant C_{v_2} versus v_2 solid circles via rigid bonds, open circles with bond stretch. The dashed curve is by eq (24), the solid curve via Benedict.

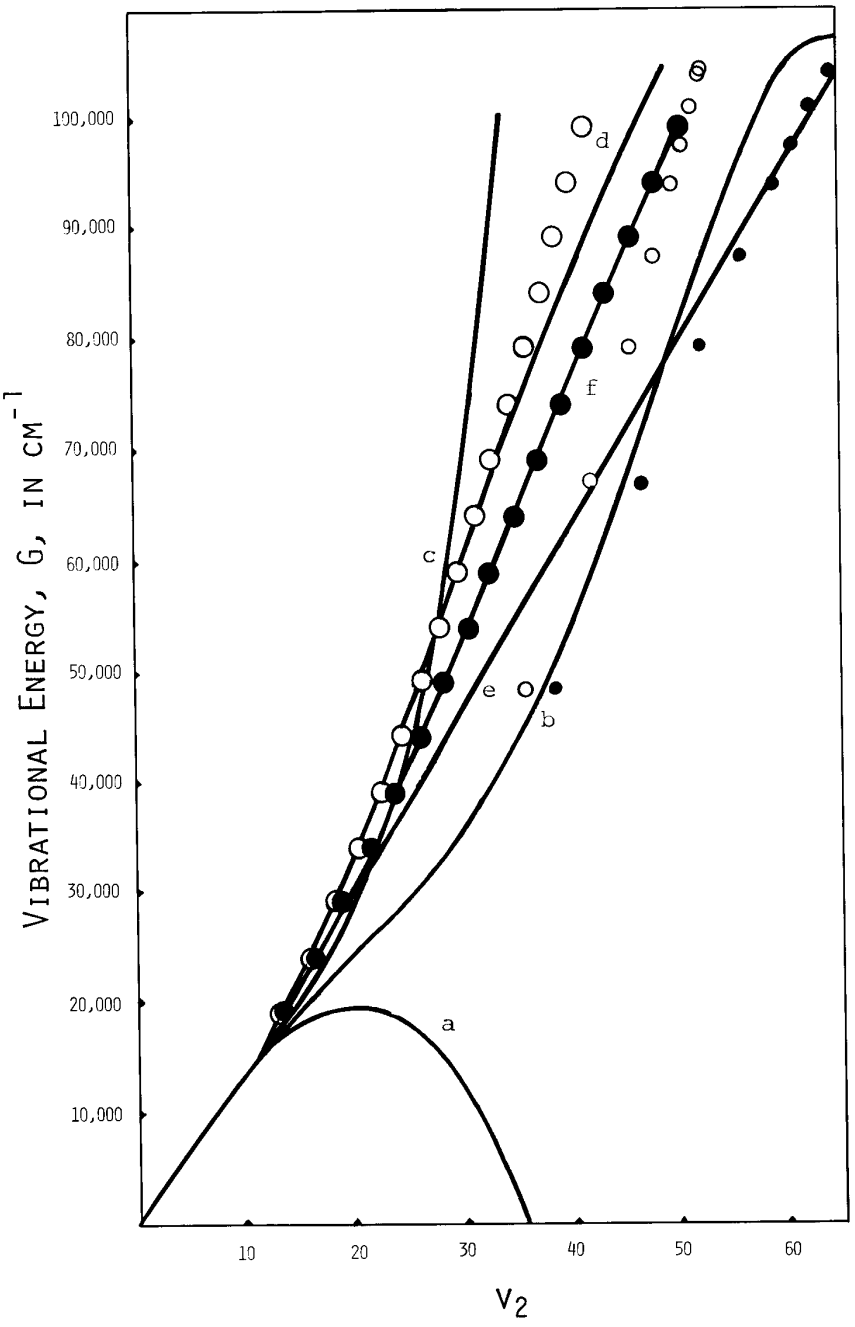

Figure 9–Vibrational bending energy, Small circles: free rotation. Large circles: with bending potential. Open circles: rigid bonds. Solid circles: with bond stretch. Curves: (a) 3 term; (b) with 2 terms added to (a); (c) 4 term fit, eq (26); (d) rational function; (e) for (d) with stretch; (f) combined locus, eq (27).

from the potential model without bond stretch. Curve "e" is also by a rational function, but fitted only to the large solid circles at low quantum number. The last curve, "f," involves a combined locus asymptotic to a rational function curve at low v_2 and to a straight line at large v_2. It is given by

$$G=(a+b)/2+[(a-b)^2+4c^2]^{1/2}/2-d \qquad (27)$$

where $a=2300(v-7)$, $c=1600$, $d=157.4661132$, and $b = 1601.337v(1 - 0.4105368v + 0.0706926v^2 - 0.006001528v^3+0.0002295548v^4)\div(1-0.4028641 v+0.06850098v^2-0.005819278v^3+0.0002301345v^4)$ where v represents v_2. It is this curve that represents values used in the present calculation of thermodynamic functions.

In comment on the many digits used for these constants, this is to be attributed not to any extreme accuracy, obviously, but at least in part to a regard for correlation between coefficients and to a desire to retain significance in difference type effects.

It is perhaps well to admit at this point that great accuracy is not claimed for the bending potential used. The application of the bending model is seen as quite successful, however, in providing a clear indication of the rather moderate magnitude of change in distant extrapolation as compared with the results for free rotation. Still, the uncertainty in these extrapolations must be very appreciable.

Centrifugal Data

As shown in an earlier publication [1], the effects on the rotational partition function for a given vibrational state due to centrifugal distortion and bond stretching may be obtained in semi-classical approximation from the integral

$$Q=8\pi^2 h^{-3}\int_{-\infty}^{\infty}\int\int \exp(-H/kT)dP_x\, dP_y\, dP_2 \quad (28)$$

with $H=hc(W_0+\mathrm{H}_1)$, where $W_0=\Sigma B_i P_i^2$ and where H_1 represents the remaining part of the Watson-type rotational Hamiltonian. This uses $B_1=C_v$, $B_2=B_v$ and $B_3=A_v$, the principal rotational constants, with $P_1=P_x$, $P_2=P_y$ and $P_3=P_z$.

The present application of the method has been carried to the evaluation of five coefficients versus temperature. In the 1979 application of the method, the evaluation was made to three coefficients, only. The hope was that the added detail would provide a better overall representation of thermal effects implied by the spectroscopic data.

There may typically be about 20 to 30 terms in current realizations of H_1, involving coefficients of various powers or products of powers of $P^2=P_x^2+P_y^2+P_z^2$, "P_{xy}^2"$=P_x^2-P_y^2$, and P_z^2. The factor $\exp(-hcH_1/kT)$ may be expanded as a Taylor series in powers of H_1. With 20 terms in H_1, running generally up to the 10th power in P_i's, but with a 12th power in P_z, there are found to be 98 terms in H_1^2 and 35 in H_1^3 in the range through the 12th power in P_i. When the terms in p^2 and P_{xy}^2 are expanded in powers of P_x^2, P_y^2 and P_z^2, the number of separate terms to use in evaluating Gaussian integrals becomes quite large. For each, the integrand is a product over $i=1$, 2, and 3 of $P_i^{2n_i}\exp(-hcB_iP_i^2/kT)$. As a result, each separate term is of the form

$$Q_v=Q_v^0\prod_{i=1,2,3}F(n_i)\,(kT/hcB_i)^{n_i} \quad (29)$$

where $F(n_i)=2^{-2n_i}(2n_i)!/n_i!$. Q_v^0 is for a classical rigid rotator for the level (v_1, v_2, v_3), symbolized by "v" as indicated earlier. The $F(n_i)$ constants are simple fractions that are functions of n_i such as $F(0)=1$, $F(1)=1/2$, $F(2)=3/4$, $F(3)=15/8$, $F(4)=105/16$, $F(5)=945/32$, $F(6)=10395/64$, etc.

A computer program has been arranged for carrying out the preparation of the correction factor as a series in powers of temperature using the empirical constants of the Watson-type Hamiltonian. With terms up to the 5th power of H_1 covered, the corresponding coefficients are computed to give the logarithm of the correction factor as a series

$$h_v=\rho_0 T(1+a_1 T+a_2 T^2+a_3 T^3+a_4 T^4). \quad (30)$$

In practical application, this has not appeared to provide a well-behaved form when used for moderately high temperatures. Accordingly, the program next computes the corresponding coefficients in a Padé approximant or rational function form,

$$h_v=\rho_0 T(1+c_1 T+c_2 T^2)/(1+d_1 T+d_2 T^2),$$

or

$$h_v=(b_0 T+b_1 T^2+b_2 T^3)/(1+d_1 T+d_2 T^2). \quad (31)$$

The coefficients in the Padé form follow from those preceding according to the relations

$$d_1=(a_1 a_4-a_2 a_3)/(a_2^2-a_1 a_3)$$

$$d_2=(a_3^2-a_2 a_4)/(a_2^2-a_1 a_3)$$

$$c_1=a_1+d_1$$

$$c_2=a_2+a_1 d_1+d_2.$$

The Padé form appears to be much better adapted to computation in ordinary circumstances. For some higher vibrational states, however, there can still be complications such as the occurrence of negative values for the coefficients c_2 and d_2 which are for the highest powers of T. Happenings of this type appear to be somewhat dependent on the source of the empirical Hamiltonian constants used.

The program is interactive in asking for values for the principal rotational constants, A, B, and C, and then for the highest power of temperature to be covered (up to 6 as set up). It then asks progressively, in a selected order for values for 30 coefficients in the Watson Hamiltonian, identifying each by a coefficient name in "string-variable" form, e. g., DELJ, etc. These happen to be in the order shown schematically by:

H=−DELJ*J**4−DELJK*JZ**2*J**2

−DELK*JZ**4−2*SDLJ*JXY**2

```
-SDLK*(JZ**2*JXY**2
+JXY**2*JZ**2)+HJ*J**6
+HJK*JZ**2**J**4+HKJ*JZ**4*J**2
+HK*JZ**6+2*SHJ*JXY**2*J**4
+SHJK*(JZ**2*JXY**2
+JXY**2*JZ**2)*J**2
+SHK*(JZ**4*JXY**2+JXY**2*JZ**4)
+CLJ*J**8+CLK*JZ**8
+CLKKJ*JZ**6*J**2
+CLJK*JZ**4*J**4+CLJJK*JZ**2*J**6
+2*SLJ*JXY**2*J**6
+SLK*(JZ**6*JXY**2+JXY**2*JZ**6)
+SLKJ*(JZ**4*JXY**2
+JXY**2*JZ**4)*J**2
+SLJK*(JZ**2*JXY**2
+JXY**2*JZ**2)*J**4+CPK*JZ**10
+CPKKJ*JZ**8*J**2
+CPKJ*JZ**6*J**4
+SPK*(JZ**8*JXY**2+JXY**2*JZ**8)
+Z12*JZ**12+Z10P2*JZ**10*J**2
+Z14*JZ**14+Z16*JZ**16
+Z18*JZ**18,                    (32)
```

where J**2 is JX**2+JY**2+JZ**2 and JXY**2 is JX**2−JY**2.

Values for the Padé constants as obtained from the available Watson Hamiltonian constants for the eight observed vibrational levels, based largely on the work of Camy-Peyret and Flaud [7] are given in table 1.

A listing of the program is included in the appendix. Further discussion of the results will be reserved for a later section dealing with table comparisons.

Rotation at High Temperature

While the Padé form for centrifugal effect seems better adapted for calculation than the simple power series form which encounters convergence problems of an erratically varying sign type, there are other consideration if extrapolation to very high temperature is required.

The rotational quantum numbers can increase up to some limiting large values as "J_a," "J_b," or "J_c," beyond which centrifugal force would cause the molecule to break apart by bond rupture. The limiting rotational energy for rotation about any principal axis would be of a general magnitude indicated by

$$D_R = B_i J_i^2 \tag{33}$$

where B_i refers to A_v, B_v or C_v, according to the axis involved. However, the affected moment of inertia at bond rupture would be appreciably increased by bond stretching over its ordinary value. A semi-classical OH bond model study on the principal rotational constants at zero vibration suggests that the ratio "r" between principal constants at maximum versus at low rotational quantum number should be about 0.195 as r_A for A, 0.260 as r_B for B, and 0.310 as r_C for C.

Table 1. Constants for low-lying vibrational states from Watson-type Hamiltonian data.

(v)	Gv	Av	Bv	Cv	b0	b1	b2	d1	d2
000	0000.0000	27.8806	14.5216	9.2777	2.4518	3.5538	1.0949	1.5266	0.5377
010	1594.7450	31.1284	14.6875	9.1291	3.2111	2.1258	1.0101	0.7945	0.3886
020	3151.6301	35.5867	14.8415	8.9745	4.3691	−.7474	3.1192	.01296	0.7349
100	3657.0532	27.1222	14.3048	9.1046	2.4668	−1.0581	0.6651	−.3572	0.2392
001	3755.9296	26.6480	14.4313	9.1382	2.4097	−.8892	0.5480	−.3130	0.2144
030	4675.1750	42.1323	14.9714	8.8350	6.8534	−4.9258	10.668	−.3500	1.5033
110	5226.5870	30.1712	14.4139	8.9520	3.1892	−1.0880	1.8797	−.2125	0.5829
011	5331.2798	29.5226	14.6136	8.9931	3.0160	−.6923	1.1666	−.1653	0.4035

This includes Padé type Wilson centrifugal effect parameters $B(I)$ and $D(I)$ for $\exp(\rho T)$, where

$\rho = \{B(0)+T^*[B(1)+T^*B(2)]\}/\{1+T^*[D(1)+T^*D(2)]\}$, with $B(0)=b0/1.0E+5$, $B(1)=b1/1.0E+8$, $B(2)=b2/1.0E+11$, $D(1)=d1/1.0E+3$, $D(2)=d2/1.0E+6$

This leads to the interesting inference that if a limiting partition function would be equal to the "volume" of an ellipsoid with semi-axes J_a, J_b and J_c, one may estimate the volume as

$$Q_M=(4/3)\pi\sigma^{-1}(D_R/A_v)^{1/2}(D_R/B_v)^{1/2} \times(D_R/C_v)^{1/2}\,\mathrm{R} \tag{34}$$

where R, the factor of centrifugal increase, is estimated as

$$R=(\mathrm{r}_A\,\mathrm{r}_B\,\mathrm{r}_C)^{-1/2}=8.0 \tag{35}$$

for low vibrational states. For high vibrational states, where little additional rotational energy is needed to bring about bond breaking, the ratio needed may be much nearer to unity. A form

$$R=[1+(R_0-1)(D_v/D_0)^s] \tag{36}$$

with $R_0=8.0$ and possibly $s=1$ may be a useful speculation as to plausible behavior. Here D_v is the additional energy D_0-G_v to reach dissociation for the vibrational state without rotation.

As to acceptable values for D_R for higher vibrational states, it appears useful, with D_M as dissociation energy including rotation, to note that by a logarithmic plot of $y=(D_M-D)/D$ versus $x=(D-G_v)/D$ for the OH diatomic potential, an approximate representation is $y=(2/9)x^{7/8}$. Estimates of a similar magnitude can also be found from the expression $y=(1/4)x$, which is a form easier to use. The latter choice provides an approximate relation $D_R=D(x+y)$, or $D=D-G_v+(D-G_v)/4=1.25(D-G_v)$.

As in the discussion leading to eq (34), an estimate for the rotational partition function may be based on an integral using an ellipsoidal shell with semi-axes $\hbar(E/A)^{1/2}$, $\hbar(E/B)^{1/2}$ and $\hbar(E/C)^{1/2}$. The "volume" of the shell between energies hcE and $hc(E+dE)$ is $2\pi\ \hbar^3\ (ABC)^{1/2}\ E^{1/2}\ dE$. In the evaluation of density of states as measured by $\prod_1^3 (h^{-1}\,dp_i\,dq_i)$, there is a factor 4π for orientation of the total momentum vector and 2π for position of the rotator in making one revolution. Thus the number of states available within the energy shell needs the factor $8\pi^2h^{-3}$ to be included, giving

$$dN=2(ABC)^{-1/2}\,E^{1/2}\,dE. \tag{37}$$

An additional factor $f=(1+\Sigma r_iE^i)$ may represent the increase due to centrifugal effects. Integration to infinite energy gives

$$Q_R^\infty=\int dQ_R=2(ABC)^{-1/2}\int_0^\infty \exp(-hcE/kT) \times(1+\Sigma r_iE^i)E^{1/2}\,dE \tag{38}$$

or

$$Q_R^\infty=2(kT/hc)^{3/2}(ABC)^{-1/2}\int_0^\infty \exp(-x)\,x^{1/2} \times[1+\Sigma r_i(kT/hc)^i\,x^i]dx \tag{39}$$

The result is

$$Q_R^\infty=\pi^{1/2}\,(kT/hc)^{3/2}(ABC)^{-1/2} \times[1+(3/2)\mathrm{r}_1(kT/hc)+(3/2)(5/2)\mathrm{r}_2(kT/hc)^2 +(3/2)(5/2)(7/2)\mathrm{r}_3(kT/hc)^3+\ldots] \tag{40}$$

Using $\mathrm{r}_i=\{\prod_{j=1}^{i}[2/(2\mathrm{j}+1)]\}e_i$, this may be identified with eq (41)

$$Q_R^\infty=\pi^{1/2}(kT/hc)^{3/2}(ABC)^{-1/2}[1+\Sigma e_i(kT/hc)^i]. \tag{41}$$

The last factor is f_v or $\exp(\rho T)$ for centrifugal effects according to eq (2).

If the integration is extended only to a rotational energy $E=D$, or for x to $x=hcD/kT$, the result for each term involves an incomplete gamma function.

$$Q_R^\infty=2(kT/hc)^{3/2}(ABC)^{-1/2}[\gamma(3/2,x_1) +\Sigma\mathrm{r}_i\gamma(i+3/2,x_1)(kT/hc)^i]. \tag{42}$$

The recurrence relation $\gamma(a+1,x)=a\gamma(a,x)-x^a\exp(-x)$ is used to relate all later terms to the first one. Values can be found for $\gamma(3/2,x)=(\pi^{1/2}/2)\,H(z)-z\exp(-z^2)$, where $x=z^2$, using $H(z)=1-\pi^{-1/2}\exp(-z^2)(z+0.2)z1^4[1-z1^4(2.5803-2.8136\ z1+4.0745\ z1^2-1.2142\ z1^3+1.1657\ z1^4-0.0091\,z1^5)]$, where $z1=1/(z+0.1)^{1/2}$.

The result for a given rotational state may be written as

$$Q_R{}^D=Q^0(Q_xf_v-Q_s) \tag{43}$$

with $Q^0=\pi^{1/2}(kT/hc)^{3/2}(A_vB_vC_v)^{-1/2}\,\sigma^{-1}$, as for a rigid rotator, σ being the symmetry number, with

$$Q_x=2\pi^{-1/2}\gamma(3/2,x_1)$$

and with f_v representing $\exp(\rho T)$ as in eq (2) or as used for Q_R^∞. Thus f_v might be used in any form that would appear suitable, such as with a Padé approximant, if acceptable. Q_s is a residual quantity

$$Q_s = 2\pi^{-1/2} x_1^{1/2} \exp(-x_1) \Sigma e_i (kT/hc)^i \times \left(\sum_{m=1}^{i} \{ \prod_{j=1}^{m} [2/(2j+1)] \} x_1^m \right),$$

a form capable of further examination.

As a variant study based on the derivation leading to eq (38), one may remove the Boltzmann factor $\exp(-hcE/kT)$ and consider the integration up to an energy E.

$$Q^E = 2(A_v B_v C_v)^{-1/2} \int_0^E (1 + \Sigma e_i E^i) E^{1/2} \, dE. \qquad (44)$$

This was tried on the ground state and some others. Conversion of the polynomial to a Padé-Wilson exponential form

$$f' = \exp[(b0\,E + b1\,E^2 + b2\,E^3) \div (1 + d1E + d2\,E^2)] \qquad (45)$$

quieted a term-wise sign fluctuation effect. However, in extension to very large E, a condition of excessively large computed Q^E was encountered. This was due to the exponential factor becoming grossly over-sized. For the ground state, as E rises from $1.E+5$ to $1.E+6$ cm^{-1}, the computed centrifugal factor rises from 6.5 to over $1.E+7$. This result is contrary to the previous estimate of a limit for the centrifugal factor of the order of $R = 8$ or less, as in eq (36). The catastrophe can obviously be avoided by enlarging the denominator by including a term $d3\,E^3$, with the ratio $b2/d3$ near to 2 or to $\ln R$.

Logically, the parameters should be chosen again in such a way that the expansion into a power series would remain unchanged through the first five coefficients. If s represents $b2/d3$, and with $B1$, $B2$, $D1$ and $D2$ to represent original values of $b1$, $b2$, $d1$ and $d2$, respectively, the revised coefficients can be obtained from

```
s1=b1**3-2*b0*b1*b2+b0**2*b2*d1
   -b0*b1**2*d1+b0**2*b1*d2
s2=b0*b1*d1*d2-b1**2*b2-b0*b2*d1**2
   -b1*b2*d1+2*b0*b2*d2-b2**2
   -b0**2*d2**2
b2=B2/[1+(s1/s2)/s]
d3=b2/s
d2=b2*(D2-b1/s)/B2
d1=[b2*(D1-b0/s)-d2*B1
   +D2*(B1-b0*D1)]/(B2-b0*D2)
b1=B1-b0*D1+b0*d1
```

With parameters so modified, the computed centrifugal factor for the ground state at $1.E+5$ and $1.E+6$ reciprocal centimeters showed reductions to 2.73 and 6.54, respectively.

The same type of control adjustment should apparently be applicable to the Padé form in terms of temperature in a normal computation. However, in actual application to a multitude of levels, there could seem to be a possibility that the final Padé constants might not always be positive, due to numerical accident. A requirement that $d3$ and $b2$ be positive can be met by using the absolute value of $B2$ for $b2$, with $d3 = b2/s$. The other parameters follow from

```
b0=B0
b1=[(B1**2-B0*B2)*(B1-B0*D1)
   -B0*B1*(B2-b2-B0*D2)
   +B0**2*(B0*d3-D1*b2)]/DEN
d1=[(B1*D1-B0*D2)*(B1-B0*D1)
   -B1*(B2-b2-B0*D2)+B0*(B0*d3
   -D1*b2)]/DEN
d2=[(B1*D2-B2*D1)*(B1-B0*D1)
   +(B2-B0*D2)*(B2-b2-B0*D2)
   +(B0*D1-B1)*(B0*d3-D1*b2)]/DEN
```

with $DEN = (B1^{**}2 + B0^{**}2 * D2 - B0 * B2 - B0 * B1 * D1)$.

This might preserve only four instead of five coefficients of the series leading to a Padé development and no absolute guarantee is known to exist against occurrence of a zero denominator.

Another simple scheme for keeping the rotational Q below the limiting Q_M value for a given vibrational level has been patterned after the familiar relation of a hyperbola to its asymptotes represented as a combination of loci. With Q_M as an excessive rotational partition function without cut-off, an estimate with cut-off included might be

$$Q=(1/2)(Q_M+Q_r)-(1/2)[4qQ_rQ_M + (Q_M-Q_r)^2]^{1/2}. \quad (46)$$

The quantity q is to be taken in a convenient form showing an acceptable temperature dependence. Results of a graphical study for rotations about principal axes, using bond stretching of the OH molecule, lead to a provisional suggestion that a usable form might be

$$q=q_1 z \exp(-z) \quad (47)$$

where $z=q_2hcD/kT$, with $q_1=0.4$ and $q_2=1.8$. Other representation schemes may reasonably be more suitable, however.

It is conceded that direct rotational cut-off effects are fairly small even for temperatures at the top of the range of the present tabulation. However, an indirect effect in the extrapolation is not quite so negligible. In making evaluations based on the empirical constants of Benedict, it was found that gross differences in behavior between $v1$ and $v3$ dependences were produced with $v1$ or $v3$ large, particularly as $v2$ was increased so as to be more than a small integer. This characteristic is attributed to the effect of the long range of the extrapolation with equations fitted to data at low quantum numbers only. A more uniform behavior has been obtained by a revised procedure for treating the empirical vibrational energy.

Energies for High Vibrational Levels

In the last several years the method for estimation of high vibrational levels appears to be changing, involving such new developments as are referred to as localized bond excitation and local mode description [10]. Special potential forms can be used for such calculations with constants converted [11] from empirical values found with a conventional valence bond system formulation and normal coordinate analysis [12]. Potential improvement based on direct comparison between computed and "observed" levels could be an ultimate objective. A hazard at the outset in this approach may be a sensitivity to the correctness of identification or assignment of spectroscopic data on which at least the original numerical constants are based. As to direct *a priori* quantum mechanical calculation of levels for the molecule as a collection of nuclei and electrons, based on general physical constants, it appears that significant advances have been made on this intrinsically difficult endeavor. Somewhat approximate agreement with vibrational fundamentals has been obtained [13,14] but whether a similar quality of prediction could be achieved for higher vibrational levels may be in an area of pure speculation. *A priori* calculation appears informative in regard to excited electronic states [15], in an energy domain beyond the range of the present treatment.

Even if a local mode description will prove ultimately more reliable than the conventional approach, it has appeared expedient to continue for the time being with the older formulation, for which the necessary parameters are at hand. It appears plausible that newly and correctly calculated levels should on the average agree tolerably well with the old values of corresponding description. This is thought to be the usual situation for a group of "interacting levels" in a so-called resonance situation.

The vibrational constants used here are based on a formulation by the late Prof. W. S. Benedict [8], described by him as preliminary. His result can be shown as

$$\begin{aligned} G(v1,v2,v3)=&3692.5965\,v1+1609.1113\,v2 \\ &+3803.6304\,v3-41.5442\,V1\,V1 \\ &-13.4642\,V2\,V2-48.0343\,V3\,V3 \\ &-28.6309\,V1\,V2 \\ &-164.2450\,V1\,V3 \\ &-19.2960\,V2\,V3 \\ &+0.0927\,V1\,V1\,V1 \\ &-0.9003\,V2\,V2\,V2 \\ &+0.2690\,V3\,V3\,V3 \\ &-0.7760\,V1\,V2\,V3 \\ &+1.9316\,V1\,V1\,V2 \\ &+0.2325\,V1\,V1\,V3 \\ &+1.0522\,V1\,V2\,V2 \\ &+1.1192\,V2\,V2\,V3 \\ &+1.5269\,V1\,V3\,V3 \\ &-0.9318\,V2\,V3\,V3, \end{aligned} \quad (48)$$

for levels with resonance shifts removed as indicated earlier.

The present proposed innovation in regard to vibrational energy is to suppress the long range effects of Benedict's fitting on the basis that the fine details of fit while relevant in the region of fit in the low quantum number range ($vi<5$) may still not be numerically reliable when extrapolated to large vi. For the various "small" quadratic and cubic terms, involving "v products" ($=p$), an extrapolation by replacement of "p" by $p/[1+(p/a)^k]$ has been used with $k=6$ and with the parameter "a" chosen differently for terms quadratic and cubic in the v's. (65 versus 460) This causes these terms to become small in the approach to the dissociation region.

For the estimation of vibrational levels in the region of large $v1$ and $v3$, the procedure adopted was to take the energy as given primarily by a quadratic jointly in $v1$ and $v3$, much as in the case with a Morse potential in a diatomic molecule. Thus, in the case with $v2=0$, the form for this main part of the vibrational energy becomes

$$GL(v1,0,v3)=\mathring{\nu}1\ v1+\mathring{\nu}3\ v3-x11\ v1\ (v1-1)$$
$$-x33\ v3\ (v3-1)-x13\ v1\ v3. \quad (49)$$

The anharmonicities for this were chosen so as to agree with energies of dissociative reactions based on thermochemical data. For $v1$ or $v3$ increasing singly with the other at zero, there is dissociation according to $H_2O=O+2H$ at about 76721 $cm^{-1}=D$. For $v1$ and $v3$ equal and advancing together, dissociation is taken to be according to $H_2O=H+OH$ at about 41280 $cm^{-1}=Dm$.

In the cases of $v1$ and $v3$ advancing singly, the energy is given as in

$$G=\mathring{\nu}\,v-x\,v\,(v-1). \quad (50)$$

With $\mathring{\nu}1=3651.145$ cm^{-1} from $G(1,0,0)-G(0,0,0)$ and also with $\mathring{\nu}3=3755.8651$ cm^{-1} from $G(0,0,1)-G(0,0,0)$, the corresponding "anharmonicity" constants follow from Birge-Sponer type relations as

$$x=2D-\mathring{\nu}-[(2D-\mathring{\nu})^2-\mathring{\nu}^2]^{1/2}. \quad (51)$$

For $D=76721$ cm^{-1}, the long range estimates are $x11=44.5045$ and $x33=47.1274$ cm^{-1}. These are raised by about 0.0004 cm^{-1} in covering small residual effects from the suppressed higher order constants at dissociation, which appears to be where $v1$ or $v3$ singly reach a value of about 41.

A somewhat similar procedure using $Dm=41280$ cm^{-1} to estimate $x13$ for $v1=v3=v$ implies the relation

$$G=\mathring{\nu}\,v-x\,v^2 \quad (52)$$

where $\mathring{\nu}=\mathring{\nu}1+\mathring{\nu}3+x11+x33$ and $x=x11+x33+x13$. The usual Birge-Sponer relations by

$$x=\mathring{\nu}^2/4Dm \text{ or } x13=\mathring{\nu}^2/4Dm-x11-x33 \quad (53)$$

give $x13=248.95779$ kaysers but the partially suppressed residual contributions of other constants at this dissociation energy (near $v1=v3=11$) raise $x13$ to 251.3489 cm^{-1}.

A multiplier factor $[1-0.0028\ v2-0.00013\ v2\ (v2-1)]$ has been introduced for $\mathring{\nu}_1\ v1+\mathring{\nu}_3\ v3$ to allow for a diminishing energy increment to dissociation as $v2$ advances upward above $v2=0$. All such adjustments are compensated for in the low quantum number range so as to preserve the behavior there according to the empirical data fit of Benedict [8].

Thermodynamic Tables for H_2O

Two sets of tabular values have been included as prospective thermodynamic quantities for the ideal gas state of the light isotopic water molecule. These are here designated by their dates of computation, which were 1982 and 1984.

For the 1982 table, appearing here as table 2, parameter values used were influenced by results of computations for a rigid bender model, adjusted further for bond length increase by centrifugal stretching due to a rotational character of motion in the bending vibration. These included indications as to the $v2$ dependence of the principal rotational constants, the extrapolation of vibrational energy to high $v2$ values, and the course of the ordinary centrifugal effects to high $v2$ and elevated temperatures, using a five parameter Padé formulation.

The 1984 table, shown here as table 3, includes the innovations of the 1982 table, and a few others, also. In the approach to dissociation at high $v1$ and $v3$, the behavior of Gv was taken as essentially quadratic in $v1$ and $v3$, in resemblance to the known diatomic behavior with a Morse potential. Special functions were used to fade out the detailed higher order terms arising out of Benedict's Gv fit at low vibrational quantum numbers. For eight low-lying vibrational states, numerical values were inserted via the computer program for observed

Table 2. Thermodynamic quantities for light isotopic water (1982 version).

T/K	$\frac{C_p^0}{R}$	$\frac{S^0}{R}$	$-\frac{G^0-H_0^0}{RT}$	$\frac{H^0-H_0^0}{RT}$	$\frac{Q\text{cut}}{Q}$	#
200	4.01111	21.09225	17.11003	3.98222	0.	3
300	4.04064	22.72269	18.72717	3.99552	0.	6
400	4.12079	23.89493	19.87912	4.01581	0.	11
500	4.23672	24.82647	20.77846	4.04801	0.	17
600	4.36880	25.61043	21.52011	4.09032	0.	26
700	4.50951	26.29436	22.15429	4.14007	0.	37
800	4.65679	26.90607	22.71068	4.19539	0.	53
900	4.80868	27.46330	23.20823	4.25507	0.	72
1000	4.96224	27.97789	23.65978	4.31810	0.	95
2000	6.17104	31.83102	26.85729	4.97373	0.	635
3000	6.78260	34.46206	28.97640	5.48566	0.	2366
4000	7.13354	36.46511	30.60809	5.85702	0.	4519
5000	7.38773	38.08513	31.94658	6.13856	0.	6524
6000	7.60934	39.45206	33.08648	6.36559	0.	8080
7000	7.79162	40.63945	34.08250	6.55695	0.	9487
8000	7.90299	41.68807	34.96896	6.71911	0.	10818
9000	7.92822	42.62120	35.76836	6.85284	0.	12075
10000	7.87725	43.45446	36.49608	6.95838	0.	13255

The final column gives the number of vibrational levels involved in the state sum.

Table 3. Thermodynamic quantities for light isotopic water (1984 version).

T/K	$\frac{C_p^0}{R}$	$\frac{S^0}{R}$	$-\frac{G^0-H_0^0}{RT}$	$\frac{H^0-H_0^0}{RT}$	$\frac{Q\text{cut}}{Q}$	#
200	4.01111	21.09218	17.10996	3.98222	0.	3
300	4.04065	22.72262	18.72710	3.99552	0.	6
400	4.12080	23.89486	19.87905	4.01582	0.	11
500	4.23676	24.82641	20.77839	4.04802	0.	17
600	4.36895	25.61038	21.52004	4.09034	0.	26
700	4.50993	26.29435	22.15423	4.14012	0.	37
800	4.65779	26.90615	22.71063	4.19552	0.	53
900	4.81075	27.46355	23.20820	4.25535	0.	72
1000	4.96610	27.97845	23.65980	4.31865	0.	95
2000	6.22473	31.84805	26.86066	4.98740	0.	651
3000	6.83435	34.50332	28.98865	5.51467	3.290E-17	2369
4000	7.13573	36.51478	30.62900	5.88579	3.328E-11	4774
5000	7.34143	38.12993	31.97291	6.15702	2.054E-08	7063
6000	7.52368	39.48479	33.11495	6.36984	4.151E-07	8973
7000	7.67781	40.65664	34.11050	6.54614	9.326E-06	10678
8000	7.77806	41.68916	34.99460	6.69456	3.320E-05	11899
9000	7.80016	42.60601	35.79032	6.81569	2.384E-04	12183
10000	7.76665	43.42708	36.51385	6.91322	4.060E-04	12183

The final column gives the number of vibrational levels involved in the final state sum. The next to the last column gives the fractional reduction in the state sum due to rotational cut-off, according to the "locus-asymptote" estimate used.

values for vibrational energy, principal rotational constants, and their five member Padé centrifugal parameters, based on reported spectroscopic data analyses using the Watson Hamiltonian formulation. A rotational cut-off approximation of a "locus-asymptote" type was also introduced, but with little apparent effect up to 10000 K.

It is natural to see the difference in values between the two tables as relevant to their uncertainty. It is presumed that the disagreement in values should be attributed to effects in changes in level distribution, which may reflect the ad hoc modification of level description for the later table.

It had appeared reasonable to maintain a favorable view of progress in raising the number of constants based on the Watson Hamiltonian data from three to five. However, it is now recognized in retrospect that some basis for reserve exists. As used, the program for finding Padé constants was able to produce the five parameters as desired even when the Hamiltonian parameters were not complete to a corresponding extent. This might be termed a "spill-over" effect akin to the forming of product terms in a series development. The highest power of T directly included as a contribution to "T times the Wilson constant" may be obtained by taking the highest net power of J's in the Hamiltonian, dividing by 2, and subtracting 1. On this basis, the ground state and first excited vibrational state, (000) and (010), may be "complete" through the 5th power. The states (020) and (030) show fitting in the 4th power, and the states (100), (001), (110) and (011) include only into the 3rd power. One may hope that a moving of the Padé process into the Hamiltonian will lead to a more uniform treatment [16].

As comment on our present use of a "preliminary" 1972 data formulation received from Professor Benedict [8], we accepted his view that his was better than that of Khachkuruzov [17], of 1959. We note that a more recent vibrational energy formulation presumably of comparable quality was published in 1983 by Bykov, Makushkin and Ulenikov [18], and could in all probability provide a similar basis for a table of thermodynamic quantities.

It appears that greater consideration should be given to recent work such as that by Child and Lawton [19] on local mode representations of vibrational states. However, at this time it is not clear how energies for the entire manifold of vibrational states would be reliably and conveniently given for the calculation of thermodynamic functions on such a basis.

Conclusion

The objective in this study has been to obtain an improved extrapolation of the ideal gas table to higher temperatures. The procedure has made use of direct data, augmented with numerical estimates based on simple physical models. It is hoped that this might provide a realistic approach to better sum of state estimation.

Although the models have involved some numerical choices that were not at all rigorous, the results may allow such comparisons as may lead to an informed appreciation of the problems remaining for the reduction of uncertainties.

References

[1] Woolley, H. W., Thermodynamic Properties for H_2O in the Ideal Gas State; Straub, J. and K. Scheffler, eds., p. 166, Pergamon: Oxford (1980).

[2] Friedman, A. S., and L. Haar, J. Chem. Phys. **22** 2051–2058 (1954).

[3] Mayer, J. E., and M. G. Mayer, Statistical Mechanics, John Wiley & Sons, Inc.: New York (1940).

[4] Watson, J. K. G., J. Chem. Phys. **45** 1360–1361 (1966); **46** 1935–1949 (1967); **48** 181–185 (1968); **48** 4517–4524 (1968).

[5] Stripp, K. F., and J. G. Kirkwood, J. Chem. Phys. **19** 1131–1133 (1951).

[6] Wilson, E. B., Jr., J. Chem. Phys. **4** 526–528 (1936).

[7] Camy-Peyret, C., and J. M. Flaud, Mol. Phys. **32** 523–537 (1976); J. Mol. Spectrosc. **59** 327–337 (1976); J. Mol. Spectrosc. **51** 142–150 (1974).

[8] Benedict, W. S., private communication.

[9] Kyro, E., J. Mol. Spectrosc. **88** 167–174 (1981).

[10] Child, M. S., and R. T. Lawton, Faraday discussions, Chem. Soc. **71** 273–285 (1981).

[11] Sorbie, K. S., and J. M. Murrell, Mol. Phys. **29** 1387–1407 (1975).

[12] Hoy, A. R.; I. M. Mills and G. Strey, Mol. Phys. **24** 1265–1290 (1972).

[13] Bartlett, R. J.; I. Shavitt and G. D. Purvis, J. Chem. Phys. **71** 281–291 (1979).

[14] Kraemer, W. P.; B. O. Roos and P. E. M. Siegbahn, Chem. Phys. **69** 305–321 (1982).

[15] Theodorakopoulos, G.; I. D. Petsalakis and R. J. Buenker, Chem. Phys. **96** 217–225 (1985); Theodorakopoulos, G.; I. D. Petsalakis, R. J. Buenker, and S. D. Peyerimhoff, Chem. Phys. Lett. **105** 253–257 (1984).

[16] Burenin, A. V.; T. M. Fevral'skikh, E. N. Karyakin, O. L. Polyansky, and S. M. Shapin, J. Mol. Spectrosc. **100** 182–192 (1983).

[17] Khachkuruzov, G. A., Optika i Spektroskopia **6** 463–474 (1959).

[18] Bykov, A. D.; Y. S. Makushkin and O. N. Ulenikov, J. Mol. Spectrosc. **99** 221–227 (1983).

[19] Child., M. S., and R. T. Lawton, Chem. Phys. Lett. **87** 217–220 (1982).

Appreciation is expressed to those who have encouraged the present effort. Lester Haar and Dr. Anneke Sengers are especially thanked.

APPENDIX

A listing of the interactive computer program, in BASIC, for carrying out the preparation of the correction factor as a series in powers of temperature using the empirical constants of the Watson-type Hamiltonian:

```
                                NOVEMBER 17, 1983

10  PR# 1: PRINT "   'CENTRI4' OF H. W. WOOLLEY, NOV. 1983": PRINT : PRINT

20  PRINT  TAB( 8);"THE CENTRIFUGAL EFFECT  OF MOLECULAR ROTATION ON IDE
    AL GAS PROPERTIES": PR# 0
30  PRINT "ENTER COMMENTS": INPUT C$: PRINT "ENTER NAME": INPUT A$: PRINT
    "ENTER DATE": INPUT D$: PRINT "ENTER DATA SOURCE": INPUT S$
40  PR# 1: PRINT  TAB( 28);A$: PRINT  TAB( 28);D$: PRINT  TAB( 5);C$: PRINT
    TAB( 5);S$: PR# 0
50  PRINT "ENTER ROTATIONAL CONSTANTS A, B & C": INPUT AZ,BX,CY
60  DIM W$(30),NT(35),KF(130),NX(130),NY(130),NZ(130),H(6,10),CO(130),CF
    (35),HH(10),HL(10),F(15)
70  DIM CN(40),XX(40),YY(40),ZZ(40)
80 FF(1) = 1:FF(2) = 2:FF(3) = 6:FF(4) = 24:FF(5) = 120:FF(6) = 720
90  PRINT "ENTER POWER OF T TO BE COVERED ((7), AS 1? 2? 3?": INPUT KH
100 F(1) = 1: FOR I = 2 TO 15:F(I) = F(I - 1) * (2 * I - 3) / 2: NEXT I
110  GOTO 1000
200  REM :PROLIFERATION AT BRANCHING
210 IK = 1:IU = 1:NC(1) = 1:IL(KL) = II
220 IK = IK + 1: IF IK ) KL THEN 260
230  IF IL(IK) = IL(IK - 1) THEN NC(IU) = NC(IU) + 1: GOTO 220
240 IU = IU + 1:NC(IU) = 1
250  IF IK ( KL THEN 220
260 IT = IU
270 FC = 1: FOR IU = 1 TO IT:FC = FC * FF(NC(IU)): NEXT IU:CT = FF(KL) /
    FC
280 MX = MX + XX(II):MY = MY + YY(II):MZ = MZ + ZZ(II):MT = MX + MY + MZ
    - 3 - KL
290 TR =  - TR * CN(II) / KL: IF MT ) KH THEN 310
300 H(KL,MT) = H(KL,MT) + TR * F(MX) * F(MY) * F(MZ) / AZ ^ (MZ - 1) / B
    X ^ (MX - 1) / CY ^ (MY - 1) * CT
310  RETURN
400  REM  :RETURNING TO A PLACE  OF BRANCHING
410 MX = MX - XX(II):MY = MY - YY(II):MZ = MZ - ZZ(II):TR =  - TR * KL /
    CN(II): RETURN
1000  REM
1010 W$(1) = "DELJ":W$(2) = "DELJK":W$(3) = "DELK":W$(4) = "SDLJ":W$(5) =
    "SDLK":W$(6) = "HJ":W$(7) = "HJK":W$(8) = "HKJ"
1020 W$(9) = "HK":W$(10) = "SHJ":W$(11) = "SHJK":W$(12) = "SHK":W$(13) =
    "CLJ":W$(14) = "CLK":W$(15) = "CLKKJ":W$(16) = "CLJK"
1030 W$(17) = "CLJJK":W$(18) = "SLJ":W$(19) = "SLK":W$(20) = "SLKJ":W$(2
    1) = "SLJK":W$(22) = "CPK"
1040 W$(23) = "CPKKJ":W$(24) = "CPKJ":W$(25) = "SPK":W$(26) = "Z12":W$(2
    7) = "Z10P2":W$(28) = "Z14":W$(29) = "Z16":W$(30) = "Z18"
1050  DATA  1,6,-1,2,0,0,-1,0,2,0,-1,0,0,2,-2,1,1,0,-2,1,0,1,-2,0,1,1
1060  DATA  2,3,-1,1,0,1,-1,0,1,1,-1,0,0,2
1070  DATA  3,1,-1,0,0,2
1080  DATA  4,4,-2,2,0,0,2,0,2,0,-2,1,0,1,2,0,1,1
1090  DATA  5,2,  -2,1,0,1,2,0,1,1
1100  DATA  6,10,1,3,0,0,1,0,3,0,1,0,0,3,3,2,1,0,3,2,0,1,3,1,2,0,3,0,2,1
    ,3,1,0,2,3,0,1,2,6,1,1,1
1110  DATA  7,6,1,2,0,1,1,0,2,1,1,0,0,3,2,1,1,1,2,1,0,2,2,0,1,2
1120  DATA    8,3,1,1,0,2,1,0,1,2,1,0,0,3
1130  DATA  9,1,1,0,0,3
1140  DATA     10,8,2,3,0,0,-2,1,2,0,2,1,  0,2 ,  2,2,1,0,4,2,0,1,-2,0,3,0
    ,-2,0,1,2,-4,0,2,1
1150  DATA  11,4,2,2,0,1,-2,0,2,1,2,1,0,2,-2,0,1,2
1160  DATA  12,2,2,1,0,2,-2,0,1,2
1170  DATA  13,15,1,4,0,0,1,0,4,0,1,0,0,4,4,3,1,0,4,1,3,0,4,3,0,1,4,0,3,
    1,4,1,0,3,4,0,1,3,6,2,2,0,6,2,0,2,6,0,2,2,12,2,1,1,12,1,2,1,12,1,1,
    2
1180  DATA   14,1,1,0,0,4
1190  DATA    15,3,1,1,0,3,1,0,1,  3,1,0,0,4
1200  DATA   16,6,1,2,0,2,1,0,2,2,1,0,0,4,2,1,1,2,2,1,0,3,2,0,1,3
1210  DATA   17,10,1,3,0,1,1,0,3,1,1,0,0,4,3,2,1,1,3,2,0,2,3,1,2,1,3,0,2
    ,2,3,1,0,3,3,0,1,3,6,1,1,2
1220  DATA  18,12,2,4,0,0,-2,0,4,0,2,1,0,3,-2,0,1,3,4,3,1,0,-4,  1,3,0,6,
    3,0,1,-6,0,3,1,6,2,1,1,-6,1,2,1,6,2,0,2,-6,0,2,2
1230  DATA   19,2,2,1,0,3,-2,0,1,3
1240  DATA   20,4,2,2,0,2,-2,0,2,2,2,1,0,3,-2,0,1,3
1250  DATA   21,8,2,3,0,1,2,2,1,1,4,2,0,2,-2,1,2,1,2,1,0,3,-4,0,2,2,-2,0
    ,1,3,-2,0,3,1
1260  DATA   22,1,1,0,0,5
1270  DATA   23,3,1,1,0,4,1,0,1,4,1,0,0,5
1280  DATA   24,6,1,2,0,3,1,0,2,3,1,0,0,5,2,1,1,3,2,1,0,4,2,0,1,4
1290  DATA   25,2,2,1,0,4,-2,0,1,4
1300  DATA   26,1,1,0,0,6
1310  DATA   27,3,1,1,0,  5,1,0,1,5,1,0,0,6
1320  DATA   28,1,1,0,0,7
1330  DATA   29,1,1,0,0,8
1340  DATA   30,1,1,0,0,9
1350  DATA  0,0,0,0,0,0,0,0,0,0,0,
1360 I = 0: SPEED= 200
1370  READ NN,N9: IF NN = 0 THEN 1420
1380  PRINT : PRINT
1390  FOR K1 = 1 TO N9:I = I + 1
1400  READ KF(I),NX(I),NY(I),NZ(I): PRINT "#";NN;", TERMS:";N9;", COEF:"
    ;KF(I);", (NX,NY,NZ): (";NX(I);",";NY(I);",";NZ(I);")": NEXT K1:NT(
    NN) = N9:LX = NN
1410  GOTO 1370
1420 KN = I: SPEED= 255
1430  FOR N = 1 TO LX: PRINT "ENTER COEFFICIENT 'CF(";N;")'  OR ";W$(N):
     INPUT CF(N): NEXT N
1440  PR# 1: PRINT "CONSTANTS IN THE ROTATIONAL HAMILTONIAN": FOR N = 1 TO
    LX: PRINT CF(N),W$(N): NEXT N: PRINT "A=";AZ;",  B=";BX;",  C=";CY:
     PR# 0
1450 I = 0: FOR N = 1 TO LX:N8 = NT(N)
1460  FOR K = 1 TO N8:I = I + 1:CO(I) = KF(I) * CF(N): NEXT K: NEXT N
1470  FOR J = 1 TO 40:CN(J) = 0: NEXT J
1480 JM = 1:CN(1) = CO(1):XX(1) = NX(1):YY(1) = NY(1):ZZ(1) = NZ(1)
1490  FOR I = 2 TO KN:KK = 0: IF CO(I) = 0 THEN 1560
1500  FOR J = 1 TO JM
1510  IF (XX(J) - NX(I)) ^ 2 + (YY(J) - NY(I)) ^ 2 + (ZZ(J) - NZ(I)) ^ 2
    = 0 THEN KK = 1: GOTO 1530
1520  GOTO 1540
1530 CN(J) = CN(J) + CO(I):J = JM
1540  NEXT J
1550  IF KK = 0 THEN JM = JM + 1:CN(JM) = CO(I):XX(JM) = NX(I):YY(JM) =
    NY(I):ZZ(JM) = NZ(I)
1560  REM
1570  NEXT I
1580  FOR J = 1 TO JM
1590  PRINT "#";J;", (XX,YY,ZZ): (";XX(J);",";YY(J);",";ZZ(J);")";", COE
    F: ";CN(J)
1600  NEXT J:KN = JM
1610  FOR MT = 1 TO 10: FOR KL = 1 TO 6:H(KL,MT) = 0: NEXT KL:HH(MT) = 0
    : NEXT MT
1620 MX = 1:MY = 1:MZ = 1:TR = 1:MT = 0
1630  FOR IA = 1 TO KN:KL = 1:I1 = IA: IF CN(I1) = 0 THEN 1930
1640  PRINT "I1=";I1;",  TR=";TR
```

```
1650  IF MT ) KH THEN IA = KN: GOTO 1930
1660 II = I1: GOSUB 200: IF KH ( KL + 1 THEN 1920
1670  FOR IB = IA TO KN:KL = 2:I2 = IB: IF CN(I2) = 0 THEN 1910
1680  IF MT ) KH THEN IB = KN: GOTO 1910
1690 II = I2: GOSUB 200: IF KH ( KL + 1 THEN 1900
1700  FOR IC = IB TO KN:KL = 3:I3 = IC: IF CN(I3) = 0 THEN 1890
1710  IF MT ) KH THEN IC = KN: GOTO 1890
1720 II = I3: GOSUB 200: IF KH ( KL + 1 THEN 1880
1730  FOR ID = IC TO KN:KL = 4:I4 = ID: IF CN(I4) = 0 THEN 1870
1740  IF MT ) KH THEN ID = KN: GOTO 1870
1750 II = I4: GOSUB 200: IF KH ( KL + 1 THEN 1860
1760  FOR IE = ID TO KN:KL = 5:I5 = IE: IF CN(I5) = 0 THEN 1850
1770  IF MT ) KH THEN IE = KN: GOTO 1850
1780 II = I5: GOSUB 200: IF KH ( KL + 1 THEN 1840
1790  FOR IG = IE TO KN:KL = 6:I6 = IG: IF CN(I6) = 0 THEN 1830
1800  IF MT ) KH THEN IG = KN: GOTO 1830
1810 II = I6: GOSUB 200
1820 II = I6:KL = 6: GOSUB 400
1830  NEXT IG:MT = MX + MY + MZ - 2 - KL
1840 II = I5:KL = 5: GOSUB 400
1850  NEXT IE:MT = MX + MY + MZ - 2 - KL
1860 II = I4:KL = 4: GOSUB 400
1870  NEXT ID:MT = MX + MY + MZ - 2 - KL
1880 II = I3:KL = 3: GOSUB 400
1890  NEXT IC:MT = MX + MY + MZ - 2 - KL
1900 II = I2:KL = 2: GOSUB 400
1910  NEXT IB:MT = MX + MY + MZ - 2 - KL
1920 II = I1:KL = 1: GOSUB 400
1930  NEXT IA
1940  FOR MT = 1 TO KH: FOR KL = 1 TO KH
1950 HH(MT) = HH(MT) + H(KL,MT)
1960  NEXT KL: NEXT MT
1970  PR# 1: PRINT : PRINT "COEFFICIENTS OF PROPORTIONAL ADDITIONS TO Q,
      BY POWERS OF T/C2"
1980  PRINT "HH:1:";HH(1);";2:";HH(2);";3:";HH(3);";4:";HH(4);";5:";HH(5
      );";6:"HH(6)
1990  GOSUB 5000
2000  PRINT "ADDITIONS TO LOG Q, BY POWERS OF  T/C2"
2010  PRINT "COEFFICIENTS:": FOR N = 1 TO KH: PRINT "POWER=";N;",  COEF.
      =";HL(N): NEXT N
2020 C2 = 1.438786: FOR N = 1 TO KH:A(N) = HL(N) / C2 ^ N: PRINT "COEF.
      OF T^";N;" :";A(N): NEXT N
2030  IF KH ( 5 THEN 2090
2040 B1 = A(2) / A(1):B2 = A(3) / A(1):B3 = A(4) / A(1):B4 = A(5) / A(1)

2050 DN = B2 ^ 2 - B1 * B3:D1 = (B1 * B4 - B2 * B3) / DN:D2 = (B3 ^ 2 -
      B2 * B4) / DN
2060 G1 = D1 + B1:G2 = D2 + D1 * B1 + B2
2070 G1 = G1 * A(1):G2 = G2 * A(1)
2080  PRINT : PRINT "D LN Q = (";A(1);" * T + (";G1;") * T ^ 2 + (";G2;"
      ) * T ^ 3) / (1 + (";D1;") * T + (";D2;") * T ^ 2 ) "
2090  PR# 0: END
5000  REM  LOG
5010 HL(1) = HH(1)
5020  IF KH ( 2 THEN 5150
5030 HL(2) = HH(2) - HH(1) ^ 2 / 2
5040  IF KH ( 3 THEN 5150
5050 HL(3) = HH(3) - HH(1) * HH(2) + HH(1) ^ 3 / 3
5060  IF KH ( 4 THEN 5150
5070 HL(4) = HH(4) - HH(2) ^ 2 / 2 - HH(1) * HH(3) + HH(1) ^ 2 * HH(2) -
      HH(1) ^ 4 / 4
5080  IF KH ( 5 THEN 5150
5090 HL(5) = HH(5) - HH(2) * HH(3) - HH(1) * HH(4) + HH(1) * HH(2) ^ 2 +
      HH(1) ^ 2 * HH(3) - HH(2) * HH(1) ^ 3 + HH(1) ^ 5 / 5
5100  IF KH ( 6 THEN 5150
5110 HL(6) = HH(6) - HH(3) ^ 2 / 2 - HH(2) * HH(4) - HH(1) * HH(5) + HH(
      4) * HH(1) ^ 2 + 2 * HH(3) * HH(2) * HH(1) + HH(2) ^ 3 / 3 - HH(3) *
      HH(1) ^ 3 - HH(2) ^ 2 * HH(1) ^ 2 * 3 / 2 + HH(2) * HH(1) ^ 4 - HH(
      1) ^ 6 / 6
5150  RETURN
6000  PR# 1: PRINT  TAB( 039);D$: PRINT  CHR$ (9);"80N";
6010  PRINT  CHR$ (9);"60P";
6020  LIST : PRINT  TAB( 039);D$: PR# 0: END
                                        NOVEMBER 17, 1983
```

Journal of Research of the National Bureau of Standards

Special Report on Electrical Standards

Report on the 17th Session Of the Consultative Committee On Electricity

Volume 92 Number 1 January–February 1987

B. N. Taylor

National Bureau of Standards
Gaithersburg, MD 20899

This report provides the background for and summarizes the main results of the 17th session of the Consultative Committee on Electricity (CCE) of the International Committee of Weights and Measures held in September 1986. Included are decisions made by the CCE which promise to have a profound effect on the standardization of national representations of the volt and ohm and thus on the international compatibility of electrical measurements. In particular, on January 1, 1990, worldwide changes in the basis for such representations are planned which will lead to an increase in the U.S. legal unit of voltage of about 9 parts-per-million (ppm) and in the U.S. legal unit of resistance of about 1.5 ppm.

Key words: Consultative Committee on Electricity; electrical units; Josephson effect; ohm; quantum Hall effect; volt.

Accepted: December 11, 1986

1. Background

The 17th session of the Consultative Committee on Electricity (CCE) of the International Committee of Weights and Measures (CIPM) met September 16–18, 1986, at the International Bureau of Weights and Measures (BIPM), which is located in Sèvres (a suburb of Paris), France. NBS Director Ernest Ambler, who was recently elected President of the CCE by the CIPM, chaired the meeting and the author attended as NBS representative.

The CCE is one of eight CIPM Consultative Committees which together cover most of the areas of basic metrology [1][1] (see fig. 1). These committees, which may form temporary or permanent 'Working Groups' to study special subjects, coordinate the international work carried out in their respective fields, assist the CIPM in supervising the work of the BIPM in these fields, and propose recommendations concerning amendments to be made to the definitions and values of units. The CIPM acts directly on these recommendations or submits them for approval to the General Conference of Weights and Measures (CGPM) if they will have a broad impact.

The BIPM, whose principal task is to ensure worldwide uniformity of physical measurements, was established by the Treaty of the Meter signed in Paris on May 20, 1875. (The number of signatories, originally 17, has now grown to almost 50.) The BIPM is supervised by the CIPM which in turn is under the authority of the CGPM. The CGPM consists of delegates from all of the member countries of the Treaty of the Meter and presently meets every four years. The CIPM consists of 18 members each representing a different country and presently meets every year. In general, a consultative committee meets every few years, has as its president a member of the CIPM, and is composed of delegates from the major national standards

About the Author: B. N. Taylor is a physicist and Chief of the Electricity Division in the Center for Basic Standards. The Center is within the NBS National Measurement Laboratory.

[1]Numbers in brackets indicate literature references.

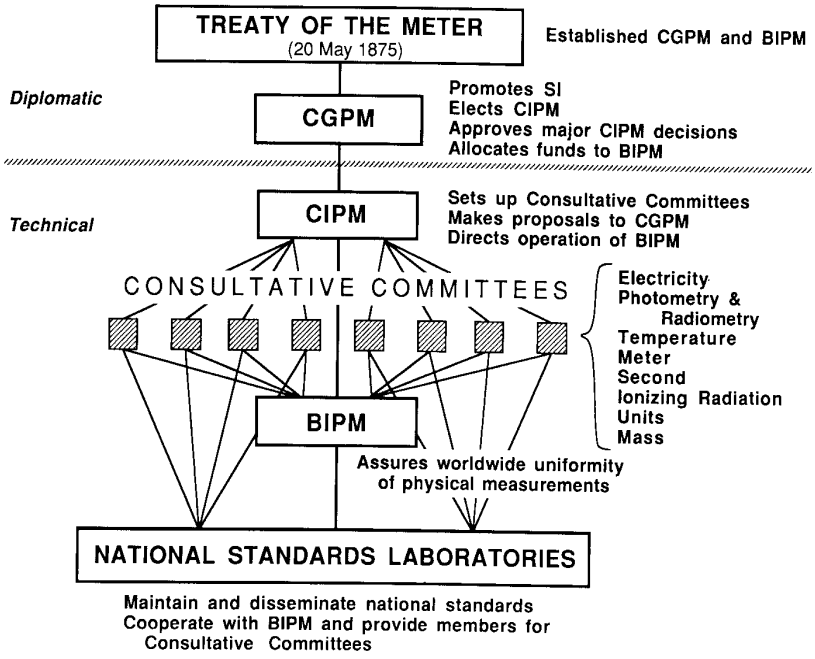

Figure 1–Schematic depiction of how basic measurement units and standards are coordinated internationally. (Treaty of the Meter: *La Convention du Mètre*; CGPM: *Conférence Général des Poids et Mesures* or General Conference of Weights and Measures; CIPM: *Comité International des Poids et Mesures* or International Committee of Weights and Measures; BIPM: *Bureau International des Poids et Mesures* or International Bureau of Weights and Measures.)

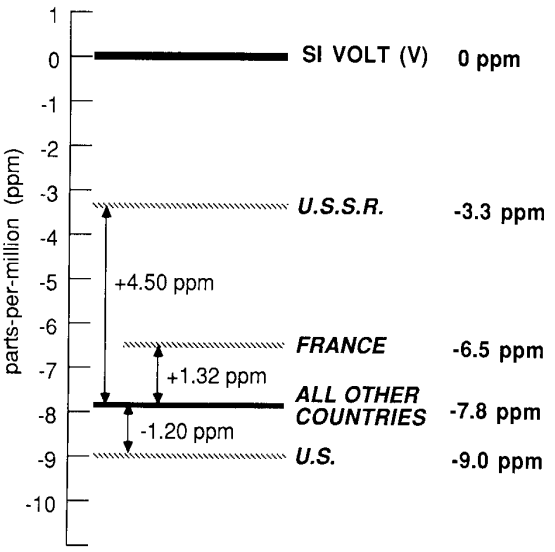

Figure 2–Graphical comparison of the representation of the SI volt of various countries based on the Josephson effect, V_{LAB}, and of V_{LAB} with the SI volt, V. The value of V_{LAB} indicated by 'All Other Countries' is based on the value of the Josephson frequency-voltage ratio $2e/h$ recommended by the CCE of the CIPM in 1972: $(2e/h)_{CCE-72} = 483594.0$ GHz/V. (See footnote 2 for those countries which use this value.)

laboratories as well as from specialized institutes, and individual members appointed by the CIPM.

The focus of the 17th session of the CCE, which was attended by some 30 individuals from 15 countries, was the use of the Josephson and quantum Hall effects to define and maintain national or laboratory representations of the units of electrical potential difference and resistance of *Le Système International d'Unités* or International System of Units (abbreviated SI): the SI volt (V) and SI ohm (Ω), respectively [2]. (The national representations are usually designated by the symbol V_{LAB} and Ω_{LAB} where LAB stands for the acronym of the national standards laboratory of the country in question, e.g., NBS.) More specifically, at its 16th session in March 1983 the CCE had concluded that [3] (see fig. 2):

(i) The value 483594.0 GHz/V for the Josephson frequency-voltage ratio $2e/h$ (e is the elementary charge and h is the Planck constant) which it had recommended at its 13th session in 1972 [4–7] for defining and maintaining national representations of the SI volt is significantly in error. (Current evidence indicates that $(2e/h)_{CCE-72}$ is about eight parts-per-million or 8 ppm smaller than the SI value of $2e/h$ and thus V_{LAB} is about 8 ppm smaller than V for those national laboratories which use the CCE value [2,8].)

(ii) It was highly likely that the recently discovered quantum Hall effect would soon be developed to the point that the quantized Hall resistance $R_H = h/e^2 = 25812.8\ \Omega$ could be used to define and maintain national units of resistance consistent with the SI ohm to

within a few tenths of a ppm. (More recent work indicates that a few hundredths of a ppm is quite feasible [9].)

The CCE was also aware of the following:

(iii) Four different values of $2e/h$ are in use in the national laboratories [2]. [The U.S., France, and the U.S.S.R. use values of $2e/h$ which differ by -1.20 ppm, $+1.32$ ppm, and $+4.50$ ppm, respectively from $(2e/h)_{CCE\text{-}72}$ and hence the national voltage units of these countries differ by these amounts from the national units of those countries which use $(2e/h)_{CCE\text{-}72}$.[2]]

(iv) The various national units of resistance, most of which are based on the mean resistance of a group of precision wire-wound resistors, differ from each other and the SI unit by up to several ppm and some are drifting in excess of 0.05 ppm per year. (Current evidence indicates that on January 1, 1986, the various Ω_{LAB} were from 0.2 ppm larger to 3.3 ppm smaller than Ω and $d\Omega_{LAB}/dt$ lies in the range -0.07 to $+0.07$ ppm/year [8].)

As a consequence of (i) through (iv), the CCE decided at its 16th session in 1983 to hold its 17th session in 1986 in order to consider the possibility of recommending for adoption a new value for $2e/h$, consistent with the SI, to be used by every laboratory which employs the Josephson effect to define and maintain its representation of the SI volt; and a value of R_H, consistent with the SI, to be used by every laboratory which chooses to employ the quantum Hall effect to define and maintain its representation of the SI ohm.[3]

Considerable preparatory work was carried out during the two years prior to the CCE's 17th session:

- Immediately after the formal close of the 1984 Conference on Precision Electromagnetic Measurements (CPEM 84, held August 20–24, 1984, in Delft, The Netherlands), active research workers from the national standards laboratories and other interested parties met informally to discuss values of $2e/h$ and R_H. Many new and relevant results were also presented at the conference itself [10].
- In the U.S., NBS Director Ambler sent a letter in early 1985 to over 30 U.S. organizations, companies, and individuals representing industry, government, science, and academia and having an interest in basic electrical measurements and standards at the highest levels of accuracy. The purpose of the letter was to give the U.S. scientific and technological communities the opportunity, well in advance of the 1986 CCE meeting, to provide NBS with advice and guidance on the subject of changing the U.S. electrical units. (The U.S. Legal Volt V_{NBS} would increase by about 9 ppm and the U.S. Legal Ohm Ω_{NBS} by about 1.5 ppm if the CCE were to recommend a new value for $2e/h$ consistent with the SI and a value of R_H also consistent with the SI.) The comments received were presented during CPEM 86 (held at NBS Gaithersburg, June 23–27, 1986) at a special session with active audience participation entitled "Changes in the Electrical Units." In addition to the U.S. presenter, viewpoints from other countries were given by speakers from the Federal Republic of Germany, Japan, and the U.K.[4] The three key points which emerged from this session were:
  - (a) Changing national voltage and resistance units will outweigh the considerable costs of making the changes if and only if complete international uniformity of all the national units of the industrialized countries is achieved.
  - (b) The changes must be well justified by the data; all of the available information must be analyzed by knowledgeable experts and no changes made unless the uncertainties in the values of $2e/h$ and R_H are sufficiently small that it is highly unlikely that further changes will be necessary in the forseeable future.
  - (c) At least one year should be allowed from the date of the official announcement that the changes will take place to the date of their actual implementation so that industry will have sufficient time to prepare itself properly.
- Many researchers took the occasion of CPEM 86 to present their latest results on values of $2e/h$ and R_H [11].
- There was an informal meeting of active research workers and other interested parties to discuss values of $2e/h$ and R_H just after the close of CPEM 86 as there was at the close of CPEM 84.

[2] These include Australia, Canada, the Federal Republic of Germany, Finland, the German Democratic Republic, Italy, Japan, The Netherlands, and the U.K., as well as the BIPM.

[3] Basing Ω_{LAB} on R_H would, of course, eliminate the drift in Ω_{LAB} (i.e., make $d\Omega_{LAB}/dt = 0$).

[4] Written versions of the talks given during the session will appear in Ref. [11].

- Fifty-nine documents were submitted to the CCE by the CCE members (i.e., by the national standards laboratories of the member countries) in support of the CCE's deliberations. These documents included new results as well as comments on the key issues facing the CCE concerning the adoption of a new value for $2e/h$ and a value of R_H.
- A detailed provisionary agenda containing some 25 items was prepared for the 1986 CCE meeting with extensive supporting material in succinct, summary form [12].

2. CCE 17th Session Discussions and Principal Decisions

2.1 Josephson Effect

The principal Josephson effect topics reviewed in detail by the CCE were [12] (i) the value of $2e/h$ used by each national standards laboratory to maintain its representation of the SI volt and the accuracy achieved; (ii) the observed agreement among national voltage standards based on the Josephson effect; (iii) the uncertainties associated with intercomparing these voltage standards using transportable standard cells and Zener diode devices; (iv) the values of $2e/h$ in SI units and their uncertainties obtained by direct force balance measurements and indirectly from fundamental constant determinations; (v) the prospects for future SI values of $2e/h$ with their expected uncertainties and dates of availability; and (vi) the need for further intercomparisons of national voltage standards and Josephson apparatus.

With regard to (i), the uncertainties achieved were noted to be generally in the range 0.01 to 0.1 ppm[5], although Josephson arrays may enable uncertainties smaller than 0.01 ppm to be achieved routinely [13]. Under (ii) and (iii), it was concluded that the agreement between national Josephson voltage standards was generally better than 0.1 ppm but that it was difficult to demonstrate this level of consistency using volt transfer standards. With regard to (iv) and (v), the CCE decided that although the data currently available (both direct and indirect) could provide a value of $2e/h$ in SI units with an uncertainty of about 0.2 ppm, additional data expected to be available within two years would significantly increase confidence in the reliability of the value. Finally, under (vi), the CCE concluded that a formal, broadly based, international comparison of national units of voltage would not be useful because of the unreliability of volt transfer standards but that those laboratories involved in determinations of $2e/h$ should attempt to compare their units using the best transfer standards at their disposal.

The result of the CCE's review of these Josephson effect topics was the following formal declaration:

Declaration E 1 (1986)

Concerning the Josephson effect for maintaining the representation of the volt.

The Comité Consultatif d'Electricité

recognizes

– that as an organ of the Convention du Mètre one of its responsibilities is to ensure the propagation and improvement of the SI, the unit system in use throughout the world,

– that worldwide uniformity and constancy over a long period of time of national representations of the volt are of great technical and economic importance to commerce and industry,

– that many national standards laboratories use the Josephson effect to maintain a highly stable representation of the volt but that not all use the same value for the quotient frequency to voltage,

– that the value of this quotient (483594.0 GHz/V) declared by the CCE in 1972 and which most national laboratories use to maintain representations of the volt is now known to be in error by a significant amount,

– that various laboratories have carried out direct realizations of the volt or determinations of fundamental constants which can yield an indirect value of $2e/h$ in SI units,

– that other national laboratories expect shortly to complete similar realizations or determinations,

is of the opinion

– that the value of the quotient frequency to voltage used to maintain a realization of the volt by means of the Josephson effect must be consistent with the SI,

– that a new value, more consistent with SI, can soon be adopted for use by all laboratories,

– that this new value should be adopted simultaneously by all countries concerned,

in consequence, the CCE

– **establishes** a Working Group charged with making a proposal to the CCE for a new value to be based upon all relevant data that become available before June 15, 1988,

– **decides** to meet in September 1988 with a view to recommending the new value of this quotient to come into effect on January 1, 1990,

[5] Throughout this paper, all uncertainties are one standard deviation estimates.

– **gives notice** that the new value is likely to be higher than the present one by about 8 parts in 10^6, furthermore, the CCE

– **recommends** that national laboratories vigorously pursue their work on the realizations of the volt, the intercomparison of these realizations, and the determination of the constants in question and communicate without delay all their results to the Working Group,

– **recommends** that laboratories do not change their value for this quotient until the new value comes into effect,

– **believes** that the value to be adopted will be sufficiently accurate, in terms of SI, that no further change will be required in the foreseeable future.

The unsatisfactory state of volt transfer standards led the CCE also to develop Recommendation E 1 (1986), the thrust of which is that the national standards laboratories "actively pursue the study and improvement of transportable standards with which the volt may be transferred from one laboratory to another . . . " Both Declaration E 1 (1986) and Recommendation E 1 (1986) were subsequently approved by the CIPM at its October 1986 meeting [14].

2.2 Quantum Hall Effect

The principal quantum Hall effect (QHE) topics reviewed in detail by the CCE were [12] (i) the values and accuracies achieved in measurements of the quantized Hall resistance $R_H = h/e^2$ in terms of national representations of the ohm; (ii) the values of R_H in SI units and their uncertainties obtained by direct calculable capacitor-based measurements and indirectly from fundamental constant determinations; (iii) the prospects for future SI values of R_H with their expected uncertainties and dates of availability; (iv) the results of recent comparisons of national units of resistance using transportable resistance standards; (v) the agreement among the present values of R_H in laboratory units and the agreement between various realizations of the SI ohm based on the calculable capacitor; (vi) the precautions required to ensure reliable results from a quantized Hall resistance sample and the availability of good samples; and (vii) the need for further intercomparisons of national units of resistance.

With regard to (i), most laboratories were able to determine R_H in terms of their national ohm with an uncertainty in the range 0.02 to 0.1 ppm. Under (ii) and (iii), the uncertainties of the values of R_H in SI units, both direct and indirect, varied between 0.020 to 0.32 ppm, and most values agreed with the value having the smallest uncertainty within 0.2 ppm. A number of new and possibly more accurate results could be expected within two years. With regard to (iv), a 0.05 ppm transfer uncertainty or even better can apparently be achieved if the transport resistors are carefully selected and used. Under (v), the CCE concluded that most measurements of R_H in laboratory units agreed within an uncertainty of 0.2 ppm but that the agreement among realizations of the SI ohm was somewhat worse. With regard to (vi), the CCE decided that while tests were available which could be used to ensure reliable results from a particular quantized Hall resistance sample, and that a number of good samples are already in hand, increased understanding of the QHE as well as additional metrologically useful samples were highly desirable. Finally, under (vii), the CCE decided that it would be useful to conduct an international comparison of 1-Ω resistance standards to facilitate the comparison of measurements of R_H in laboratory units.

The result of the CCE's review of these quantum Hall effect topics was the following formal declaration:

Declaration E 2 (1986)

Concerning the quantum Hall effect for maintaining a representation of the ohm.

The Comité Consultatif d'Electricité

recognizes

– that as an organ of the Convention du Mètre one of its responsibilities is to ensure the propagation and improvement of the SI, the unit system in use throughout the world,

– that worldwide uniformity and constancy over a long period of time of national representations of the ohm are of great technical and economic importance to commerce and industry,

– that the application of the quantum Hall effect as a means of maintaining a stable representation of the ohm is being developed rapidly in many national standards laboratories,

– that the quantum Hall effect is providing very reproducible results from one laboratory to another, but that the number of usable samples available is insufficient for present needs,

– that experience is leading to tests that provide assurance of both reproducible and accurate results from a selected sample,

– that no laboratory has yet adopted a value of the quantized Hall resistance R_H to maintain its laboratory representation of the ohm,

– that various laboratories have determined R_H in SI units using both the calculable capacitor and determinations of fundamental constants,

– that additional results for R_H in SI units are

expected to become available in the near future,

is of the opinion

– that the same value of R_H should be adopted simultaneously by all those laboratories that decide to use the quantized Hall resistance as their representation of the ohm,

– that this value should be consistent with SI,

– that such a value can soon be adopted,

in consequence, the CCE

– **establishes** a Working Group charged with making a proposal to the CCE for a value of R_H to be based upon all relevant data that become available up unitl June 15, 1988 and with developing detailed guidelines for the proper use of the quantum Hall effect to maintain a representation of the ohm,

– **decides** to meet in September 1988 with a view to recommending the value of R_H to come into effect on January 1, 1990,

– **gives** notice that the adoption of this value for R_H may lead to a change in national and the BIPM representations of the ohm; this change should in general not exceed 2 parts in 10^6,

furthermore, the CCE

– **recommends** that national laboratories

  – vigorously pursue their work to understand better the quantum Hall effect,

  – encourage the increased availability and distribution of good quantum Hall effect samples,

  – determine the value of R_H in SI units both by the direct realization of the ohm and the determination of appropriate fundamental constants,

  – carry out bilateral comparisons as seem appropriate, and communicate without delay all their results to the Working Group,

– **recommends** that the BIPM organize during 1987/88 an international comparison of one ohm resistance standards in connection with the quantum-Hall effect work,

– **recommends** that no laboratory should adopt a value of R_H for its representation of the ohm or use the quantum Hall effect to alter the present drift rate until the recommended value comes into effect,

– **believes** that the value to be recommended in 1988 will be sufficiently accurate, in terms of SI, for no change to be required in the foreseeable future.

The less than satisfactory current state of understanding of the QHE and the limited availability of good samples led the CCE also to develop Recommendation E 2 (1986) which encourages (a) studies of QHE sample manufacture and characterization, (b) the provision of an adequate supply of high quality QHE devices for metrological purposes by industry and research laboratories, (c) better theoretical and experimental understanding of the QHE, and (d) comparisons of QHE devices under the auspices of the BIPM. Both Declaration E 2 (1986) and Recommendation E 2 (1986) were also subsequently approved by the CIPM at its October 1986 meeting [14].

3. Conclusion

If all proceeds as planned, that is, if the several new values for $2e/h$ and R_H in SI units which are expected to become available by June 15, 1988, agree with earlier results within acceptable limits, then the CCE at its 18th Session in September 1988 will officially recommend for adoption a new value for the Josephson frequency-voltage ratio $2e/h$ consistent with the SI, and a value of the quantized Hall resistance $R_H = h/e^2$ also consistent with the SI, to be used by all national standards laboratories and the BIPM to define and maintain their representations of the volt and ohm. These new values, which would be implemented simultaneously throughout the world starting January 1, 1990, are anticipated to have an uncertainty of between 0.1 and 0.3 ppm. Moreover, the uncertainty associated with using the Josephson and quantum Hall effects to define and maintain representations of the volt and ohm should generally be in the range 0.01 to 0.1 ppm. As a consequence, starting January 1, 1990, the practical electrical units for voltage, resistance, and current of most industrialized countries will be equivalent within an uncertainty no greater than about 0.1 ppm and these units will be consistent with their respective SI units within an uncertainty no greater than about 0.3 ppm. Although implementing these new representations will require adjusting a large industrial inventory of standards and instruments by significant amounts (e.g., in the United States the U.S. Legal Volt will increase about 9 ppm and the U.S. Legal Ohm about 1.5 ppm), the benefits of international uniformity of electrical measurements and their consistency with the SI which will result from the unit changes should completely outweigh the costs of making them.

References

[1] Com. Intl. Poids Mes. Com. Consult. d'Electricité, Trav. 16e Session, 1983 (Bur. Intl. Poids Mes., Sèvres, France, 1983), p. E 105.

[2] Taylor, B. N., J. Res. Natl. Bur. Stand. **91** 299 (1986).
[3] Ref. [1], pp. E 3, E 9, E 111, E 116; and Giacomo, P., Metrologia **20** 25 (1984).
[4] Com. Intl. Poids. Mes. Com. Consult. d'Electricité, Trav. 13e Session, 1972 (Bur. Intl. Poids Mes., Sèvres, France, 1972), p. E 13; Terrien, J., Metrologia **9** 40 (1973).
[5] P. V. Séances Com. Intl. Poids Mes., 61e Session, **40** (Bur. Intl. Poids Mes., Sèvres, France, 1972), pp. 22, 100.
[6] Com. Intl. Poids Mes. Com. Consult. d'Electricité, Trav. 14e Session, 1975 (Bur. Intl. Poids Mes., Sèvres, France, 1975), p. E 6; Terrien, J., Metrologia **11** 179 (1975).
[7] P. V. Séances Com. Intl. Poids Mes., 64e Session, **43** (Bur. Intl. Poids Mes., Sèvres, France, 1975), p. E 7.
[8] Taylor, B. N., and T. J. Witt, Document CCE/86–46 submitted to the 16e Session of the Comité Consultatif d'Electricité, CIPM, 1986 (to be published in Ref. [12]).
[9] Delahaye, F.; D. Dominguez, F. Alexandre, J. P. Andre, J. P. Hirtz, and M. Razeghi, Metrologia **22** 103 (1986).
[10] See the relevant papers in IEEE Trans. Instrum. Meas. **IM–34** (June 1985).
[11] IEEE Trans. Instrum. Meas. **IM–36** (June 1987, to be published).
[12] Com. Intl. Poids Mes. Com. Consult. d'Electricité, Trav. 17e Session, 1986 (Bur. Intl. Poids Mes., Sèvres, France, to be published).
[13] Hamilton, C. A.; R. L. Kautz, R. L. Steiner, and F. L. Lloyd, IEEE Device Lett. **EDL–6** 623 (1985); Niemeyer, J.; L. Grimm, W. Meir, J. H. Hinken, and E. Vollmer, Appl. Phys. Lett. **47** 1222 (1985).
[14] P. V. Séances Com. Intl. Poids Mes., 75e Session, **54** (Bur. Intl. Poids Mes., Sèvres, France, 1986, to be published).

Journal of Research of the National Bureau of Standards

Conference Report

COMPUTER SECURITY—FOR TODAY . . . AND FOR TOMORROW

The Institute for Computer Sciences and Technology (ICST) and Department of Defense (DoD) National Computer Security Center (NCSC) jointly sponsored the Ninth National Computer Security Conference held at the National Bureau of Standards. The September 1986 conference attracted more than 800 people from government, industry, and academe eager to share information and to learn of new approaches and future trends in "trusted" computer systems. A "trusted" computer system is one that employs sufficient hardware and software integrity measures to allow simultaneous processing of multiple levels of classified or sensitive information. Stated another way, the term "trusted" computer system simply means we can rely on the computer itself to protect information from unauthorized use or modification.

Under the theme "Computer Security—for Today . . . and for Tomorrow," the conference provided a forum for technology interchange among developers of trusted systems and a place where computer users could exchange ideas and learn of new ways to apply some of the current computer and information security technology.

Background

Computers were first used to solve our information processing and dissemination problems. Security design principles, in general, were not used in building most commercial computer systems. This vulnerability, coupled with large amounts of highly sensitive and classified information processed by computers, resulted in an awareness that the security objectives of maintaining confidentiality, integrity, and availability of computer systems could not be assured.

Through its Computer Security and Risk Management Program, the Institute for Computer Sciences and Technology has played a vital and unique role in helping to protect government computer systems from intentional and accidental destructive acts. The activities of the program were established in 1965 by the Brooks Act and affirmed in 1980 by the Paperwork Reduction Act. Since 1972, ICST has issued cost-effective standards and guidelines for protecting computerized information from numerous threats including human error, natural hazards, and unauthorized users. The program encompasses research and development of security standards, test methods, transfer of technology to potential implementors and vendors, and technical assistance to advance new uses of computer technology. To carry out its computer security program, ICST researchers work cooperatively with a broad spectrum of organizations from Federal, State, and local governments; industry computer users and manufacturers; research organizations; and voluntary standards groups. While ICST's computer security program primarily assists Federal agencies in meeting their computer security responsibilities, the private sector is making increasing use of the program's services and resources.

Still faced with a lack of trusted computer systems upon which to depend in multiple classification processing environments, DoD organizations adopted a policy whereby system access was denied to all except those cleared to the highest level of classification of any information contained in the computer system. Enforcing such policy, however, required considerable duplication of resources and placed a strain on security clearance procedures.

In 1978 the Assistant Secretary of Defense for Communications, Command and Control and Intelligence established the DoD Computer Security Initiative to achieve widespread availability of trusted computer systems for use within DoD. This initiative was intended to foster development of computers by industry that would provide a high degree of integrity for protecting sensitive and classified information.

Since the start of the DoD Computer Security Initiative, industry has met the challenge of the security problem. Several trusted computer systems have been developed for use within the DoD. Evaluation procedures have been established for determining the environments for which a particular trusted system is suitable. The "Department of Defense Trusted Computer System Evaluation Criteria," published August 15, 1983, establishes a uniform set of basic requirements and evaluation classes for accessing the effectiveness of security controls built into computer systems. This document is commonly referred to as the "Orange Book." The evaluation criteria, as defined in the Orange Book, are divided into four broad hierarchical divisions representing enhanced security protection: D, C, B, and A. Each division represents a major improvement of security controls found in a computer system. The highest division "A" is reserved for systems providing the most comprehensive security. Furthermore, the problems of computer security have gained greater importance and attention in government at all levels and in business. In recent years, the initiative has been expanded to encourage research that is responsive to a broad class of computer security needs. Computer manufacturers continue research for the development of additional trusted systems that can be effectively used by not only the DoD, but civil agencies and the private sector.

The Technology Transfer Program continues to be an important element of the DoD Computer Security Initiative. In 1979, ICST joined with DoD to assist in stimulating a higher awareness of both the information security problems and solutions. Mr. Stephen Walker, who was then Chairman of the Computer Security Technical Consortium and Dr. Dennis Branstad, ICST, (now an NBS Fellow), organized the first of a series of meetings that would become an invaluable source for information exchange.

Since that first meeting held at the National Bureau of Standards in 1979, attendance and active participation have grown, and meetings have progressed from seminar to symposium to conference. The growth in participation represents an increase in information security awareness as well as a parallel maturation of the technology and its use. The combined efforts of ICST and DoD have brought about much of this progress.

About the 1986 Conference

Two parallel tracks, one of which addressed managerial computer security issues and the other technical issues, allowed conferees to focus on areas that were of interest or visit sessions in both categories to gain a broad perspective of trends in securing information systems. While many of the papers presented at this conference addressed issues relevant to trusted computer systems designed to support military computer applications, topics which dealt with a broader and more practical utilization of computer security technology were also discussed. Some of the management issues explored included education and awareness training, risk management, contingency planning, and computer security auditing. Some of the technical issues discussed included secure operating systems, security models, verification techniques, database security, and network security.

Speakers for both tracks included computer industry leaders, computer security practitioners and researchers from the United States and abroad. Brief summaries of a few specific contributions follow.

Opening the Conference

ICST Director, James Burrows and NCSC Director, Patrick Gallagher welcomed the conference participants. Mr. Burrows stressed the need for alliances between users and suppliers to meet future needs for secure applications. Mr. Gallagher discussed NCSC activities and called for cooperative efforts from the government, industry, and academe to solve security problems.

The keynote speaker, Walter S. Harner, Director of Complex Systems Technology for International Business Machines (IBM), said that industry had made progress in developing computer systems with security features but that there were still many issues to be addressed. He called for uniform standards for secure systems with extensions defined for special applications such as national security.

Database Issues

Several papers dealt with the integrity issue for trusted database systems. Each addressed the infer-

ence and aggregation problems as well as other security threats. Inference occurs when the user is able to infer some fact from the information that has been presented. Aggregation occurs when data combined from different sources results in a data item that has a higher classification than its individual components.

Rhonda Henning and Swen Walker, both from NCSC, presented a joint paper with Ms. Henning reporting on various system configurations which support database management systems (DBMS) and the security tradeoffs inherent in each. She pointed out that the incorporation of security features into a commercial DBMS is not an easy task, that a trusted DBMS will depend upon the careful inclusion of appropriate security controls, a sufficient audit trail, and a thorough recovery capability. She concluded that problems vital to database security were not fully understood and that only when these issues were properly addressed could DBMS be considered secure. She suggested that building prototype database management systems could provide insights into the problem.

Similarly, Roger Schell, Gemini Computers, Inc., and Dorothy Denning, SRI International, presented a joint paper which addressed integrity issues essential to the operation of secure database systems. Dr. Schell discussed all aspects of mandatory (classification/clearance) and discretionary (need-to-know) integrity controls both of which can protect data from malicious tampering and destruction as well as from accidental modification and destruction. Dr. Schell pointed out that database integrity rules should be included in an overall integrity policy because they provide users with considerable assurance that the data can be protected against many errors.

Peter Troxell, PAR Government Systems Corporation, discussed the hardware and software components which must be present in a "trusted" DBMS. He presented two approaches, Views and Integrity-Lock, both of which have been proposed as solutions to the trusted database design. He discussed the strengths and weaknesses of each of the proposed architectures. He concluded that further work must be done on how to implement the discretionary security policy onto a database.

Toward Improving Operational Systems

Many claims have been made about the degree of protection afforded by dial-up communications security devices. Gene Troy, ICST, reviewed a wide variety of hardware devices that are on the market. He discussed the limitations of these dial-up security devices, pointing out their flaws and implementation weaknesses. Mr. Troy recommended a series of approaches to overcoming these problems.

Also on the topic of improving operational systems, Hal Feinstein, MITRE Corporation, discussed security problems faced by civilian agencies operating unclassified, but sensitive systems. He pointed out that much of the security technology has been developed for the protection of classified information and that this technology cannot be effectively applied to unclassified environments of the Federal Government. Mr. Feinstein reviewed the multi-level sensitivity sharing problem suggesting that the risks can be reduced by good software security engineering and basic security enhancements to the operating system. He emphasized the need to develop a consistent, government-wide classification or ranking system for sensitive information similar to the labeling structure used in military environments. He further suggested that such a classification system would allow managers to more adequately determine the level of protection needed for handling and transmitting sensitive applications and data. Mr. Feinstein proposed a classification system ranging from non-sensitive to extremely sensitive. He pointed out that while these sensitive classifications conform to the military labeling structure, they are without national security implications.

Verification and Analysis

David Balenson, ICST, described the NBS Message Authentication Code Validation System (MVS) which permits remote, automated testing of systems employing message authentication for conformance to various standards. Mr. Balenson addressed topics which led to the development of the MVS, the standards it validates, its design philosophy, the requirements placed on vendors who wish to validate their devices, performance characteristics, and the results of the validations performed to date. Mr. Balenson explained that security standards have been developed within ICST and the Financial Community to authenticate computer data and electronic financial transactions. He pointed out that these standards, Federal Information Processing Standards Publication (FIPS PUB) 113 and the American National Standards Institute (ANSI) X9.9, make use of the Data Encryption Standard (DES) cryptographic algorithm to calculate a cryptographic checksum or Message Authentication Code (MAC) which is used to detect the accidental or intentional modification of com-

puter data. Miles Smid and Elaine Barker, also from ICST, are co-authors of the paper presented by Mr. Balenson.

F. Javier Thayer, MITRE Corporation, proposed a discipline for verifying software. Three interactive processes were proposed: a modeling process, a theorem-proving process, and a review and acceptance process. Suggestions were made for improving the development of these processes. He recommended that the modeling process should develop formal mathematical models of natural language requirements or specifications. He referred to the modeling-process as the most critical part of verification. In the theorem-proving process, the second process of formal verification, mathematical proofs of the conjectures generated during the modeling process should be constructed and analyzed. He pointed out that the review and acceptance process generally means ascertaining that the verification satisfies requirements agreed upon by the customer and verifier. He emphasized that this review and acceptance process should not only satisfy the requirements set forth by the customer, but should point to the soundness of the principles used in the verification. He called attention to the idea that the review process should allow for interaction between the reviewers and the verifiers. The ideas presented here were principally drawn from a review of the design verification of the Restricted Access Process (RAP). Co-authors of the work presented by Mr. Thayer included Dale Johnson, and William Farmer also of MITRE Corporation.

Foundations

Pamela Cochrane, Trusted Information Systems, Inc., reported the initial findings of a research project undertaken to investigate the feasibility of creating a trusted version of the Mach-1 operating system being developed at Carnegie-Mellon University. Ms. Cochrane, explained how Accent, the progenitor of Mach-1, is being used to conduct initial analysis, since both systems are message-based and focus on ports (kernel-managed message queues). She explained that her organization's research was targeted toward a class B3 Trusted Computing Base (TCB). The DoD Trusted Computer Security Evaluation Criteria (TCSEC) defines B3 systems as those highly resistant to penetration. Specifically, B3 systems preserve the integrity of sensitivity labels and use them to enforce a set of mandatory access control rules. Systems with B3 ratings are further characterized by a commitment to satisfy the reference monitor requirement that the system mediate all accesses to objects by subjects, be tamperproof, and be small enough to be subjected to analysis and tests.

Ms. Cochrane discussed two different approaches to labeling that are being probed. These approaches are 1) Kernel Mediation Approach—associating labels with ports and processes managed by the kernel; and 2) Server Mediation Approach—modifying the existing access group structure and using the Authentication, Authorization, and Name Servers to provide mandatory access control. She concluded that current investigations indicate that the Accent system could be modified to generate a viable B3 level operating system, and that the Kernel Mediation Approach, with labeling of all subjects and objects and a minimized TCB, is a strong candidate for B3. Further investigation of both approaches will continue. The research activities discussed in this paper were cooperative efforts of Ms. Cochrane, Martha Branstad, D. Elliot Bell, and Stephen Walker who are staff members of Trusted Information Systems, Inc.

Vendor Activities

Honeywell Information Systems has the only two commercial products available on the NCSC Evaluated Products Lists above Class C2 (this class enforces individual user accountability through login procedures, auditing of security-related events, and resource isolation). The Multics Product is rated as a class B2 system (provides structured protection); the Secure Communication Processor (SCOMP) was rated A1 (verified protection), the highest rating available.

Lester Fraim, Honeywell, Corp., discussed Honeywell's strategy for developing future products that will meet high-level security requirements. He informed the audience of the research activities of the Honeywell Secure Computing Technology Center. He spoke of Honeywell's plans to build on the technology of the SCOMP product, as well as integration of new technology as it becomes available, into sound technical solutions.

Conclusion

As was evidenced throughout the conference, research activities are aggressively being pursued toward development of technologies that will enhance the integrity and security of our nation's computing systems and networks. It is widely recognized, however, that a great deal of research and

development is needed before a significant number of "trusted" computing systems become available. With continued contributions from Federal Government, private industry, and academe this goal is certain to become a reality.

Proceedings from this conference are available upon request. You may write or call Irene Isaac, ICST, (301) 975-3360. Next year's conference will be held at the Baltimore Convention Center, Baltimore, MD, so that a larger audience may be accommodated. The conference will be announced in early 1987.

Irene E. Isaac
Computer Security Management
and Evaluation Group
Institute for Computer Sciences
and Technology
National Bureau of Standards
Gaithersburg, MD 20899

Journal of Research of the National Bureau of Standards

Conference Report

SYMPOSIUM ON OPTICAL FIBER MEASUREMENTS

One might expect that, as a technology matures, associated measurement problems would be solved and research in those areas would diminish. That view is supported by examination of the programs of some of the major international conferences related to optical fiber communications, which have shown a steady decline in the percentage of papers related to measurements. It is not supported by experience with the biennial Symposium on Optical Fiber Measurements. Rather, it appears that the need for such a specialized meeting on the topic of measurements continues to grow.

The 4th Symposium, sponsored by NBS in cooperation with the Optical Society of America and the IEEE Optical Communications Committee was held September 9-10, 1986, at the NBS Boulder Laboratories. It drew nearly 350 people from 17 countries to hear 29 contributed and 5 invited papers. The papers of this years' program were exceptionally diverse, both in subject and origin. In only two technical areas, chromatic dispersion and mode-field diameter measurements, was it possible to schedule a full session on a single topic. In origin, there were 21 organizations in 9 countries represented in the program. Over 40 percent of the papers were from outside the United States.

One reason for the continued interest in fiber measurements, suggested by W. T. Anderson of Bell Communications Research in an invited paper that opened the Symposium, is that while the properties of silica fibers are near their fundamental limits, more complete exploitation of their capacity continues to add to the characterization requirements.

Continuing concern with chromatic dispersion measurements arises from a growing interest in designing single-mode fiber communications systems for very high data rate operation. The limitation imposed by the fiber in these systems is a combination of material dispersion and waveguide dispersion, which cause different spectral components from the source to propagate at slightly different velocities. Material dispersion, which is related to the second derivative of the refractive index with wavelength, is fairly predictable, passing through zero at a wavelength near 1.3 μm. Waveguide dispersion, which depends on the shape of the refractive index profile, adds to the material dispersion, shifting the wavelength of zero total dispersion (i.e., the optimum operating wavelength) accordingly.

System designers need to know both the wavelength, λ_0 of zero total dispersion, and the variation of the dispersion around that wavelength. The latter requires a satisfactory model. A paper by Reed and Philen of AT&T Bell Laboratories concluded that a three term Sellmeier dispersion relation, well known in optics, is an adequate model for the most common types of fiber. For so-called dispersion shifted fibers, designed to have λ_0 near the wavelength of minimum loss at 1.55 μm, however, they found that it was necessary to use a more complex form of the Sellmeier equation.

Early dispersion measurement techniques required elaborate and expensive equipment, hence a strong interest in simpler measurements. A paper from Phillips Glass reports very encouraging results with a method called the phase-shift technique. In this technique the phase shift of a modulated source is monitored as its wavelength is scanned. The authors conclude that an accuracy of better than 0.5 ps/nm · km can be achieved but to

do so will require a temperature stabilization of the fiber to better than 1 K during the measurement.

Because the losses of modern fibers are extremely low, a much greater concern is attached to losses incurred in splices. One aspect of this problem is the need to establish and test high quality splices in the field. Techniques for field testing were reviewed in an invited paper by Reinhard Engle of Siemens and Everett McNair of Siecor. Another aspect is adequate specification of the mode profiles of single mode fiber. Several contributed papers seemed to conclude that it is relatively easy to achieve measurement consistency on step index single mode fibers but that more advanced index profile designs still pose problems.

Three invited talks discussed programs of related and future interest to fiber measurement specialists. These included a discussion of source and detector characterization by Ito and Kurumada of NTT, a summary of the characterization of advanced fibers and devices by Payne, et al., of the University of Southampton and British Aerospace, and a discussion of the problems associated with characterizing planar optical waveguides by Alferness of AT&T Bell Laboratories.

The Technical Digest for the Symposium on Optical Fiber Measurements, 1986, contains summaries of all invited and contributed papers. It is available as NBS Special Publication 720 from the Superintendent of Documents, U.S. Government Printing Office, Washington, D.C. 20402 ($8.00).

G. W. Day and D. L. Franzen
Program Chairman and General Chairman,
respectively for the Symposium
Electromagnetic Technology Division
National Bureau of Standards
Boulder, CO 80303

Volume 91 (1986)
Contents and Errata

Journal of Research of the National Bureau of Standards

UNITED STATES DEPARTMENT OF COMMERCE • Malcolm Baldrige, *Secretary*
NATIONAL BUREAU OF STANDARDS • Ernest Ambler, *Director*

In This Volume: *Issue 1 Jan.–Feb.*

Articles *Special Issue: pH Measurements in Rainwater*

Issue 2 Mar.–Apr.

Articles — *Special Issue: Biomedical Sampling*

Technical News Briefs

Conference Report

Issue 3 May–June

Articles

Conference Report

Technical News Briefs

Issue 4 July–Aug.

Articles

Conference Report

Technical News Briefs

Issue 5 Sept.–Oct.

Articles

Technical News Briefs

Issue 6 Nov.–Dec.

Articles

News Briefs and Reports

ERRATA

Corrections to be noted in Volume 91 of the JOURNAL OF RESEARCH of the National Bureau of Standards

Page	Line	Now reads in part	Should read
82	22, col. 1	[3]	[33]
84	6, col. 1	[36]	[34]
92	Ref. 36	Clin. Chem. **24** 353 (1978).	Clin. Chem. **24** 303 (1978).
167	16, col. 2	$\frac{dI}{dv} = K \cdot \log_e$	
168	1, col. 1	$\left[\frac{1+\eta^2-\mu^2+\sqrt{1+2(\eta^2-\mu^2)+(\eta^2+\mu^2)^2}}{2\eta^2}\right]$ (1)	$\frac{dI}{dv} = K \cdot \log_e \left[\frac{1+\eta^2-\mu^2+\sqrt{1+2(\eta^2-\mu^2)+(\eta^2+\mu^2)^2}}{2\eta^2}\right]$ (1)
169	7, col. 2	D_{water}	$\dot{D}_{water}$
175	47, col. 1	T. E. Feuchtwang	T. E. Feuchtwang [22]
197	Eq 3-5	10^6	10^{-6}
200	cap., Fig. 22	61 cm × 25 cm	92 cm × 61 cm × 25 cm
209	fn. 7	and C. F. Quate	S. A. Elrod, A. L. deLozanne and C. F. Quate
211	fn. 9	The author is not aware of any other published results which show . . .	The author is aware of only one other published result which shows . . .
217-220			The computer program on p. 217 is correct to the line, "Listing of DNSITY," one-third down left column, p. 218. Place a 3 at this point, a 2 at "GET WORK FUNCTION," two-thirds down left column, p. 219, and a 4 at "DIVISION, NATIONAL BUREAU OF STANDARDS," seventh line from bottom of left column, p. 220. The program should be read in the sequence thus indicated.
289	13, col. 2	The ten are column entries in	The entry in column ten is
296	13, col. 2	are given cellulose	are cellulose
327	14, col. 1	aliquoting	aliquanting
327	54, col. 1	10 °C	110 °C

☆U.S. G.P.O. 1987-181-096:40013

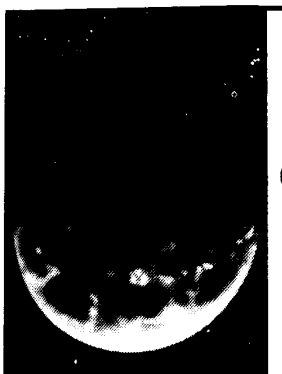

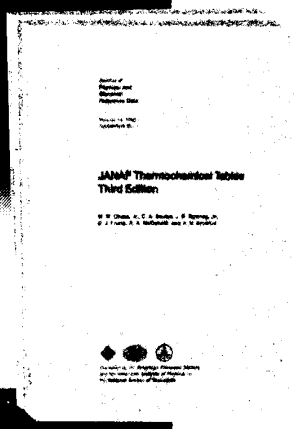

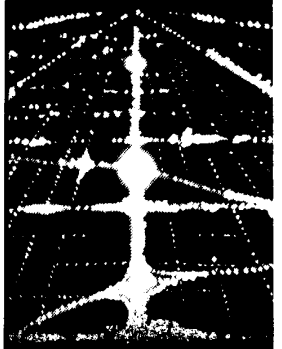

JUST PUBLISHED!

JANAF THERMOCHEMICAL TABLES

Third Edition

A Major Supplement from JOURNAL OF PHYSICAL AND CHEMICAL REFERENCE DATA

Presenting Reliable Data Utilized by Chemists, Chemical Engineers, and Materials Scientists from Around the World for Over 25 Years

JOURNAL OF PHYSICAL AND CHEMICAL REFERENCE DATA is very pleased to publish the Third Edition of the JANAF THERMOCHEMICAL TABLES.

Since the first version appeared 25 years ago, the JANAF THERMOCHEMICAL TABLES have been among the most widely used data tables in science and engineering. You'll find:

- Reliable tables of thermodynamic properties of substances of wide interest
- A highly professional approach with critical evaluations of the world's thermochemical and spectroscopic literature
- A concise and easy-to-use format

This Third Edition presents an extensive set of tables including thermodynamic properties of more than 1800 substances, expressed in SI units. The notation has been made consistent with current international recommendations.

There is no other reference source of thermodynamic data that satisfies the needs of such a broad base of users.

Order your 2-volume set of the JANAF THERMOCHEMICAL TABLES today! You'll get over 1890 pages of valuable information that is crucial to your research—in two hardback volumes.

SUBSCRIPTION INFORMATION

The JANAF THERMOCHEMICAL TABLES, THIRD EDITION is a two-volume supplement of *Journal of Physical and Chemical Reference Data.*

1896 pages, 2 volumes, hardcover
ISBN 0-88318-473-7
Supplement Number 1 to Volume 14, 1985

U.S. & Canada	**$130.00**
All Other Countries	**$156.00**
(Postage included.)	

All orders for supplements must be prepaid.

Foreign payment must be made in U.S. currency by international money order, UNESCO coupons, U.S. bank draft, or order through your subscription agency. For rates in Japan, contact Maruzen Co., Ltd. Please allow four to six weeks for your copy to be mailed.

For more information, write **American Chemical Society,** Marketing Communications Department, 1155 Sixteenth Street, NW, Washington, DC 20036.

In a hurry? Call TOLL FREE **800-424-6747** and charge your order!

Editors:
M.W. Chase, Jr.
Nat'l Bureau of Standards
C.A. Davies
Dow Chemical U.S.A.
J.R. Downey, Jr.
Dow Chemical U.S.A.
D.J. Frurip
Dow Chemical U.S.A.
R.A. McDonald
Dow Chemical U.S.A.
A.N. Syverud
Dow Chemical U.S.A.

Published by the **American Chemical Society** and the **American Institute of Physics** for the **National Bureau of Standards**